R-08-106

Numerical modelling of solute transport at Forsmark with MIKE SHE

Site descriptive modelling SDM-Site Forsmark

Lars-Göran Gustafsson, Mona Sassner
DHI Sverige AB

Emma Bosson, Svensk Kärnbränslehantering AB

December 2008

Svensk Kärnbränslehantering AB
Swedish Nuclear Fuel
and Waste Management Co
Box 250, SE-101 24 Stockholm
Tel +46 8 459 84 00

ISSN 1402-3091
SKB Rapport R-08-106

Numerical modelling of solute transport at Forsmark with MIKE SHE

Site descriptive modelling SDM-Site Forsmark

Lars-Göran Gustafsson, Mona Sassner
DHI Sverige AB

Emma Bosson, Svensk Kärnbränslehantering AB

December 2008

Summary

The Swedish Nuclear Fuel and Waste Management Company (SKB) is performing site investigations at two different locations in Sweden, referred to as the Forsmark and Laxemar areas, with the objective of siting a final repository for high-level radioactive waste. Data from the site investigations are used in a variety of modelling activities. This report presents model development and results of numerical transport modelling based on the numerical flow modelling of surface water and near-surface groundwater at the Forsmark site. The numerical modelling was performed using the modelling tool MIKE SHE and is based on the site data and conceptual model of the Forsmark areas described in /Johansson and Öhman 2008/ and /Johansson 2008/, respectively.

This report presents solute transport applications based on both particle tracking simulations and advection-dispersion calculations. The MIKE SHE model described in /Bosson et al. 2008/ is the basis for the transport modelling presented in this report. Simulation cases relevant for the transport from a deep geological repository have been studied, but also the pattern of near-surface recharge and discharge areas. When the main part of the modelling work presented in this report was carried out, the flow modelling of the Forsmark site was not finalised. Thus, the focus of this work is to describe the sensitivity to different transport parameters, and not to point out specific areas as discharge areas from a future repository (this is to be done later, within the framework of the safety assessment). In the last chapter, however, results based on simulations with the re-calibrated MIKE SHE flow model described in /Bosson et al. 2008, Chapter 6/ are presented.

The results from the MIKE SHE water movement calculations were used by cycling the calculated transient flow field for a selected one-year period as many times as needed to achieve the desired simulation period. The solute source was located either in the bedrock or on top of the model. In total, 15 different transport simulation cases were studied. Five of the simulations were particle tracking simulations, whereas the rest were performed with the MIKE SHE advection-dispersion module. Sensitivity analyses were made in order to study the effect of the number of computational layers, i.e. the relation between numerical dispersion and the vertical grid resolution, the influence of dispersion in the saturated zone, and the influence of sorption in the saturated zone.

In the advection-dispersion simulations, input concentrations were given either as a pulse source or as a constant source in the bedrock layer at c. 140 m.b.s.l. (metres below sea level), or as a constant infiltration source in the top layer. In the particle tracking simulations reported here, particles were initially introduced in the top layer or in the deeper bedrock layer at approximately 140 m.b.s.l. In some simulation cases, particles were introduced through a concentration source in the deeper bedrock layer corresponding at c. 140 m.b.s.l. or as an infiltration source in the top layer. These scenarios were modelled primarily to enable comparisons with the corresponding advection-dispersion cases.

The simulation results show that the solute introduced at a level of 140 m.b.s.l. was transported both upwards and downwards, although the main transport direction was upwards. The solute that was transported towards the ground surface was mainly transported through deformation zones below the lakes and the watercourses. In some of these zones, transport was rather fast and the solute was transported to the surface in only a few months. However, the solute was also transported towards the sea, but the transport towards the sea was much slower than that in the deformation zones. In large parts of the area, the transport towards the sea was very slow, although in some highly water-conductive parts the process was faster. In these zones with higher horizontal hydraulic conductivity in the bedrock, the solute was mainly transported in the horizontal direction towards the sea, cutting off the vertical transport upwards.

Furthermore, results from the transport simulations illustrate that the applied infiltration source produces solute mass in recharge areas only, although a horizontal solute transport from higher-altitude recharge areas to lower-lying discharge areas (e.g. lakes) would be expected. It seems that on the time scale considered in the present modelling the littoral zones act as hydraulic barriers around some of the lakes. This means that the spreading through horizontal transport in the upper layers in these areas is less important than the effects of vertical flow directions.

The dispersion processes transports solutes from the advective zones into more stagnant zones. The results show that this process is important when evaluating the risk of solute spreading into zones in which the transport pattern is more diffuse. Therefore, it is important to estimate the dispersion coefficients and to avoid numerical dispersion. Furthermore, since sorption leads to a delay in the peak arrival time, it is an important factor to include in simulations when the estimation of the solute peak arrival time is crucial.

Sammanfattning

Svensk Kärnbränslehantering (SKB) genomför för närvarande platsundersökningar inom två potentiella områden för lokalisering av ett slutförvar för utbränt kärnbränsle i Sverige, nämligen Laxemar och Forsmark. Data från platsundersökningarna används i ett flertal modellaktiviteter. Denna rapport presenterar resultat från numeriska transportberäkningar, baserade på en numerisk flödesmodellering av ytvatten och ytligt grundvatten i Forsmark. Den numeriska modelleringen utfördes med modellverktyget MIKE SHE och baseras på de platsdata och den konceptuella modellen över Forsmark som beskrivs i /Johansson och Öhman 2008/ respektive /Johansson 2008/.

Den här rapporten presenterar transportmodelleringar baserade både på s k partikelspårning och på advektions-dispersionsberäkningar. MIKE SHE-modellen som finns beskriven i /Bosson m fl. 2008/ utgör basen för transportmodelleringen i denna rapport. Beräkningsfall som är relevanta för att studera transporten från djupa geologiska lager har undersökts, men även mönster för ytnära in- och utströmningsområden för grundvatten. När huvuddelen av modellarbetet som presenteras i denna rapport utfördes var flödesmodelleringen av Forsmark fortfarande inte slutförd. Därför har fokus i denna rapport lagts på att beskriva känsligheten med avseende på olika transportparametrar och inte på att peka ut specifika utströmningsområden från ett framtida slutförvar (detta görs senare inom ramen för säkerhetsanalysen). I det sista kapitlet presenteras dock resultat baserade på den omkalibrerade MIKE SHE-flödesmodell som beskrivs i /Bosson m fl 2008, kapitel 6/.

Resultaten från flödesmodelleringen som gjorts med MIKE SHE användes genom att det transienta flödesfältet för en utvald ettårsperiod kördes cykliskt så många varv som behövdes för att den önskade simuleringsperioden skulle erhållas. Källan där det lösta ämnet tillfördes (antingen som partiklar eller som en specificerad koncentration) placerades antingen djupt nere i berget eller ovanpå modellen. Totalt kördes 15 olika transportsimuleringar. Fem av simuleringarna var partikelspårningar och resten advektions-dispersionssimuleringar. Känslighetsanalyser gjordes för att studera effekten av antalet beräkningslager, d v s sambandet mellan numerisk dispersion och modellens upplösning i vertikalled, effekten av att inkludera dispersion i den vattenmättade zonen, samt effekten av sorption i den mättade zonen.

I advektions-dispersionsberäkningarna angavs tillförd massa antingen som en pulskälla i de djupare berglagren, på ca 140 m u h (meter under havsnivån), eller som en konstant infiltrationskälla i det översta lagret i modellen. I de partikelspårningsberäkningar som redovisas i denna rapport, introducerades partiklarna i översta lagret samt i ett djupare berglager på ca 140 m u h. I vissa beräkningsfall introducerades också partiklar genom en koncentrationskälla i det djupare berglagret eller i ytlagret. Dessa beräkningar gjordes främst för att möjliggöra jämförelser med motsvarande advektions-dispersionsfall.

Simuleringarna visar att den lösta massa som applicerades på motsvarande ca 140 m u h transporterades både uppåt och nedåt, även om huvudriktningen var uppåt. Den massa som rörde sig uppåt mot ytan transporterades i huvudsak genom deformationszoner i berget under sjöarna och vattendragen. I vissa av dessa zoner skedde transporten ganska snabbt och föroreningsmassan transporterades till ytan på bara några månader. Det tillförda ämnet transporterades dock även mot havet, men den transporten var avsevärt långsammare än transporten genom deformationszonerna. I stora delar av området tog transporten mot havet mycket lång tid, även om transporten i en del högkonduktiva områden var betydligt snabbare. I dessa zoner med högre horisontell hydraulisk konduktivitet i berget transporterades det lösta ämnet framförallt horisontellt mot havet och längs flödesvägar som skär av den vertikala transporten mot ytan.

Resultaten från transportberäkningarna visar också att när det tillförda ämnet appliceras på ytan och sedan får infiltrera ner i modellen produceras massa enbart i inströmningsområden, trots att man kunde förvänta sig en horisontell transport från högre belägna inströmningsområden till lägre liggande utströmningsområden (t ex sjöar). Det tycks som om litoralzonerna fungerar som hydrauliska barriärer runt en del av sjöarna. Detta innebär att spridningen genom horisontell transport i de övre lagren är betydligt mindre än effekterna av vertikala flödesriktningar.

Dispersionsprocesserna transporterar massa från de advektiva zonerna till de mer stagnanta zonerna. Resultaten visar att denna process är viktig när man utvärderar risken för förorenings-spridning till zoner med ett mera diffust transportmönster. Det är därför viktigt att uppskatta dispersionskoefficienter och att undvika numerisk dispersion i modellen. Det är dessutom viktigt att även ta hänsyn till sorption. Eftersom sorption leder till en försening av toppnivån i koncentrationen är det en viktig faktor att inkludera i simuleringarna när uppskattning av tiden för maxkoncentrationen är av intresse.

Contents

1 Introduction

1.1 Background

The Swedish Nuclear Fuel and Waste Management Company (SKB) is performing site investigations at two different locations in Sweden, referred to as the Forsmark and Laxemar areas, with the objective of siting a final repository for high-level radioactive waste. Data from the site investigations are used in a variety of modelling activities; the results are presented within the frameworks of Site Descriptive Models (SDM), Safety Assessment (SA), and Environmental Impact Assessment (EIA).

The SDM provides a description of the present condition at the site, which is used as a basis for developing models intended to describe future conditions in the area. This report presents model development and results of numerical transport modelling based on the numerical flow modelling of surface water and near-surface groundwater at the Forsmark site. Data from the Forsmark 2.3 data freeze (March 31, 2007) constitute the most recent input to the modelling. The numerical modelling was performed using the modelling tool MIKE SHE and is based on the site data and conceptual model of the Forsmark areas described in /Johansson and Öhman 2008, Johansson 2008/. The present work is a part of the modelling performed for the final version of the Forsmark SDM to be produced during the site investigation stage. This SDM version is referred to as SDM-Site Forsmark and is reported in /SKB 2008/.

Modelling of radionuclide transport is an important part of the analyses performed in order to support the safety assessments. This report presents solute transport applications based on both particle tracking (in the following sometimes shortened to PT) simulations and advection-dispersion (AD, for brevity) calculations. Simulation cases relevant for the transport from a deep geological repository have been studied, but also the pattern of near-surface recharge and discharge areas. When the modelling work presented in this report was carried out, flow modelling of the Forsmark site was not finalised. Thus, the focus of this work is to describe the sensitivity to different transport parameters, and not to point out specific areas as discharge areas from a future repository (this is done later in the safety assessment). However, results from transport simulations performed based on the final, re-calibrated flow model are also presented in this report.

1.2 Objective and scope

The general objectives of the site descriptive modelling of the Forsmark area and the specific objectives of the SDM-Site Forsmark modelling are presented in /SKB 2008/. The present report is a background report describing the numerical modelling of solute transport in Forsmark.

The objectives of the modelling reported in this document are to:

1. Analyse solute transport from potential sources at large depth in the bedrock into the near-surface system, and from sources on the ground surface into the bedrock.
2. Analyse the sensitivity of solute transport results to selected model parameters.

1.3 Setting

The Forsmark area is located approximately 120 km north of Stockholm, in northern Uppland within the municipality of Östhammar. Figure 1-1 shows the regional model area and the so-called candidate area considered by the site investigation and within the site descriptive modelling. Also some lakes and other objects of importance for the hydrological modelling are shown in the figure.

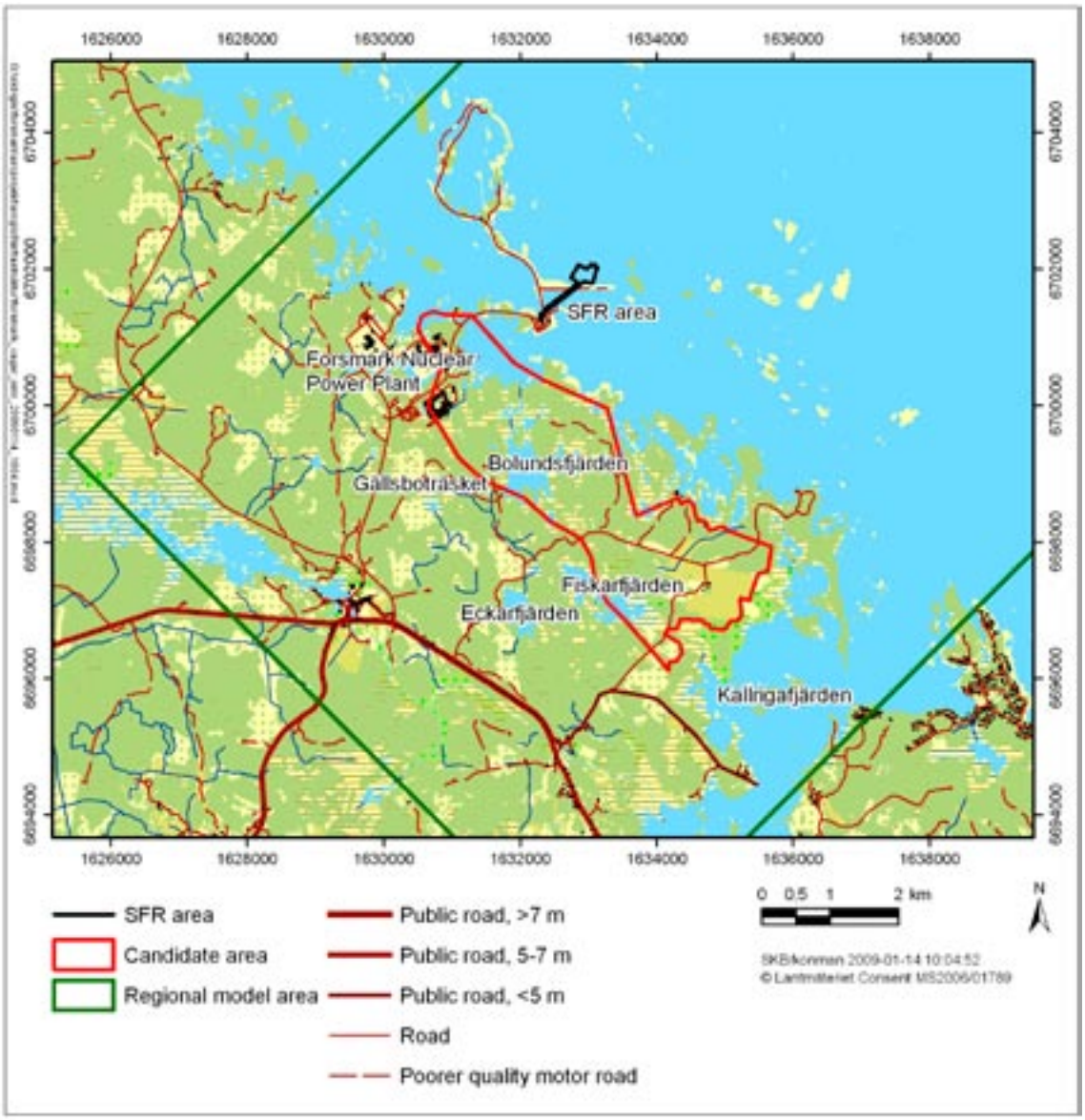

Figure 1-1. *Map of the land part of the regional model area and some objects of particular interest for the hydrological modelling.*

The candidate area is the area initially prioritised for potentially hosting the geological repository. This means that the repository possibly could be built somewhere within this area, not that it would occupy the whole area. This implies that more detailed investigations have been performed inside the candidate area than in the rest of the regional model area, at least for that some of the site investigation disciplines (see /SKB 2008/ for details). The candidate area is situated in the immediate vicinity of the Forsmark nuclear power plant and the underground repository for low- and medium-active nuclear waste, SFR. It is located along the shoreline of Öregrundsgrepen (a part of the Baltic), and extends from the nuclear power plant and the access road to the SFR facility in the northwest to the Kallrigafjärden bay in the southeast. The candidate area is approximately 6 km long and 2 km wide.

A description of the meteorological, hydrological and hydrogeological conditions in the Forsmark area is presented in /Johansson 2008/. /Lindborg (ed.) 2008/ gives a description of the whole surface and near-surface system, including the most recent models of, e.g. the topography and the Quaternary deposits.

1.4 Related modelling activities

Several modelling activities have provided the various external input data and models required for the present modelling and the preceding SDM site modelling. The numerical flow model, which is the basis for the transport modelling, was developed using the MIKE SHE tool. The ground surface, as obtained from the topographic model of the site, is the upper model boundary. The modelling activities that provided inputs to the various parts of this work can be summarised as follows:

- The SDM Forsmark 2.2 hydrogeological modelling performed with the ConnectFlow modelling tool /Follin et al. 2007/ delivered the hydrogeological model of the rock and the bottom boundary condition used in the basic setup of the model and in the sensitivity analysis.
- The Forsmark version 2.2 and 2.3 geological models of the Quaternary deposits /Hedenström et al. 2008, Hedenström and Sohlenius 2008/ provided the geological-geometrical framework for the stratigraphical description used in the MIKE SHE flow model.
- The SDM-Site conceptual modelling of the hydrology and near-surface hydrogeology at the Forsmark site /Johansson 2008/ provided a basic hydrogeological parameterisation and a hydrological-hydrogeological description to be tested in the numerical modelling.
- The MIKE SHE model described in /Bosson et al. 2008/ is the basis for the transport modelling presented in this report. However, the transport modelling presented here was a parallel activity to the flow modelling and an early version of the flow model was used in most of the simulations. The final flow model presented in /Bosson et al. 2008/ was used only in the later stages of the transport modelling; the results of this modelling are described in Chapter 6 of the present report.

The relations between the near-surface and bedrock hydrogeological models are discussed in /Follin et al. 2007/ and /SKB 2008/.

1.5 This report

This report provides a presentation of the modelling activities listed as parts 1 and 2 in Section 1.2. Chapter 2 describes the modelling tool and the governing equations of the transport calculations. Chapter 3 presents the input data and the different simulation cases studied. In Chapter 4 the results are presented in terms of recharge and discharge areas and flow paths in the bedrock and the Quaternary deposits. In Chapter 5, the methodology and the results of the sensitivity analysis are described. In Chapter 6 results from simulations based on the final, re-calibrated flow model are presented, and, finally, in Chapter 7 the work is summarised and the conclusions are presented.

2 Solute transport modelling with MIKE SHE

The modelling tool used in the analysis is based on MIKE SHE, developed by DHI. MIKE SHE is a dynamic, physically based, modelling tool that describes the main processes in the land phase of the hydrological cycle. The code used in this project is software release version 2007 /DHI Software 2007/.

In MIKE SHE, the precipitation can either be intercepted by leaves or fall to the ground. The water on the ground surface can infiltrate, evaporate or form overland flow. Once the water has infiltrated the soil, it enters the unsaturated zone. In the unsaturated zone, it can either be extracted by roots and leave the system as transpiration, or it can percolate down to the saturated zone. MIKE SHE is fully integrated with a channel-flow code, MIKE 11. The exchange of water between the two modelling tools takes place during the whole simulation, i.e. the two programs run simultaneously. The modelled processes are summarised in Figure 2.1. For a detailed description of the processes included in MIKE SHE and MIKE 11, see /Werner et al. 2005/ and /DHI Software 2007/.

Solute transport simulations with the MIKE SHE model may be performed by either the particle tracking module or the advection-dispersion module. In both cases, the three-dimensional flow field calculated by the MIKE SHE water movement module is the basis for the transport simulations. General principles for the two methods are given below.

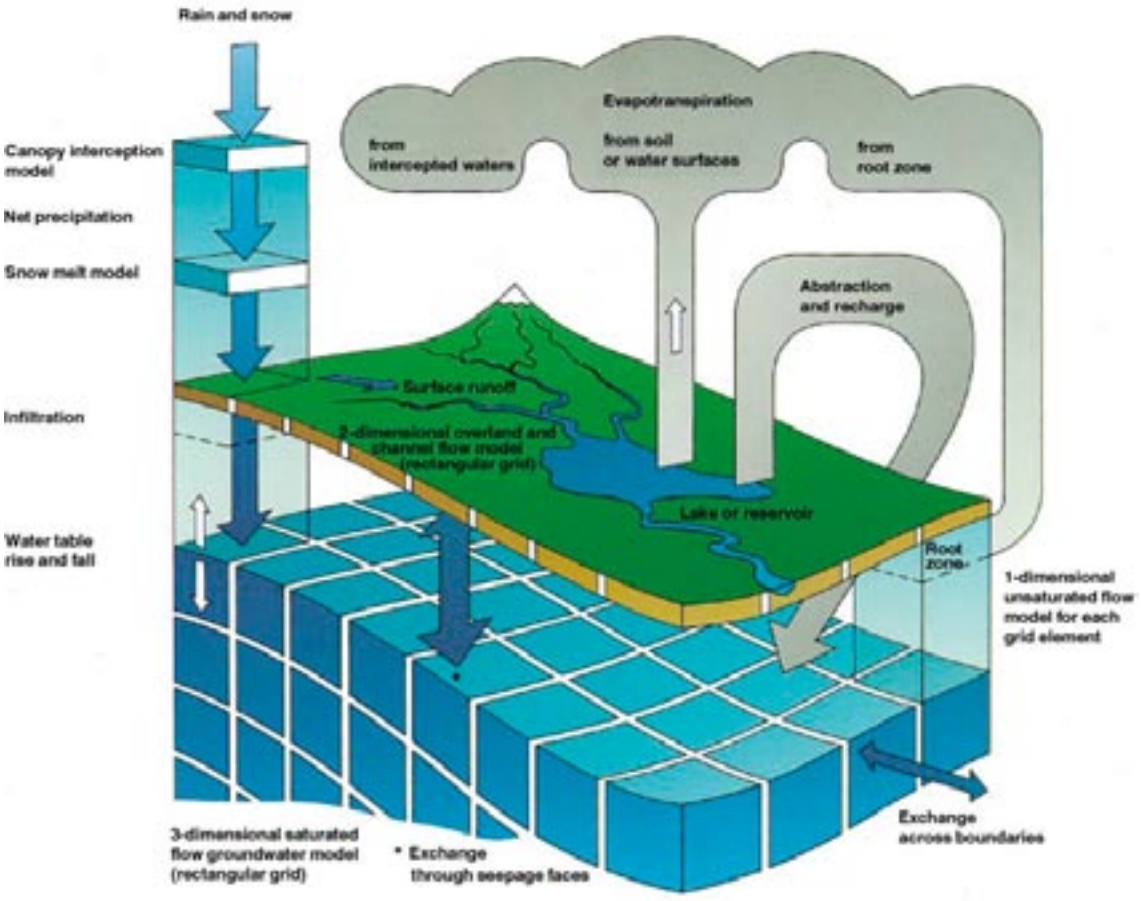

Figure 2-1. *Overview of the model structure and the processes included in MIKE SHE /DHI Software 2007/.*

2.1 Particle tracking modelling

Particle tracking modelling is in the MIKE SHE model system per definition a purely advective transport, without any dispersion effects. This means that the substance is moved with the Darcy flow vectors, and nothing else. The particles can have any location in the water movement grid cells, which means that they can be started at any selected position within cells and their locations monitored also within the cells. In this sense, the description of the movement of the particles is independent of the numerical resolution. This gives a very distinct result, which is often also easy to evaluate regarding destinations and flow paths. However, the transport itself is obviously affected by the numerical model resolution, since it determines the resolution of the velocity field that transports the particles.

In particle tracking simulations, hypothetical inert particles or "water parcels" are traced as they are transported by the groundwater flow field in the model volume. The resulting flow paths provide important information as such; they connect the selected starting points with groundwater discharge points or other exit points on the model boundaries. Furthermore, travel or residence times along the flow paths can be calculated.

The three-dimensional flow field calculated by MIKE SHE is the basis for the advective transport of the particles. In addition to the input required for the flow modelling, the particle tracking simulations require input data on the number of particles introduced and the starting point of each particle.

In MIKE SHE, particle tracking calculations can be performed for the saturated zone only. When a particle moves from the saturated zone to another compartment of the model, that particle is not traced any further. It is registered to which sink/compartment the particle moves, and the time step, transport distance and actual position of the particle are also registered. Thus, it is possible to get information on where the particle leaves the saturated zone and where it goes. A more detailed description of the methodology of the particle tracking calculation is given in /Bosson and Berglund 2006/ and /DHI Software 2007/.

2.2 Advection-dispersion modelling

With the MIKE SHE tool, it is possible to calculate advective-dispersive solute transport in all the different parts of the hydrological cycle that are considered in the flow modelling. At present, however, three alternatives are possible for simulating transport in the different MIKE SHE modules:

- transport in the saturated (groundwater) zone can run as a stand-alone module,
- transport in the saturated zone can be run in combination with transport in the overland water module,
- transport in all modules can be modelled simultaneously.

The solute transport module for the saturated zone in MIKE SHE allows the user to calculate transport in 3D, 2D, or even 1D. However, the transport formulation is controlled by the water movement discretisation. If the vertical discretisation is uniform (except for the top and bottom layer) the transport scheme is described in a fully three-dimensional numerical formulation. If the numerical layers have different thicknesses a multi-layered 2D approach is used, where each layer exchanges solute mass with other layers as sources and sinks.

Temporal and spatial variations of the solute concentration in the soil matrix are described mathematically by the advection-dispersion equation and solved numerically by an explicit, third-order accurate solution scheme. The forcing function for advective transport is the cell-by-cell groundwater flow, as well as groundwater head, boundary, drain and exchange flows, which are all read from the MIKE SHE water movement results files.

Advection-dispersion modelling includes, except advective transport, also dispersion, which allows the substance to move in other directions than that given by the modelled velocity field. The strength of the solute transport through dispersion is controlled by given dispersivities in different directions. The physical interpretation behind the dispersion is diffusion and small scale heterogeneities that are not part of the model description, but affect the solute spreading in reality. The more accurately the spatial variability in the hydrogeological properties is described, which requires a sufficiently fine grid and detail in the representation of the variations in the groundwater velocity, the smaller dispersivities need to be applied in the model.

A drawback with the advection-dispersion description of solute transport is that the model may create so-called numerical dispersion, i.e. dispersion that arises in the numerical model although the given dispersivities may be zero. This phenomenon arises when the grid cells are too large in relation to the advective velocities.

Several reaction processes can be added to the MIKE SHE solute transport calculations, including

- sorption and desorption,
- degradation,
- plant uptake.

Sorption-desorption models represent a number of chemical reactions and physical processes that associate solutes with surfaces of solid phases. If these processes occur sufficiently fast compared with the water flow velocity, they can be described by an equilibrium sorption isotherm. Different equilibrium sorption isotherms have been identified from experimental results. The MIKE SHE advection-dispersion module includes three of the most commonly applied isotherms, namely the linear, the Freundlich and the Langmuir sorption isotherms.

MIKE SHE is also able to simulate solute transport in fractured media through a so-called dual porosity description, which involves a mobile and an immobile phase. Further details on available process models are found in /DHI Software 2007/.

3 Description of simulation cases

3.1 Input data

Solute transport analyses presented in this report are based on the Forsmark 2.3 MIKE SHE model described in /Bosson et al. 2008/. Simulation cases relevant for the transport from a deep geological repository are studied, but also the pattern of recharge and discharge areas in the Quaternary deposits. The source of the dissolved substance is located either in the bedrock or in the uppermost layer of the model.

The modelling activities described in this chapter, and in terms of results in Chapters 4–6 include particle tracking simulations and advection-dispersion simulations. In both cases, the transport results in Chapters 4 and 5 are based on the flow model described in /Bosson et al. 2008, Chapter 4/. In most of the transport simulation cases, however, the number of calculation layers is increased to approximately the double compared to the flow modelling. The reason for this is to avoid numerical dispersion when the advection-dispersion model is applied. This is described in more detail below, and numerical dispersion is analysed in Chapter 5. As explained above, the transport simulations in Chapter 6 of this report are based on the final, re-calibrated MIKE SHE flow model, which is described in /Bosson et al. 2008, Chapter 6/.

The results from the MIKE SHE water movement calculations are used by cycling the transient flow modelling results for a selected one-year period as many times as needed to achieve the desired simulation period. The effective porosity of the bedrock is imported from the ConnectFlow bedrock modelling /Follin et al. 2007/; this dataset is also used to describe the specific yield in the water movement calculations. The effective porosity of each Quaternary deposit material is assumed to be equivalent to the specific yield of that material.

In the advection-dispersion modelling reported here, input concentrations are given either as a pulse source (during one month), or as a constant solute source in the bedrock layer corresponding to a level of c. 140 m.b.s.l. (metres below sea level), or as a constant infiltration source in the top layer. In the particle tracking scenarios reported here, particles (one in each grid cell) are initially introduced in the top layer, or in the bedrock layer at c. 140 m.b.s.l. In some simulations, particles are introduced through a concentration source (during one month) at 140 m.b.s.l. in the bedrock, or as an infiltration source in the top layer. These simulations are primarily done to enable comparisons with the corresponding advection-dispersion scenarios.

3.2 Simulation cases

In total, 15 different transport simulation cases were modelled, see Table 3-1. Five of the simulations were particle tracking simulations, whereas the rest were made with the advection-dispersion module.

The first two particle tracking cases, referred to as *PT0-top* and *PT0-bedrock*, were modelled with the original number of calculation layers from the flow model, i.e. 14 layers. In *PT0-bedrock*, one particle is introduced in each cell at 140 m.b.s.l. while in *PT0-top* one particle is introduced in each cell in the uppermost calculation layer. The simulation time was 300 years in both simulation *PT0-top* and *PT0-bedrock*. The simulations were based on the calculated transient flow modelling results using the simulated one-year period from October 2003 to October 2004 as input. This means that the model results from the MIKE SHE Water movement calculation for this one-year period were cycled 300 times. The results from *PT0-bedrock* are presented in Section 4.1.1 and the *PT0-top* results are presented in Section 4.2.1.

Table 3-1. Specification of solute transport model simulations (QD stands for Quaternary deposits).

Simulation ID	Source location	Source definition	Number of layers	Dispersivities (longitudinal, transverse), m	Sorption Kd-value, m^3/g
PT0-top	top layer	one particle per cell	14	N/A	N/A
PT0-bedrock	140 m.b.s.l.	as PT0-top	14	N/A	N/A
AD1	140 m.b.s.l.	one month fixed concentration	14	0.2, 0.01	no sorption
AD2	140 m.b.s.l.	as AD1	30	0.2, 0.01	no sorption
AD3	140 m.b.s.l.	as AD1	22	0.2, 0.01	no sorption
AD3-constant	140 m.b.s.l.	fixed continuous concentration	22	0.2, 0.01	no sorption
AD4	140 m.b.s.l.	as AD1	22	20, 0.2	no sorption
PT5	140 m.b.s.l.	as AD1	22	N/A	N/A
AD6	140 m.b.s.l.	as AD1	22	0.2, 0.01	QD: 10^{-7} bedrock: 10^{-10}
AD7	140 m.b.s.l.	as AD1	22	0.2, 0.01	QD: 10^{-7} bedrock: 0
AD10	infiltration	fixed continuous concentration	22	0.2, 0.01	no sorption
AD11	infiltration	as AD10	22	20, 0.2	no sorption
PT12	infiltration	as AD10	22	N/A	N/A
AD13	140 m.b.s.l.	as AD1	22	0.2, 0.01	no sorption
PT5-repository	140 m.b.s.l.	one particle per cell in repository area only	22	N/A	N/A

The first three advection-dispersion model simulations, referred to as *AD1*, *AD2*, and *AD3*, were carried out as a sensitivity analysis in order to evaluate whether the model was affected by so called numerical dispersion, i.e. dispersion that may arise in the numerical model although the given dispersivities may be zero. This phenomenon arises when the grid cells are too large in relation to the advective velocities.

In all of these simulations the source was applied in the bedrock at a level of approximately 140 m.b.s.l. The source was applied as a pulse with a duration of one month. It was applied all over the model area with a uniform concentration of 1 g/m^3. The initial concentration in the model was 0 g/m^3. The results from the MIKE SHE water movement calculations were used by cycling the flow for a one-year period, in this case from May 2004 to May 2005. In all three simulations, the solute dispersion was isotropic with a longitudinal dispersivity of 0.2 m and a transverse dispersivity of 0.01 m. These dispersivities correspond to a very low degree of solute dispersion.

The *AD1* model contained the original number of computational layers from the flow model, which is 14 layers. As shown in Table 3-2, the number of computational layers was in *AD2* increased to 30, whereas in *AD3* the number of layers was 22. In all simulations with a bedrock source, the source was applied in the original layer L10 (at a level corresponding to 140 m.b.s.l.). The results from *AD1*, *AD2* and *AD3* are compared in Section 5.1.

Table 3-2. Division of the *AD1*, *AD2* and *AD3* models into computational layers.

Original computational layer number	AD1	AD2	AD3
L1 (Quaternary deposits)	1	1	1
L2 (Quaternary deposits)	1	1	1
L3 (bedrock)	1	5	3
L4 (bedrock)	1	3	2
L5 (bedrock)	1	3	2
L6 (bedrock)	1	3	2
L7 (bedrock)	1	3	2
L8 (bedrock)	1	3	2
L9 (bedrock)	1	3	2
L10 (bedrock)	1	1	1
L11 (bedrock)	1	1	1
L12 (bedrock)	1	1	1
L13 (bedrock)	1	1	1
L14 (bedrock)	1	1	1
Total number of layers	14	30	22

The solute source in simulations *AD1-AD3* was applied as a pulse during one month. In order to make sure that the conclusions drawn based on this simulation were not influenced by seasonal flow patterns, an additional simulation with the *AD3* setup was made, this time with a constant concentration source through the whole simulation. This simulation is referred to as *AD3-constant*. The results from *AD3* and *AD3-constant* are presented in Section 4.1.2.

The next advection-dispersion simulation is *AD4*, which is the same as *AD3* except for the dispersion coefficients. In *AD4*, the longitudinal dispersivity equals 20 m and the transverse dispersivity is 0.2 m. The dispersion coefficients correspond to a higher degree of solute dispersion. The purpose of the simulation is to study the effect of the dispersion coefficients on the results.

To be able to study also the effect of a smaller dispersion, a particle tracking simulation with the same conditions as *AD3* and *AD4* was also made; this simulation is referred to as *PT5*. In a MIKE SHE particle tracking simulation, the transport is purely advective, i.e. the solute dispersion is zero. The source in *PT5* was based on the same concentration source as in *AD3*, i.e. a concentration pulse with a duration of one month, applied uniformly over the model area with a concentration of 1 g/m^3. The number of particles introduced in each time step was calculated based on the calculated mass flow and a specified particle mass of 50 g. The same period for the MIKE SHE Water movement results (May 2004 to May 2005) were used for *PT5*, as for *AD3* and *AD4*. The results from *AD3*, *AD4* and *PT5* are compared in Section 5.2.1.

The next two simulations, referred to as *AD6* and *AD7*, were made in order to study the effect of adding sorption processes. Sorption was added by a linear equilibrium sorption isotherm. The linear sorption isotherm is mathematically the simplest isotherm and can be described as a linear relationship between the amount of solute sorbed onto the soil material and the aqueous concentration of the solute. In *AD6*, the sorption coefficient, K_d, in the Quaternary deposits is set to $1.0 \cdot 10^{-7}$ m^3/g and in the bedrock to $1.0 \cdot 10^{-10}$ m^3/g. In *AD7*, the sorption coefficient in the Quaternary deposits is the same as for *AD6*, i.e $1.0 \cdot 10^{-7}$ m^3/g, while the coefficient in the bedrock is zero. The results from *AD3*, *AD6* and *AD7* are compared in Section 5.3.

In the following three simulation cases, the pollution source is applied as an infiltration source, i.e. the source is introduced to the groundwater through infiltration. As a consequence, the amount of solute introduced to the model depends on the amount of infiltration. The first two of the three simulations are with the advection-dispersion module, they are referred to as *AD10* and *AD11*, and the third simulation is with the particle tracking module, referred to as *PT12*. Except for the source description, these simulation cases are equivalent with *AD3*, *AD4* and *PT5*, respectively.

The infiltration source in *AD10* and *AD11* is continuous with a concentration of 1 g/m^3. The initial concentration in the model is 0 g/m^3. The same holds for *PT12*, and the numbers of particles introduced are calculated based on a particle mass of 50 g. The results from *AD10*, *AD11* and *PT12* are compared in Section 5.2.2.

In all of the simulations discussed above, only the saturated zone was included in the transport calculations. In the final simulation, *AD13*, all simulation components, except the river component, are included, i.e. the overland component, OL, the unsaturated zone component, UZ, and the saturated zone, SZ, are all active. In *AD13*, the source is applied in the same way as in *AD3*. The results from *AD13* are presented in Section 4.1.2.

In the advection-dispersion transport simulation cases *AD1* to *AD6*, all with the bedrock source, the simulation time was set to 200 years. For the cases with the infiltration source, *AD10* and *AD11*, the simulation time was set to 20 years. For *AD13*, the simulation time was set to 50 years. However, due to very long simulation times, not all simulations were concluded at the time of evaluating the results. As a consequence, some of the figures in Chapters 3 and 4 may contain graphs that are cut off prior to the intended simulation time.

After completion of the transport simulations described above, a re-calibration of the water flow model was made /Bosson et al. 2008, Chapter 6/. With the re-calibrated flow model, some of the already simulated cases were redone and also a new simulation case was defined, *PT5-repository*, in which particles were released at a level of c. 140 m.b.s.l. within the intended repository area only. Results from the simulations with the re-calibrated flow model are presented in Chapter 6. The *PT5* simulation with particle injection in all cells at 140 m.b.s.l. was repeated with the updated flow field. In Chapter 6 this case is referred to as *PT5-allover*, in order to distinguish it from the *PT5-repository* case.

4 Results

4.1 Deep bedrock source

4.1.1 Particle tracking

In total, 22,867 particles (one in each cell) were introduced in case *PT0-bedrock*. The overall results after 300 years, expressed in terms of where the particles left the saturated zone, i.e. to which other model compartments or boundaries they went, are summarised in Table 4-1. The dominating sink is the combined overland compartment/unsaturated zone. It is not possible to separate these two sinks.

An illustration of the numbers in Table 4-1 is shown in Figure 4-1. The figure shows the position of each particle where it has left the saturated zone and moved to a specific sink. The different sinks are marked with different colours. The green dots represent the particles that moved to the combined Overland flow-Unsaturated zone sink. Since the majority of the green dots are situated in the lakes and close to water courses, i.e. in water-saturated areas, it is reasonable to assume that the majority of the 37% registered in this sink moved to the Overland flow compartment.

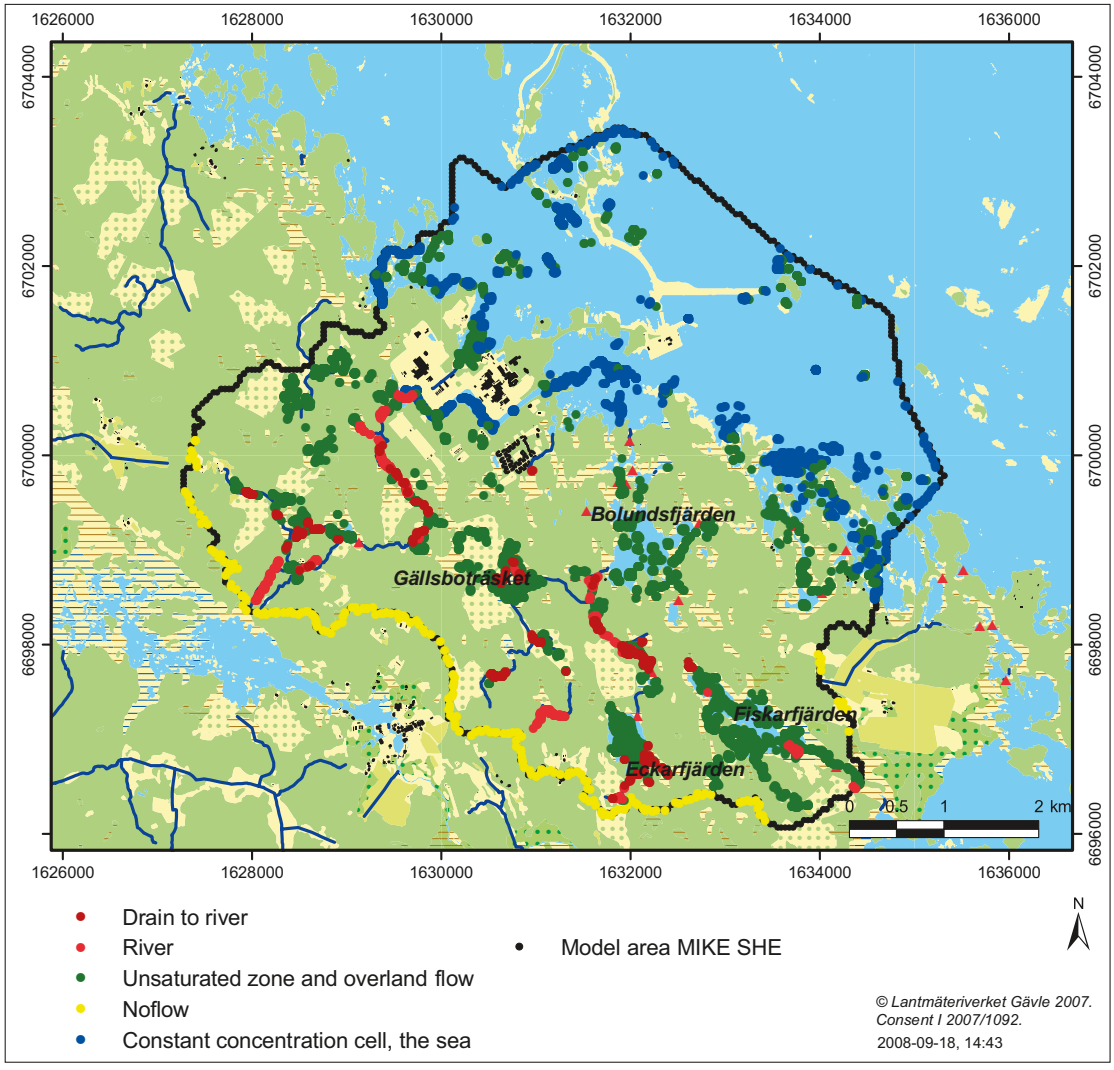

Figure 4-1. *Positions of the particles when they left the saturated zone. The type of sink each particle moved to is marked in the figure.*

Table 4-1. Distribution of particles on different sinks after 300 years in the *PT0-bedrock* simulation.

Sink	Number of particles	%
Particles removed to OL-UZ*	8,571	37
Particles removed directly to streams	907	4
Particles removed by drain to streams	798	3
Particles gone to the sea	3,514	16
Particles left in model	9,077	40
Sum	22,867	100

*OL-UZ is the combined Overland flow-Unsaturated zone sink.

Figure 4-1 above is also an illustration of the discharge areas of particles in the uppermost calculation layer. The majority of the particles discharges in lakes and stream valleys. Among the particles that move to the sea, the majority discharges in the littoral zone. Figures 4-2 to 4-5 shows the accumulated particle count in each cell in calculation layer 2, 4, 6 and 9. Calculation layer 2 contains the lower part of the Quaternary deposits. The lower level of calculation layer 4 is placed at 30 m.b.s.l., the lower level of calculation layer 6 is at 70 m.b.s.l., and that of calculation layer 9 is at 130 m.b.s.l. If the accumulated particle count is zero no particles have moved through that cell; thus, the figures give an illustration of the discharge and recharge areas in each layer.

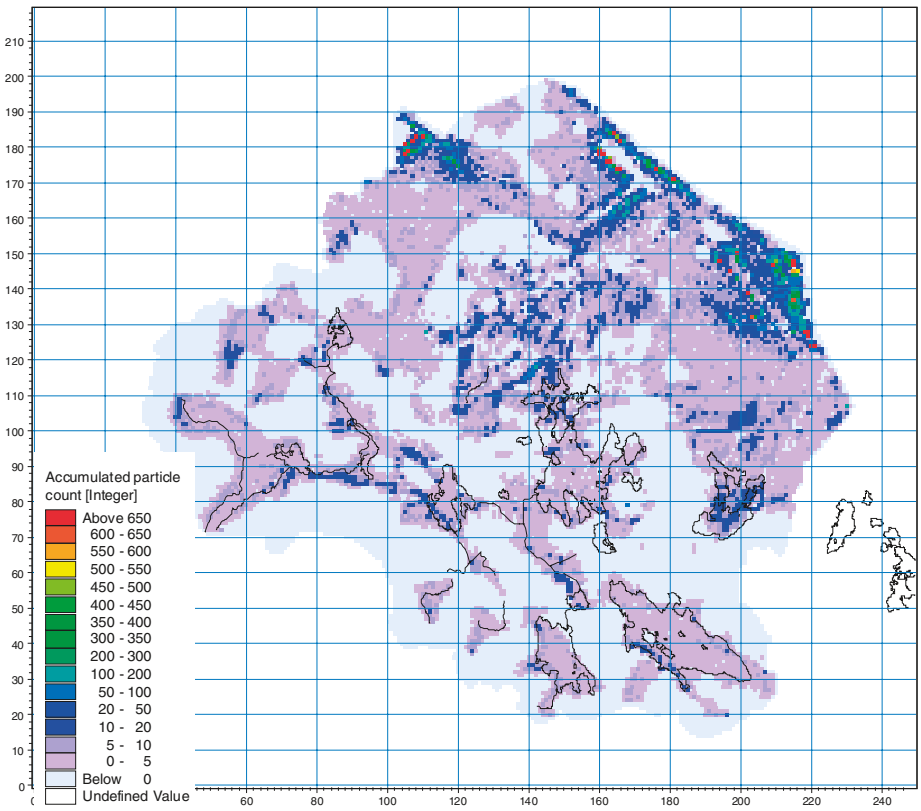

Figure 4-2. *Accumulated particle count after 300 years in layer 9 (130 m.b.s.l.). As an orientation, the shorelines of the lakes and the water courses are marked in the figure.*

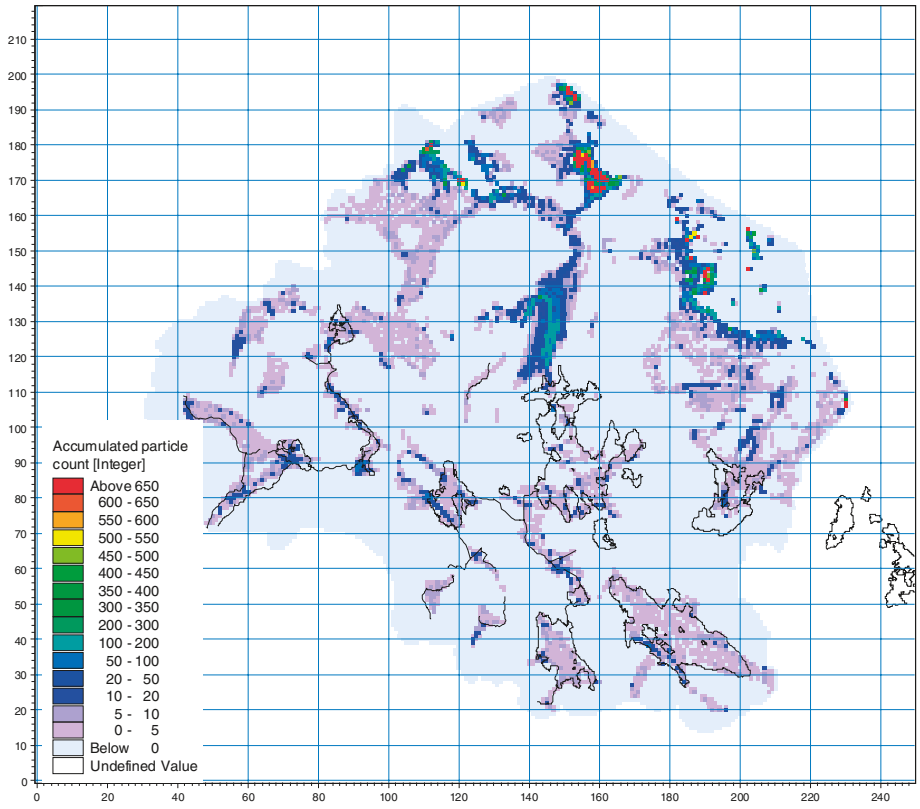

Figure 4-3. *Accumulated particle count after 300 years in layer 6 (70 m.b.s.l.). As an orientation, the shorelines of the lakes and the water courses are marked in the figure.*

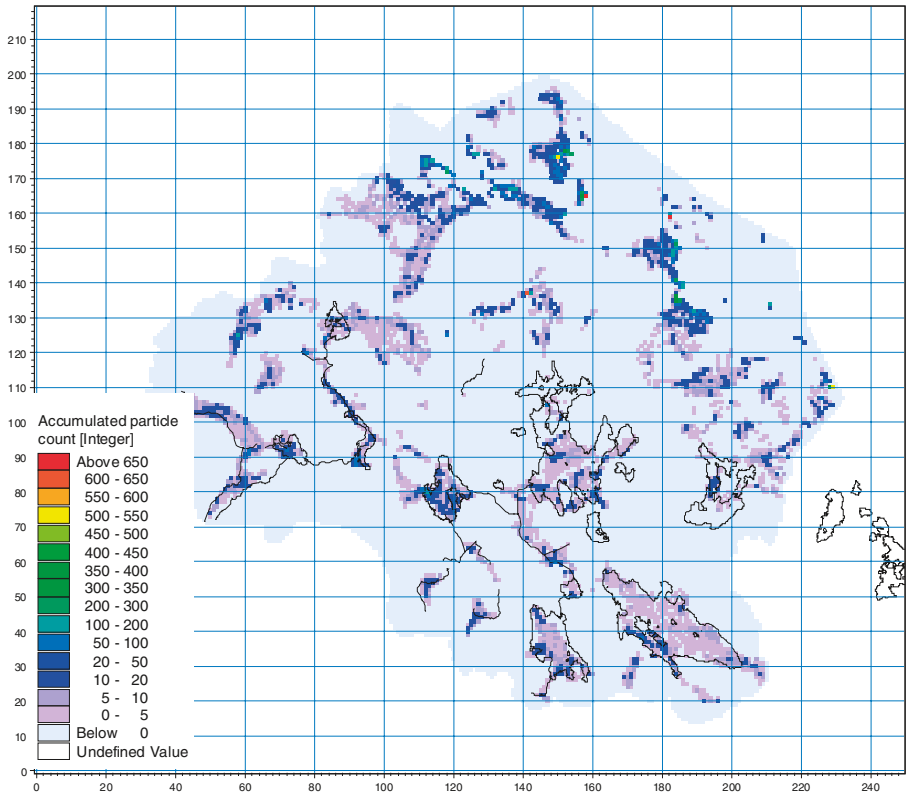

Figure 4-4. *Accumulated particle count after 300 years in layer 4 (30 m.b.s.l.). As an orientation, the shorelines of the lakes and the water courses are marked in the figure.*

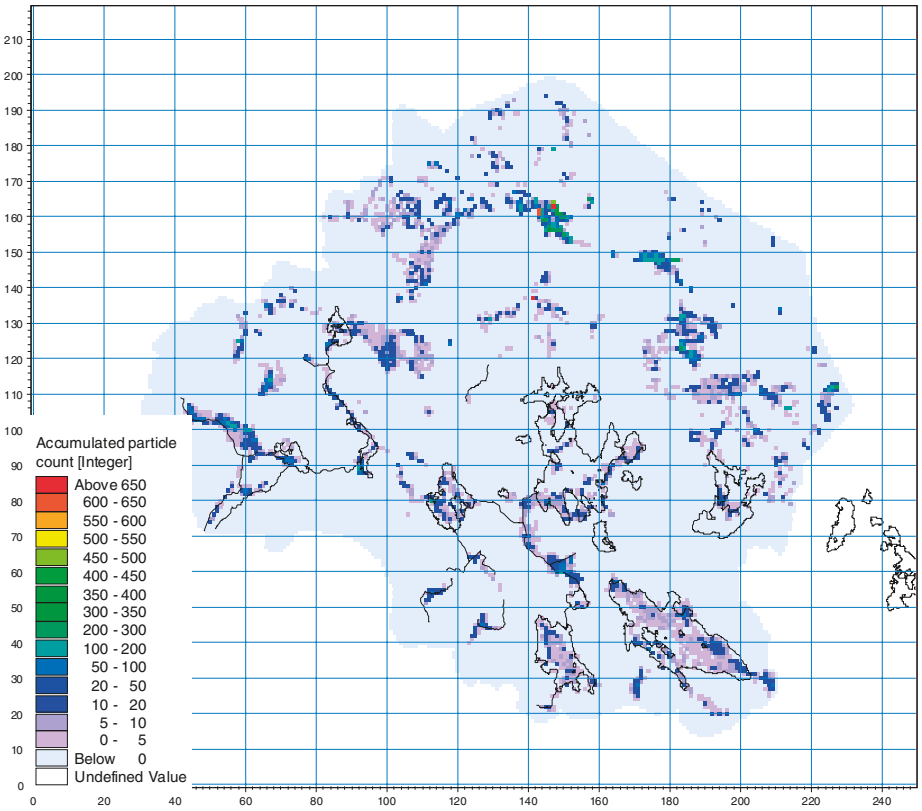

Figure 4-5. *Accumulated particle count after 300 years in layer 2 (in the Quaternary deposits). As an orientation, the shorelines of the lakes and the water courses are marked in the figure.*

Studying the accumulated particle count from layer 9 to layer 2, it is possible to see how the particles move towards high conductive areas in the bedrock and discharge areas at the surface. There is a clear concentration of particles in the horizontal sheet joints represented in layer 6, this high-conductive area short-circuits the water flow and many particles move out to the sea in this layer. Figure 4-5 shows the accumulated particle count in layer 2, i.e. the discharge areas from the bedrock to the Quaternary deposits. Lakes, stream valleys and low bathymetric points at the sea bottom are the main discharge areas from the bedrock to the Quaternary deposits and sea bottom sediments.

4.1.2 Advection-dispersion modelling

For the advection-dispersion transport modelling with a bedrock source, results are shown for the simulation case *AD3*. Figures 4-6 to 4-8 show *AD3* simulation results for three different layers at three different times. Two of the layers are bedrock layers and one is a Quaternary deposit layer. The figures show concentrations in the model layers after 2 months, 2 years and 10 years simulation time. In all Figures 4-6 to 4-8, the scale of the solute concentration is the same.

Figure 4-6 shows concentration plots from a bedrock layer at a level of approximately 130 m.b.s.l. (layer L9). The layer is situated just above the layer of the solute source. The figure illustrates that the solute concentration is high at the beginning of the simulation, but then decreases rather fast as the solute mass is transported away from the layer. It is also seen that the concentration initially is high in connection with the more high-conductive zones in the bedrock. As time goes, the concentration in the high-conductive zones decreases and instead the concentration is higher in connection to the sea.

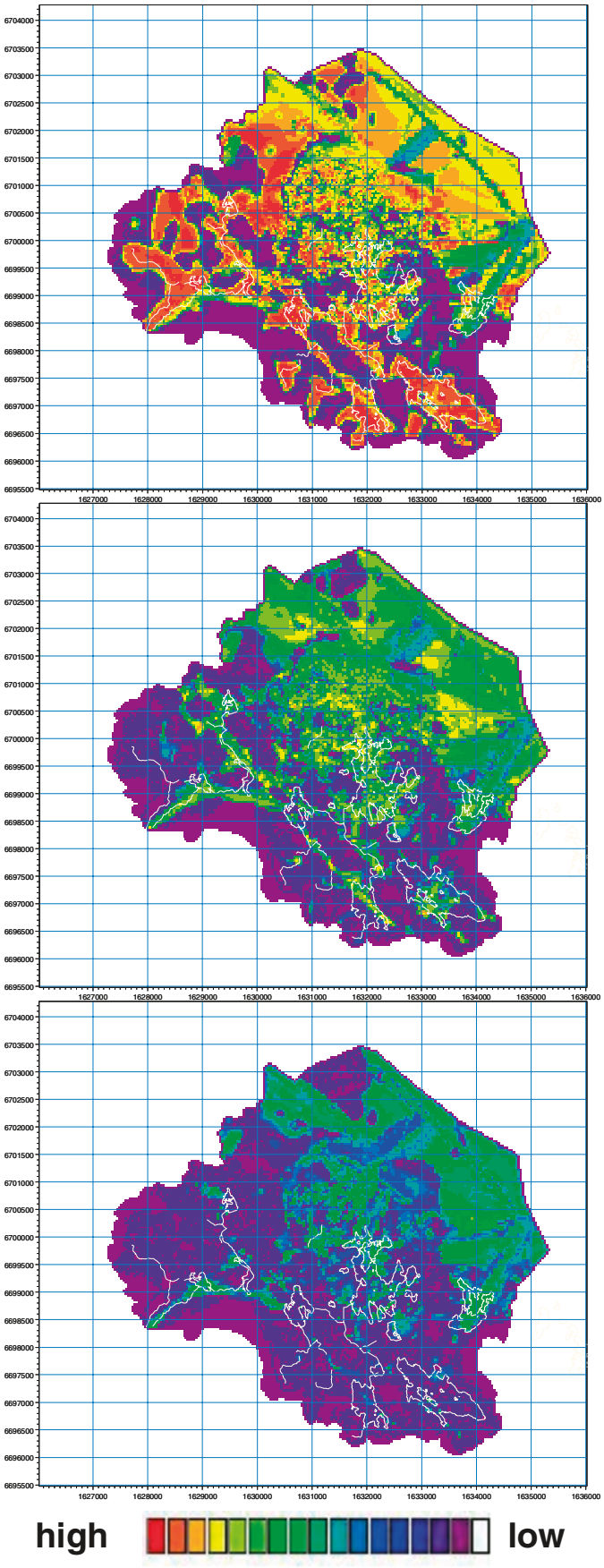

Figure 4-6. *Concentration in the bedrock at approximately 130 m.b.s.l. in an AD simulation with a pulse source in the bedrock. The uppermost figure is after 2 months, the middle figure after 2 years and the bottom figure after 10 years. As an orientation, the shorelines of the lakes and the water courses are marked in the figure.*

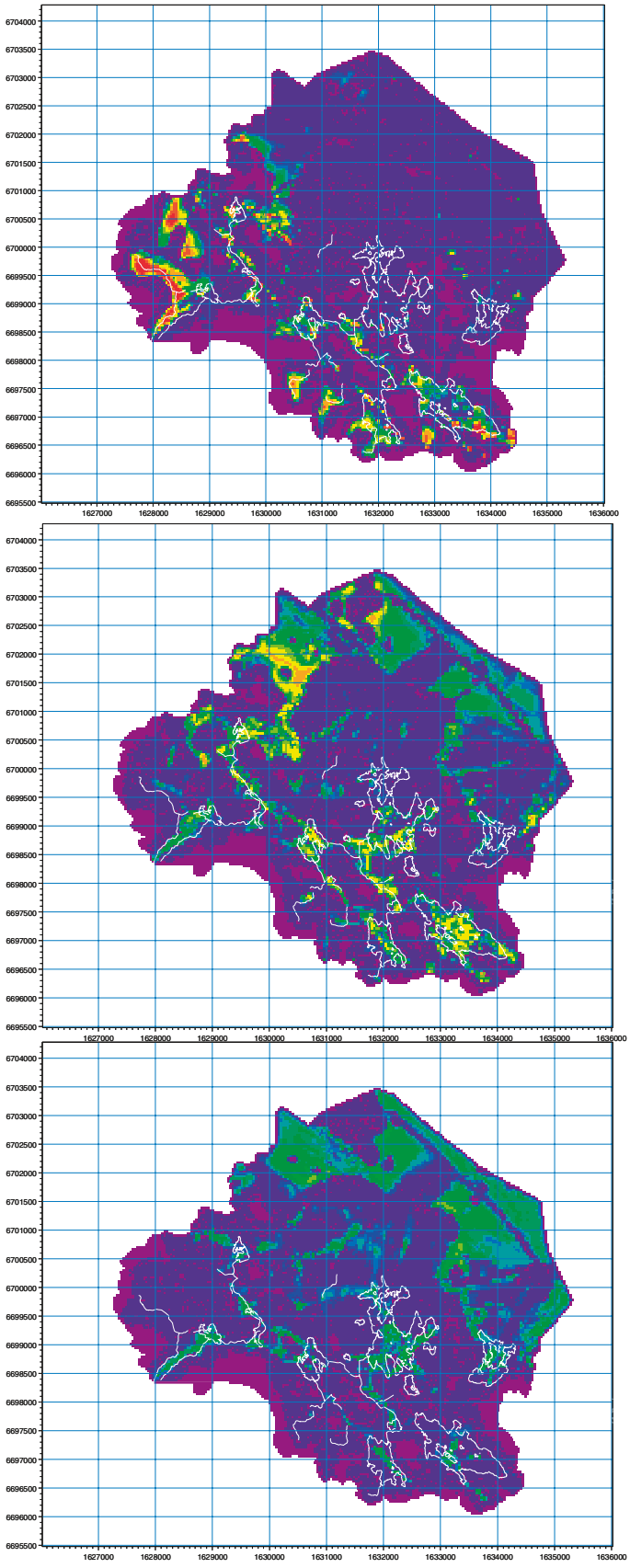

Figure 4-7. *Concentration in the bedrock at approximately 70 m.b.s.l. in an AD simulation with a pulse source in the bedrock. The uppermost figure is after 2 months, the middle figure after 2 years and the bottom figure after 10 years. As an orientation, the shorelines of the lakes and the water courses are marked in the figure.*

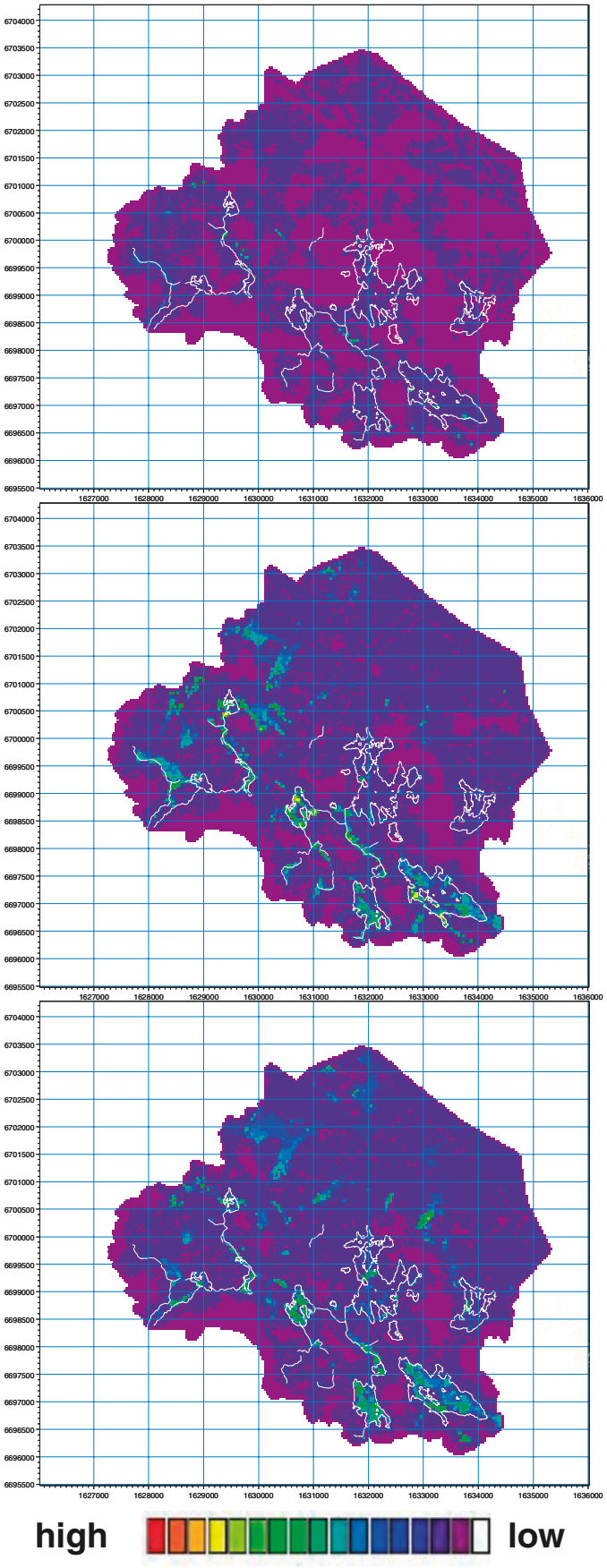

Figure 4-8. *Concentration in calculation layer 2 in the Quaternary deposits in an AD simulation with a pulse source in the bottom layer. The uppermost figure is after 2 months, the middle figure after 2 years and the bottom figure after 10 years. As an orientation, the shorelines of the lakes and the water courses are marked in the figure.*

Figure 4-7 shows concentration plots from the bedrock layer at approximately 70 m.b.s.l. (layer L6) containing areas with high horizontal hydraulic conductivities in the northern part of the model area (close to the sea). The figure illustrates that the concentration after 2 months is high only in the fractured zones under the lakes and watercourses. After 2 years the concentrations in the most high-conductive zones have decreased, whereas in other areas they have increased. After 10 years the concentration pattern is almost the same as for layer L9, i.e. the remaining solute is concentrated to the sea area and under the lakes.

Figure 4-8 shows concentration plots from calculation layer 2, which is the lower layer in the Quaternary deposits. The figure shows that after 2 months almost no solute has yet reached the Quaternary deposits. After 2 years it is seen that the solute has reached the upper part of the model. The figure shows that the solute is mainly transported upwards through the deformation zones that are connected to the lakes and water courses. This is further established in the plot showing concentrations after 10 years, where it is also seen that the lake areas are solute recipients.

In order to confirm that the patterns illustrated in Figures 4-6 to 4-8 are not results of seasonal flow patterns depending on the fact that the solute source was added for one month only, a transport simulation with a constant bedrock source was made, referred to as *AD3-constant*. All other parameters are exactly the same as for *AD3*. Figure 4-9 illustrates concentration plots in bedrock layer L6 for the simulation with a constant pollution source. Concentration plots are shown for simulation times 2 months, 2 years and 10 years. The figure should be compared to Figure 4-7. It is shown that the flow patterns observed in *AD3* are further confirmed.

To further illustrate the solute transport pattern, a vertical profile through the model area is taken. The profile is taken according to Figure 4-10. Figure 4-11 shows the vertical profile at three different time steps. The uppermost figure shows the concentration plume after 2 months simulation time, the middle figure after 2 years, and the bottom figure after 10 years. The white band at a level of about 140 m.b.s.l. is the layer in which the solute source is applied. The signs S and N indicate the orientation of the profile according to Figure 4-10. It is illustrated in the figure that parts of the applied solute mass are transported downwards. The main part is, however, moving upwards, mainly towards the sea and the lake areas.

Figure 4-12 is the same as Figure 4-11, but looking only at the upper part of the model, above the solute source. The figure further shows that the solute transport mainly takes place towards the sea and the lake areas. It also illustrates that some solute is transported rapidly while some is moving slowly.

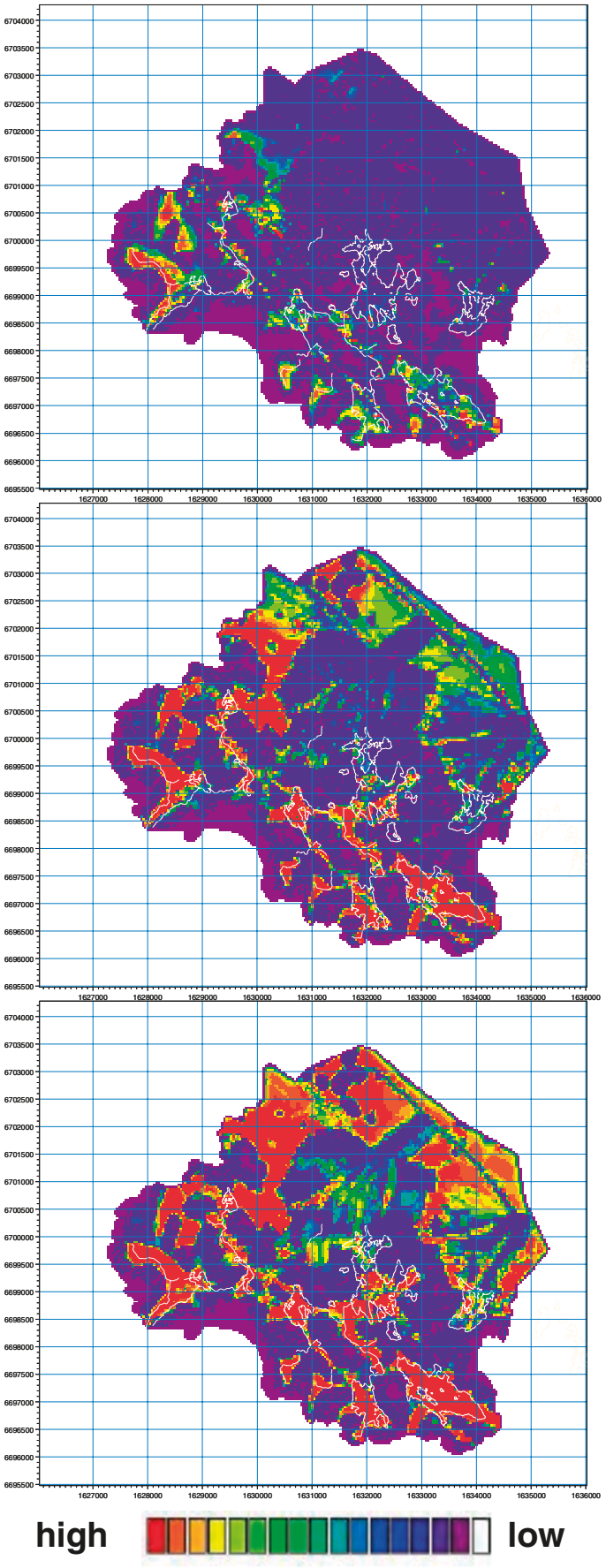

Figure 4-9. *Concentration in the bedrock at approximately 70 m.b.s.l. in an AD simulation with a constant source in the bedrock. The uppermost figure is after 2 months, the middle figure after 2 years and the bottom figure after 10 years. As an orientation, the shorelines of the lakes and the water courses are marked in the figure.*

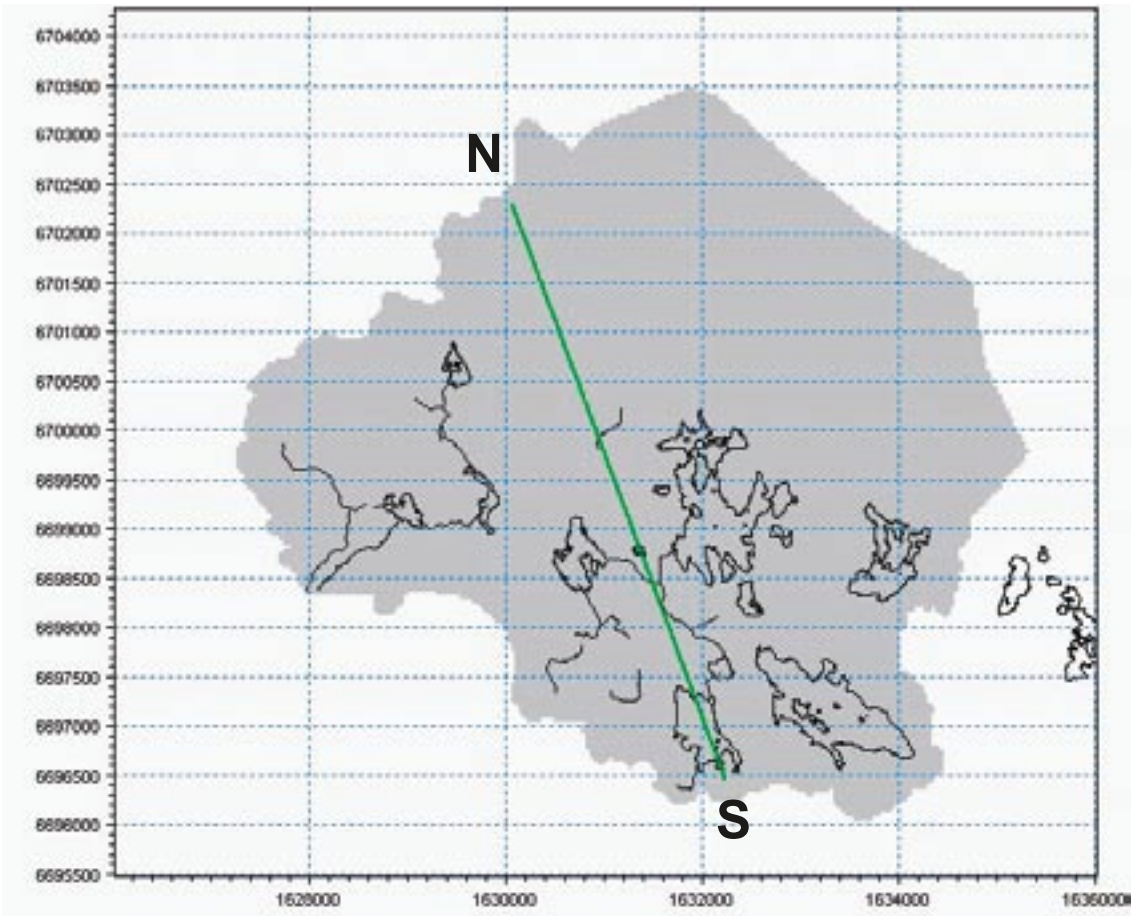

Figure 4-10. *The green line indicates the position of the vertical profile for which transport results are illustrated. The letters S and N indicates south and north direction, respectively.*

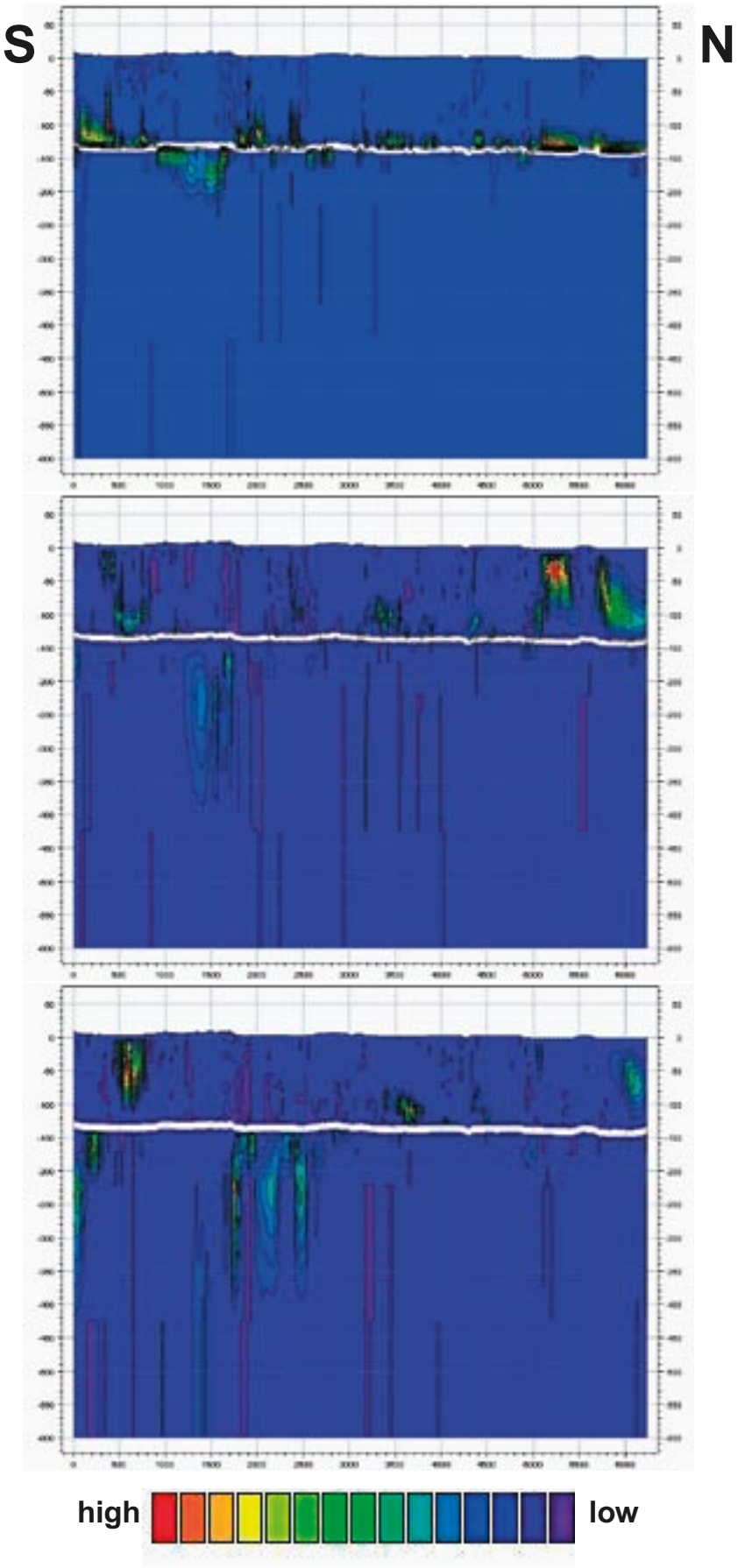

Figure 4-11. *Vertical profile through the model area in the south-north direction. The upper figure shows the concentration pattern after 2 months, the middle after 2 years and the bottom figure after 10 years.*

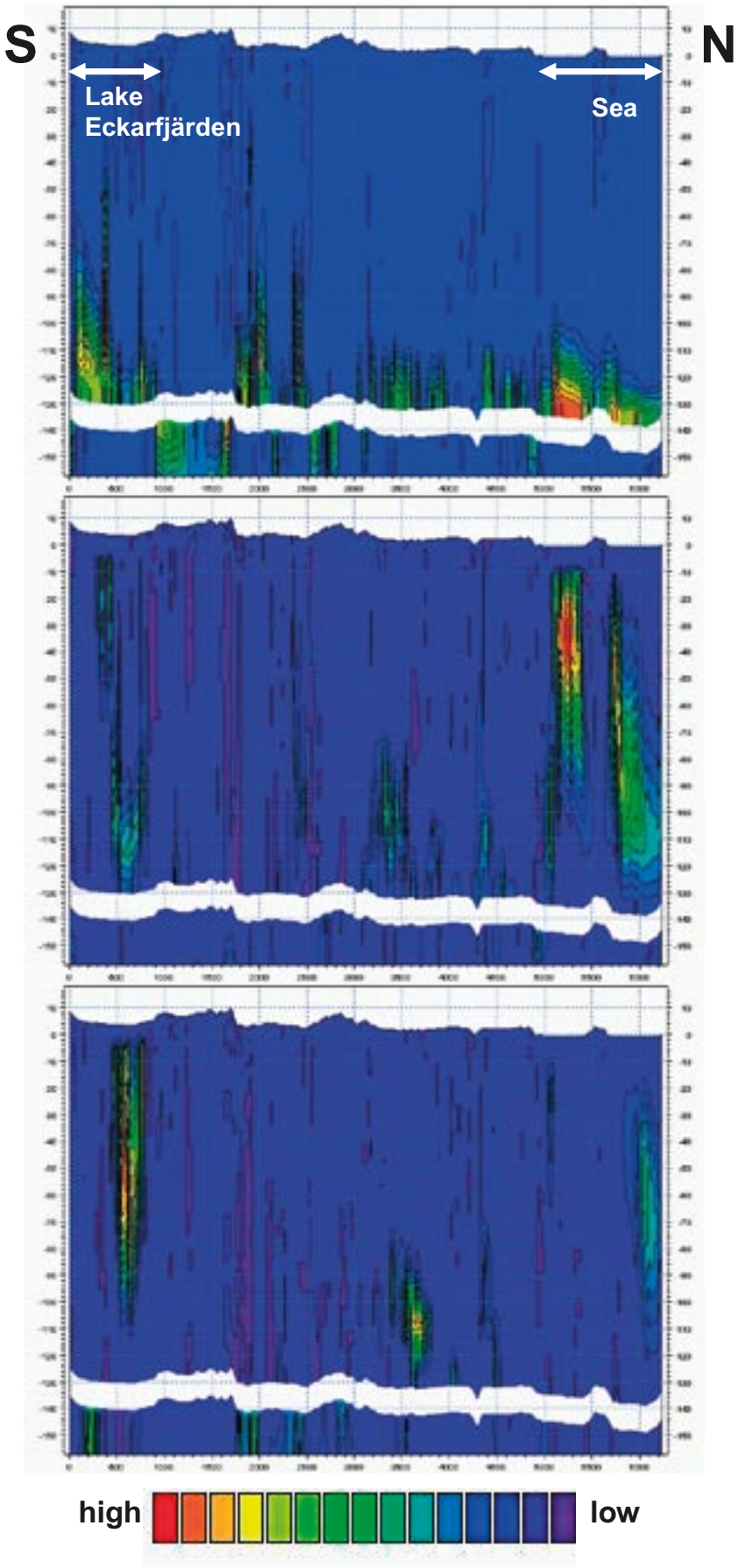

Figure 4-12. *Vertical profile for the uppermost 150 m through the model area in the south-north direction. The upper figure shows the concentration pattern after 2 months, the middle after 2 years and the bottom figure after 10 years.*

Since the solute transport mainly takes place towards the sea and lake areas, a more detailed profile for Lake Eckarfjärden is taken to illustrate the transport directions under the lake. The position of the profile is illustrated in Figure 4-13. Figure 4-14 shows the results for the upper 20 m of the profile at two different times, the upper figure after 1 year and the lower figure after 15 years. In the figures, it is seen that the solute transport towards the lake area initially is vertical. Once the solute reaches the upper layers, consisting of lake sediments, the transport is slowed down and after 15 years it is seen that the transport is faster towards the sides of the lake than in the middle of the lake area.

In parts of the model area, zones with high horizontal hydraulic conductivity in the bedrock are located. In the model, one layer with such high-conductive areas is represented between approximately 60 and 70 m.b.s.l., see Figure 4-15, and another in the interval 100–110 m.b.s.l. Within these areas, the solute transport is mainly directed horizontally towards the sea, which is illustrated in Figure 4-16. Figure 4-17 shows the position of the profile shown in Figure 4-16.

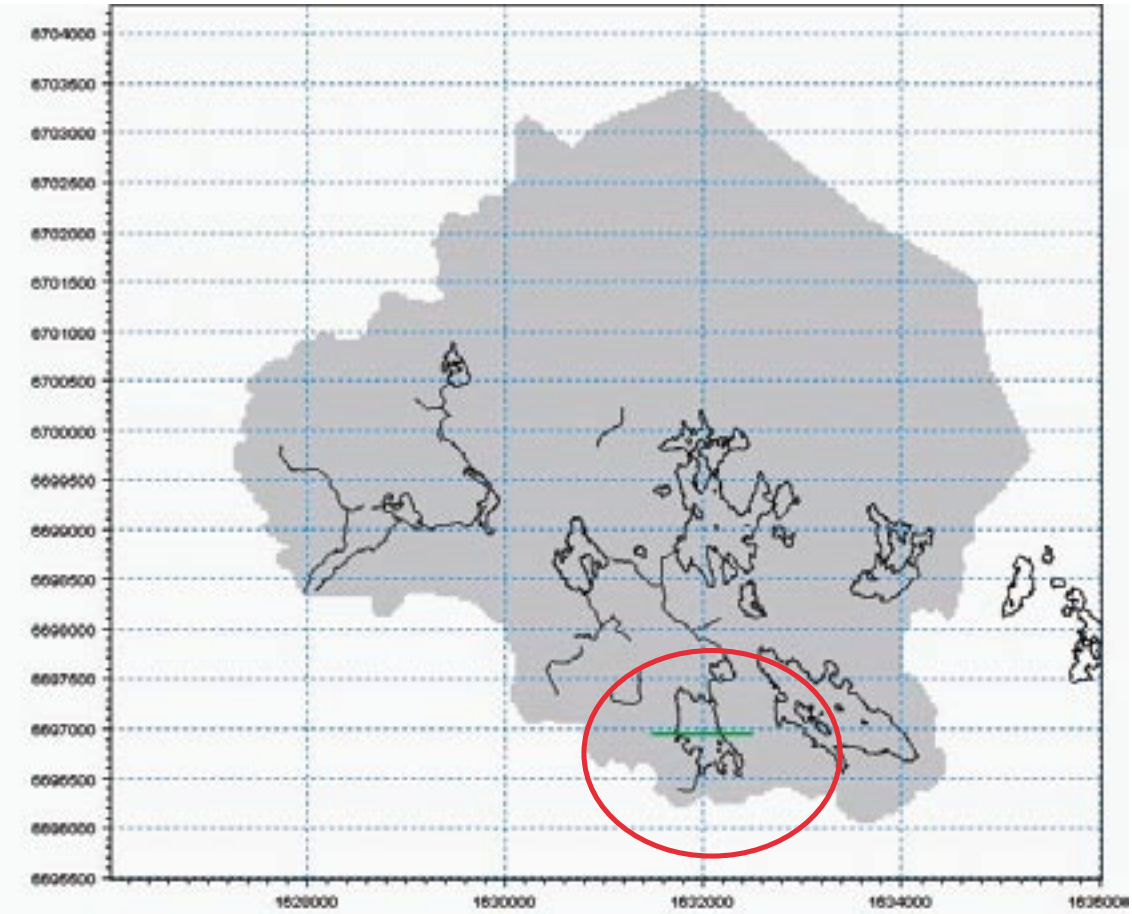

Figure 4-13. *The green line indicates the position of the vertical profile for which transport results are illustrated in Figure 4-14.*

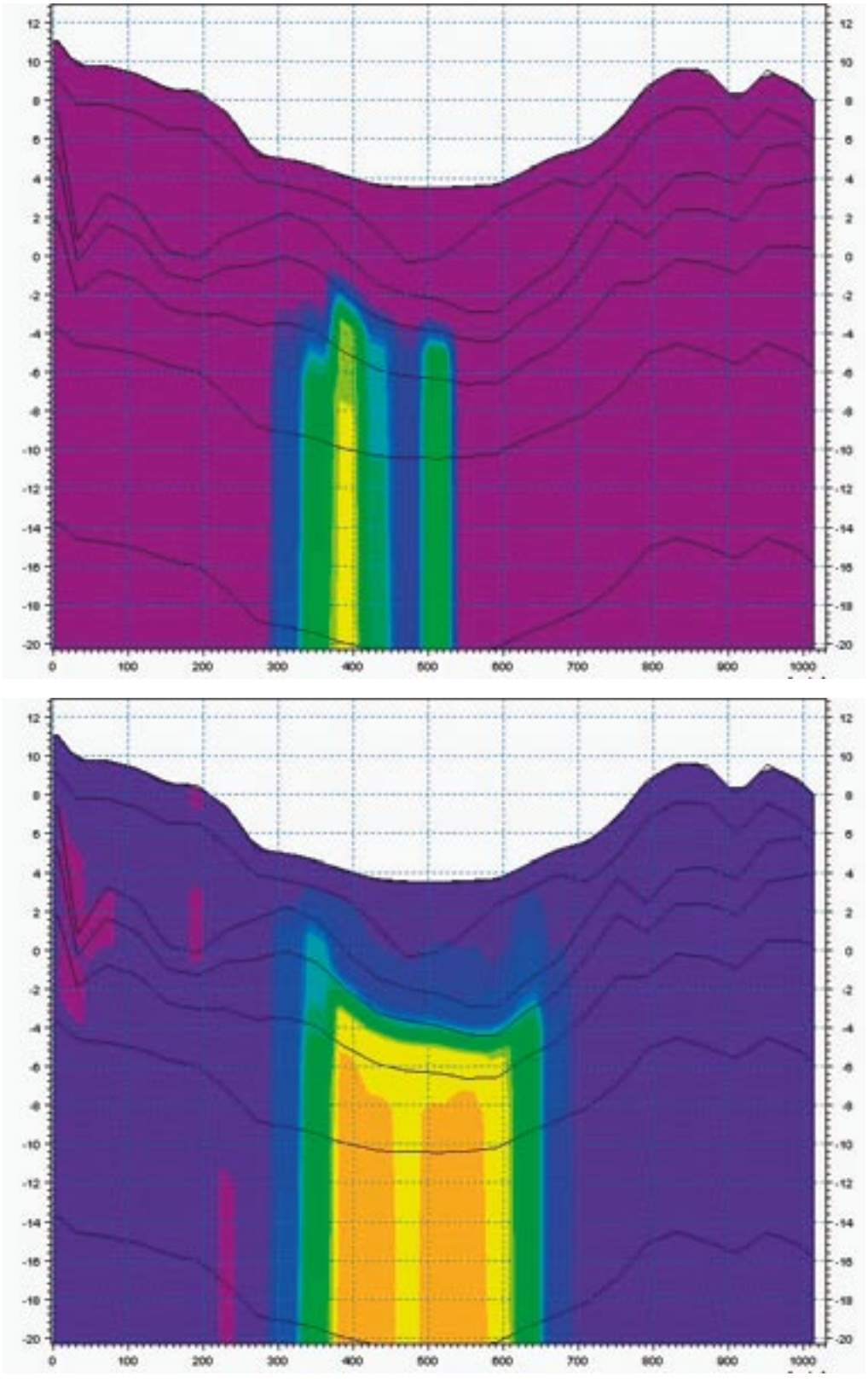

Figure 4-14. *Vertical profile through Lake Eckarfjärden. The upper figure shows the solute concentration for the upper 20 meters after 1 month and the lower figure after 15 years of simulation.*

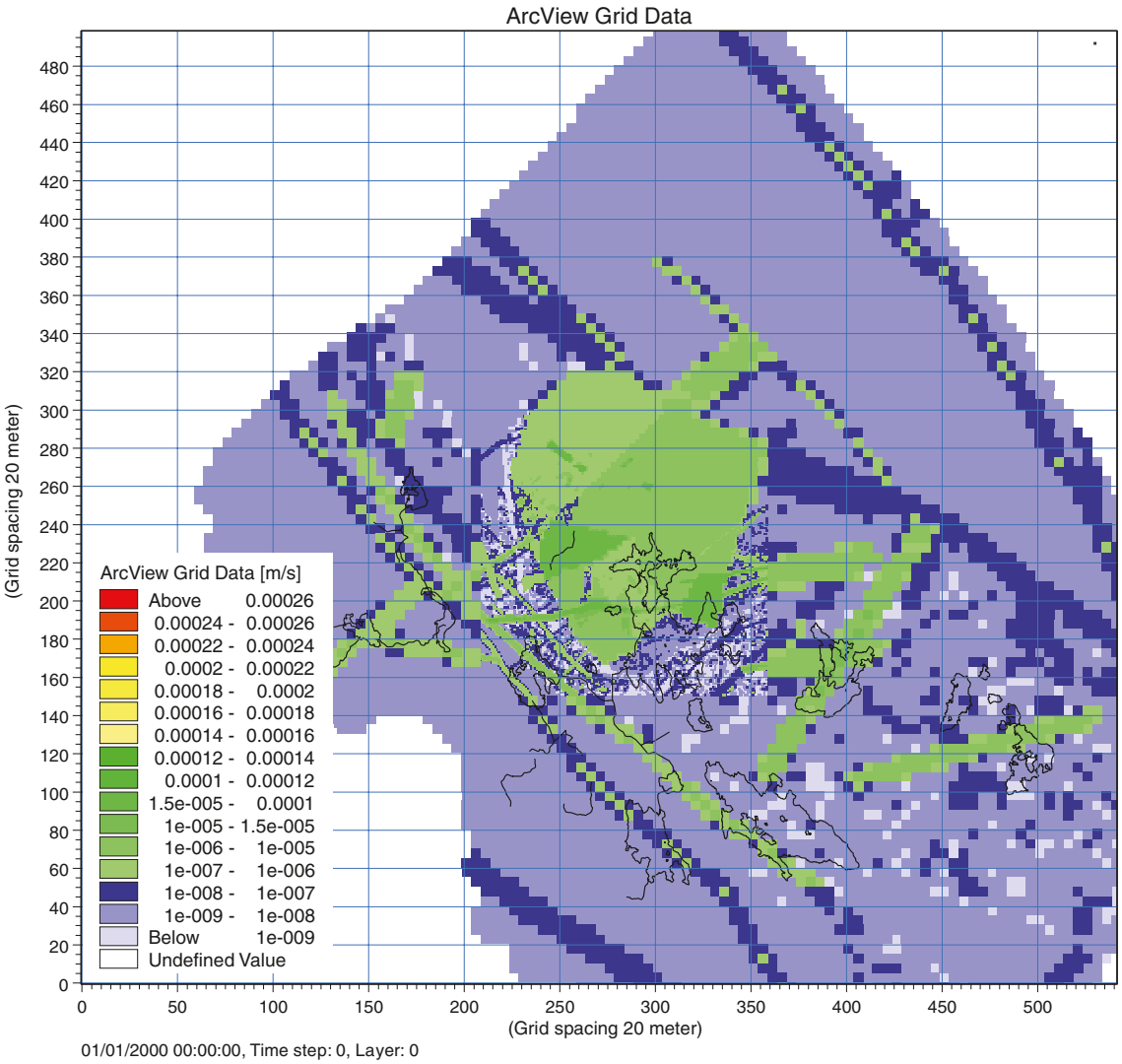

Figure 4-15. *Horizontal hydraulic conductivity (m/s) at 60–70 m.b.s.l. in the model. The lakes and the streams in the area are marked in the figure.*

In Figure 4-16 the uppermost figure shows the concentration plume after one year of simulation. The solute is still moving mainly in the vertical direction, but at the depth of the lower layer with higher horizontal conductivity zones, located at approximately 100 m.b.s.l., the solute is transported mainly in the horizontal direction. This is illustrated by the solute concentration after 10, 20 and 30 years. Parts of the mass are transported to the upper layer with high horizontal conductivity, located at approximately 70 m.b.s.l., and at that level it starts moving towards the sea. This can be seen in the graph showing the results after 20 years in Figure 4-16.

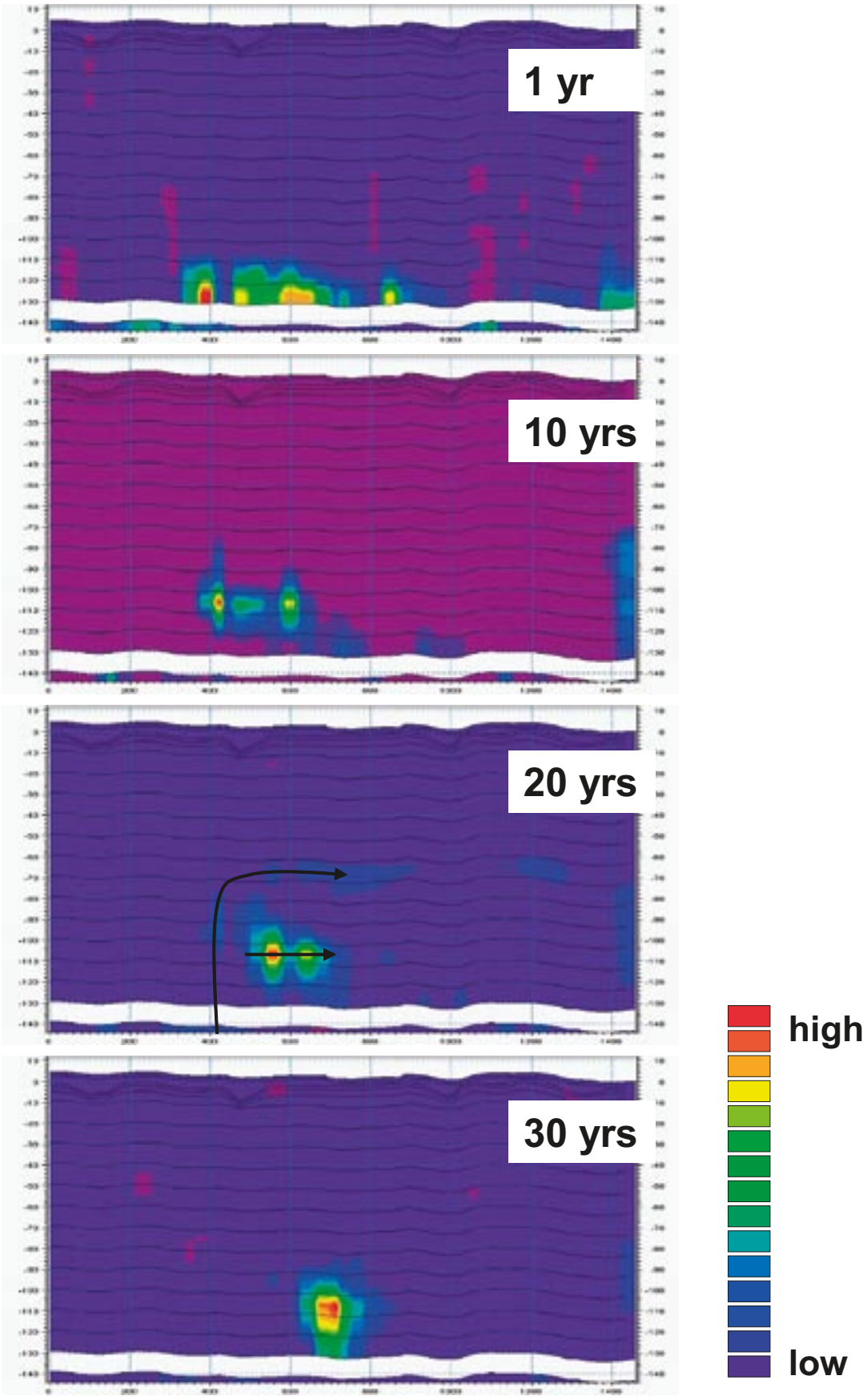

Figure 4-16. *Vertical profile through the uppermost 150 m, with location according to Figure 4-17. The upper figure shows the concentration pattern after 1 year, the second after 10 years, the third after 20 years, and the bottom figure after 30 years of simulation time.*

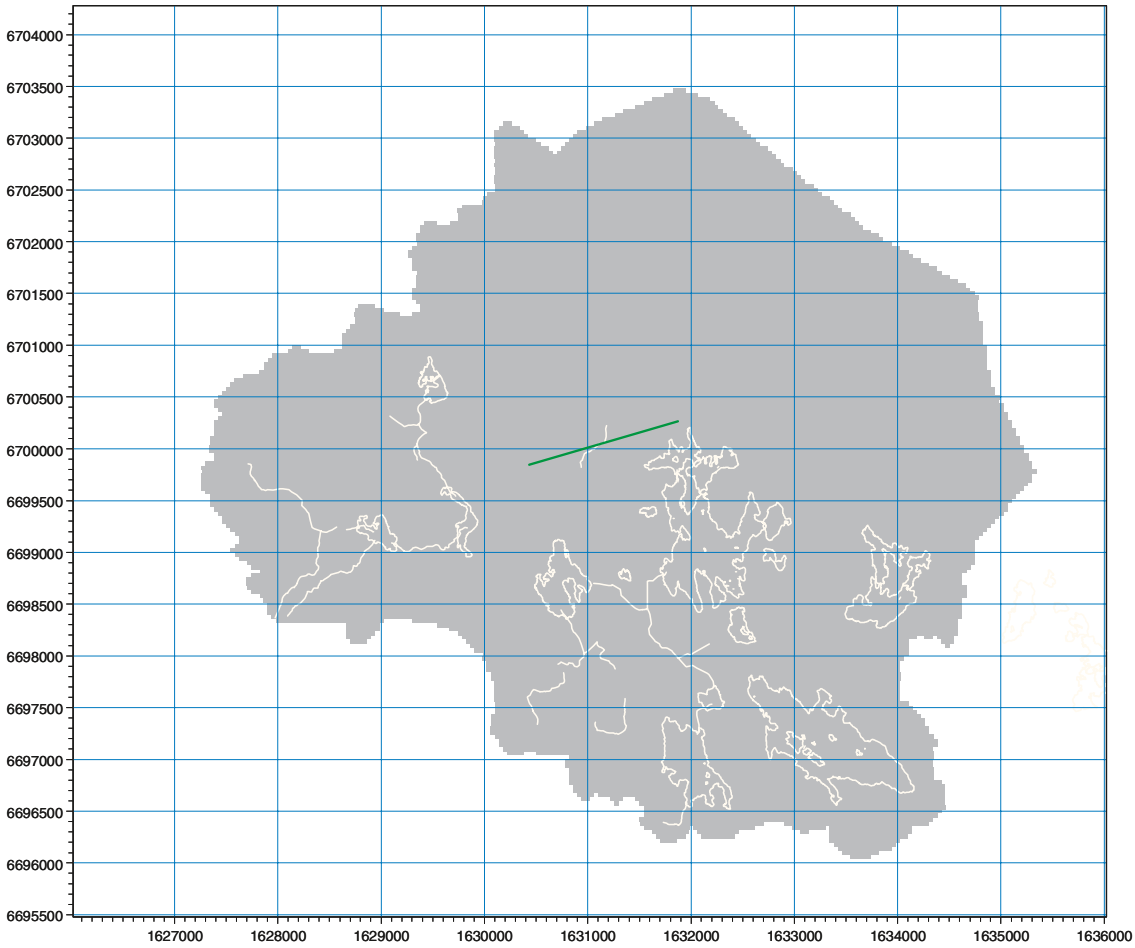

Figure 4-17. *The green line indicates the position of the vertical profile for which transport results are illustrated in Figure 4-16.*

The difference in transport velocity between different parts of the model area is illustrated by examples of time series in Figure 4-19. Figure 4-18 shows the positions of the three points for which time series are illustrated. Cell (58, 87) is situated in a fractured area with a water-course, cell (176, 121) is in the sea close to the shore, and cell (145, 38) is situated in Lake Eckarfjärden.

In Figure 4-19, the uppermost graph shows the times series for the three points in layer 9, i.e. just above the solute source. The figure shows that all three points have concentration peaks only a few weeks after the solute transport has begun. However, although the peak is at almost the same time, the maximum concentration values differ and so do the shapes of the curves. The middle figure shows the concentration curves in the upper bedrock layer, i.e. at approximately 70 m.b.s.l. The differences in peak times and peak concentrations are further enhanced. The lower figure shows the concentration curves in the Quaternary deposits. The difference between fast and slow transport areas is clearly illustrated. The three points were more or less randomly selected, and are not thought to represent areas of extremely fast or slow solute transport.

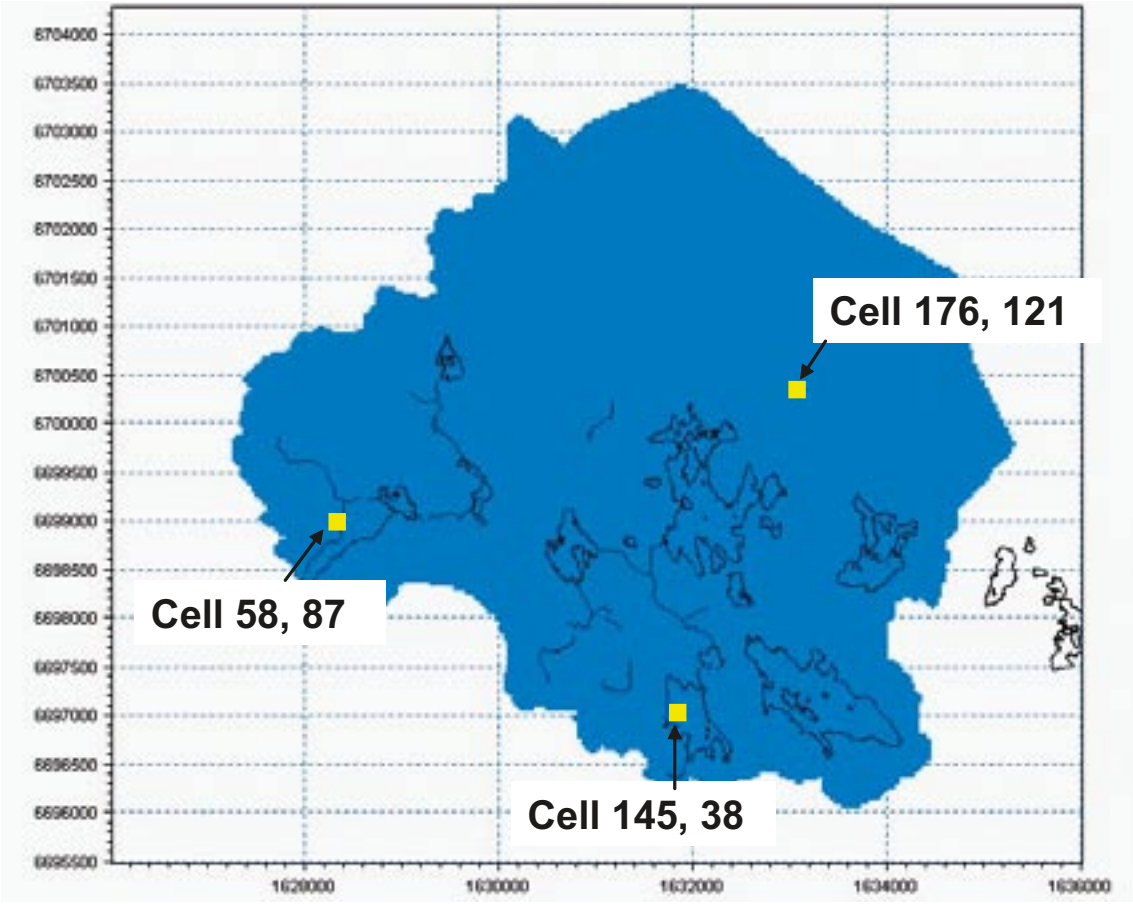

Figure 4-18. *Points for which times series of solute concentrations are illustrated. As an orientation, the shorelines of the lakes and the water courses are marked in the figure.*

Table 4-2 shows a summary of model sinks where the solute leaves the saturated zone. Each sink parameter is compared to the total applied source mass. Results are illustrated after 5 years as well as after 75 years. After 5 years, less than 25% of the solute mass has left the saturated zone. After 75 years, more than 70% has left the saturated zone. The main part of the solute that leaves the saturated zone goes to the unsaturated zone, but a relatively large fraction is transported to the sea.

Table 4-2. Summary of model sinks for case *AD3* after 5 and 75 years of AD-simulation with a source in the bedrock at c. 140 m.b.s.l.

	Cumulative mass in % of total applied source mass	
	After 5 years	After 75 years
Saturated zone storage	75.6	29.4
Saturated zone to unsaturated zone	12.7	29.1
Saturated zone baseflow to streams	2.1	3.2
Saturated zone drain to streams	1.0	2.0
Saturated zone to sea	6.8	24.7
Saturated zone flow to boundary	1.7	10.9
Saturated zone drain to boundary	0.1	0.7
Total source to saturated zone	100.0	100.0

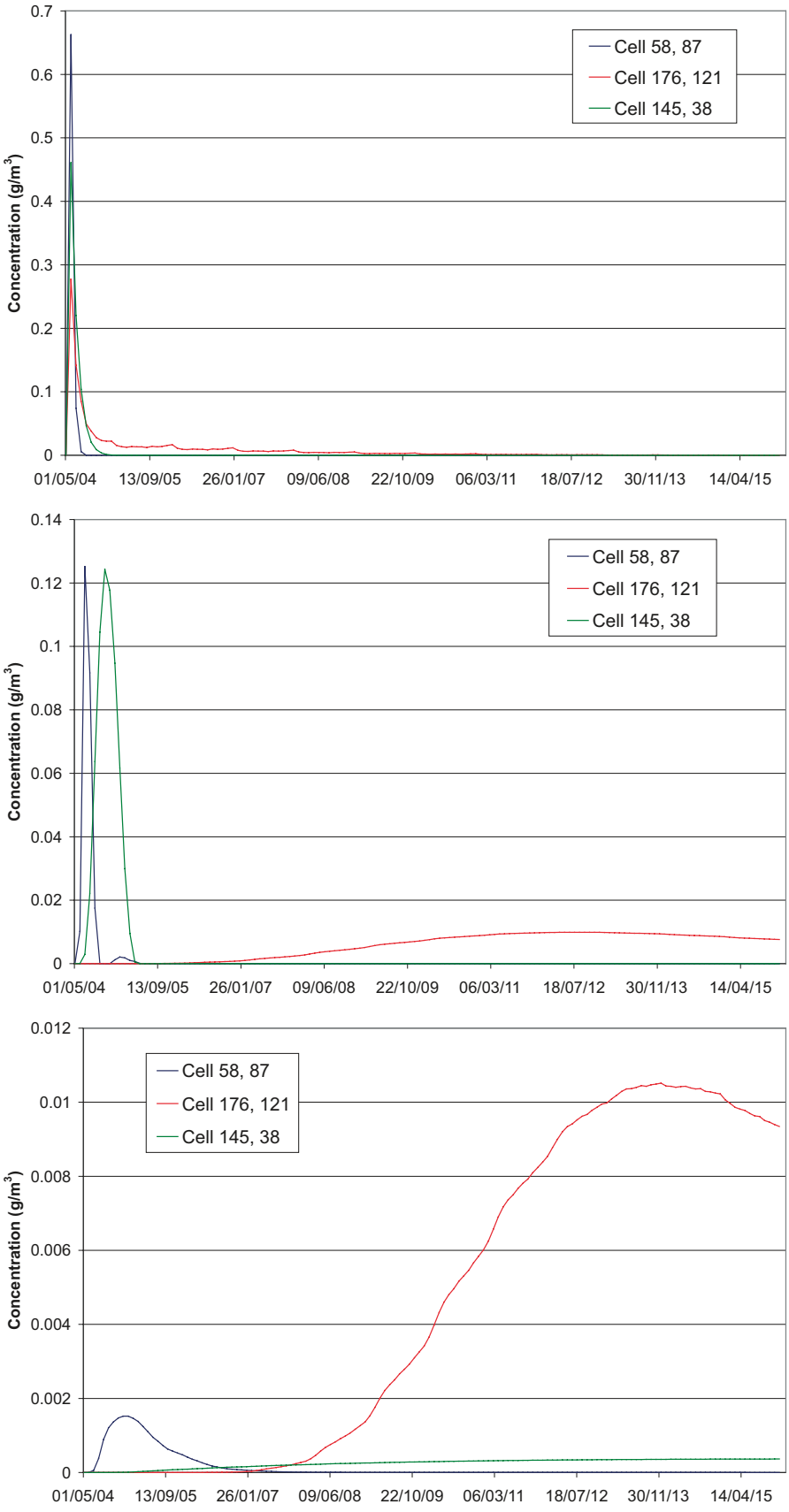

Figure 4-19. *Time series of solute concentrations in three different points. The upper graph is from a bedrock layer at 130 m.b.s.l., the middle figure from a bedrock layer at 70 m.b.s.l., and the lower figure from layer 2 in the Quaternary deposits. Cell (58, 87) is situated in an area with fractured bedrock, cell (176, 121) is in the sea, and cell (145, 38) is situated in Lake Eckarfjärden. Note that the scale on the y-axis is not the same in all figures.*

Evaluation of the continued transport from the compartments in Table 4-2 demands that all flow components are included in the transport modelling. In case *AD13*, all flow components except the river (streams) component are included. Table 4-3 shows a summary of model sinks from the saturated zone in case *AD13*. These results illustrate that the main part of the solute that goes to the unsaturated zone in Table 4-2 is actually going to the overland component. A comparison between Table 4-1 and Table 4-3 shows that the same result is obtained in the PT and AD simulations, i.e. the main part of the solute goes to the unsaturated zone or the overland component. Table 4-3 also confirms the argument discussed in connection to Table 4-1, i.e. that most of the solute is transported to the overland component.

Figure 4-20 illustrates the solute mass in the overland component. The upper graph shows the concentration after 2 months and the lower graph the concentration after 2 years. The figure shows the same patterns as seen in Figure 4-8, i.e. the solute is concentrated to deformation zones in connection to lakes and water courses.

4.2 Infiltration source

4.2.1 Particle tracking

In case *PT0-top*, one particle in each cell was introduced in the uppermost layer of the model. The overall results after 300 years, expressed in terms of where the particles left the saturated zone, i.e. to which other model compartments or boundaries they went, are summarised in Table 4-4. In total, 16,703 particles were introduced to the model. Particles placed in an unsaturated cell or a cell in contact with a river link is directly excluded from the simulation. At the sea, the uppermost calculation layer has a prescribed head describing the sea water level, thus no particles are introduced in the sea. This is the reason to the reduced number of particles introduced in case *PT0-top* compared to *PT0-bedrock*. The dominating sink is the combined Overland flow-Unsaturated zone compartment, 78% of the particles moves to the unsaturated zone or the overland compartment.

Table 4-3. Summary of model sinks for *AD13* with all MIKE SHE components included after 5 years of simulation with a source at c. 140 m.b.s.l.

	Cumulative mass in % of total applied source mass
Saturated zone storage	75.9
Saturated zone to unsaturated zone	1.3
Saturated zone to overland	10.5
Saturated zone baseflow to streams	2.1
Saturated zone drain to streams	1.5
Saturated zone to sea	6.8
Saturated zone flow to boundary	1.7
Saturated zone drain to boundary	0.1
Total source to saturated zone	100.0

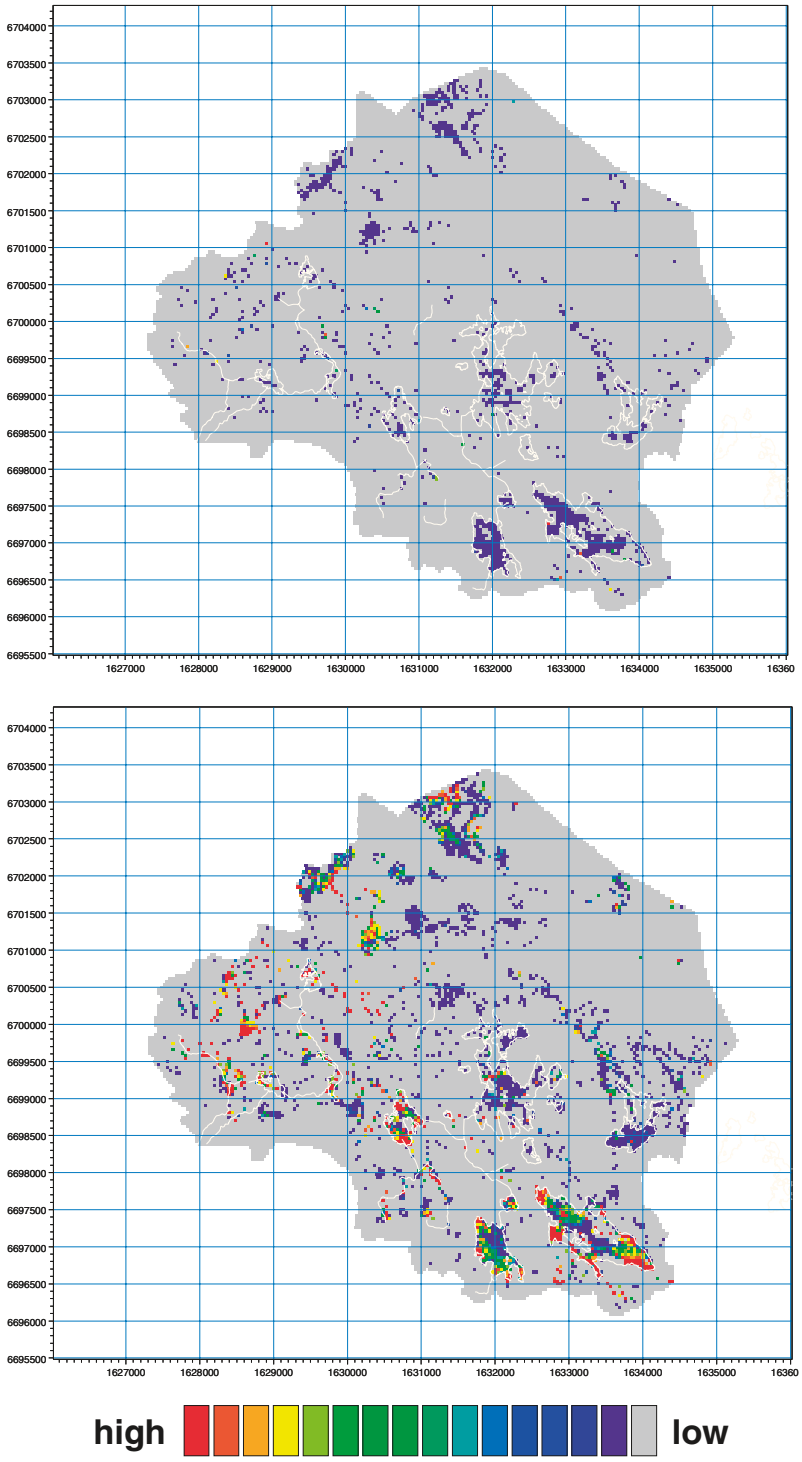

Figure 4-20. *Overland mass/area for simulation case AD13 (top: after 2 months, bottom: after 2 years). As an orientation, the shorelines of the lakes and the water courses are marked in the figure.*

Table 4-4. Distribution of particles on different sinks after 300 years in the *PT0-top* simulation.

Sink	Number of particles	%
Particles removed to OL-UZ*	13,024	78
Particles removed directly to streams	861	5
Particles removed by drain to streams	1,173	7
Particles gone to model boundary	497	3
Particles gone to the sea	601	4
Particles left in model	547	3
Sum	16,703	100

*OL-UZ is the combined Overland flow-Unsaturated zone sink.

The accumulated particle counts in layers 2, 3, 6 and 9 are presented in Figures 4-21 to 4-24. The accumulated particle counts in the lake areas are in most cases zero. Figure 4-22, showing the accumulated particle count in layer 3, illustrates the recharge areas between the Quaternary deposits and the uppermost bedrock. Still, there are no clear patterns of recharge and discharge areas, except from below the lakes. The areas below the lakes have not received any particles. Deeper in the bedrock, in layer 6 and 9 the pattern of the fracture zones is clearer. Many particles reach layer 6 and move towards the areas with high horizontal conductivity. Only a few percent of the particles reach calculation layer 9. Fractures and deformation zones with a gradient directed downwards receive in total 966 particles.

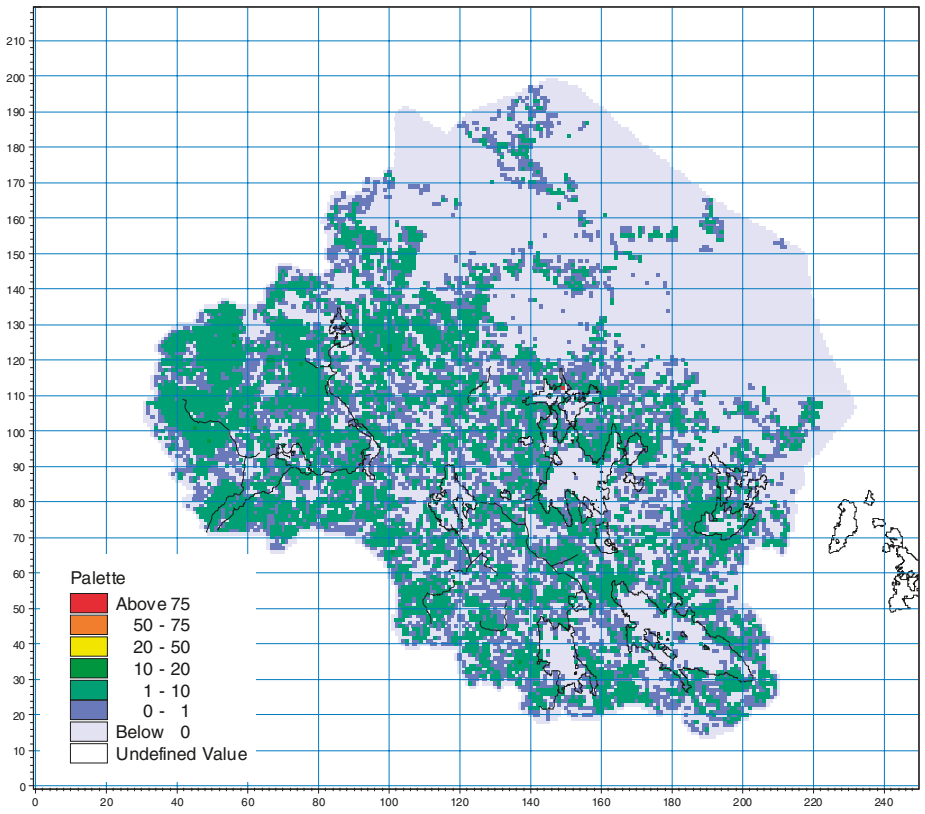

Figure 4-21. *Accumulated particle count after 300 years in layer 2, the lower layer in the Quaternary deposits. Locations of streams and lake shorelines are also marked in the figure.*

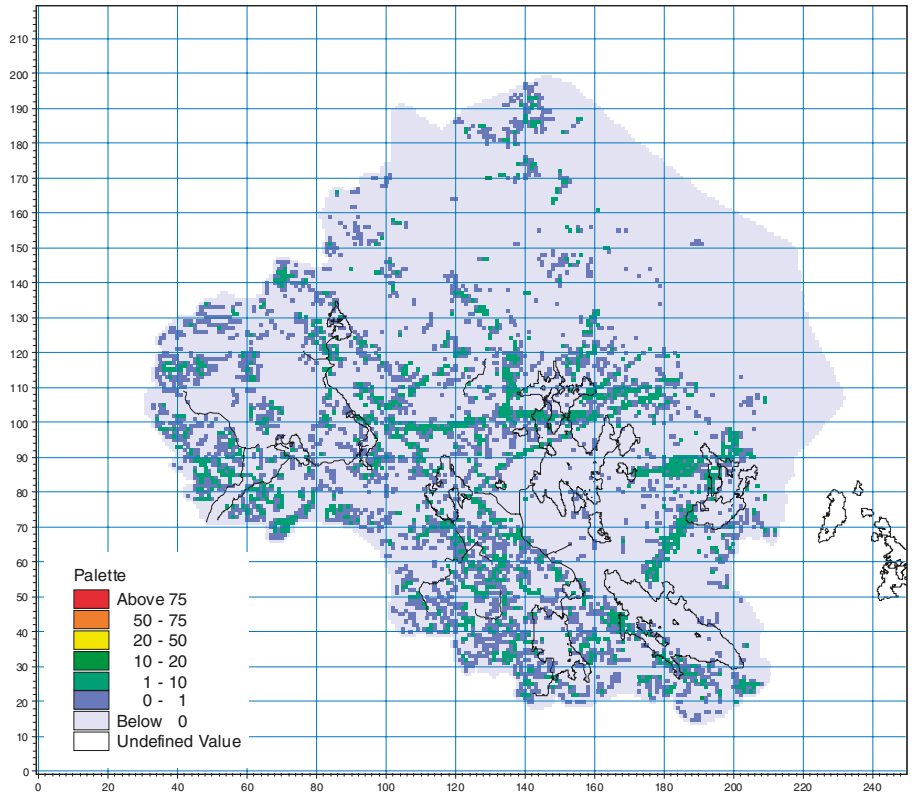

Figure 4-22. *Accumulated particle count after 300 years in layer 3, the uppermost layer of the bedrock (at approximately 10 m.b.s.l.). Locations of streams and lake shorelines are also marked in the figure.*

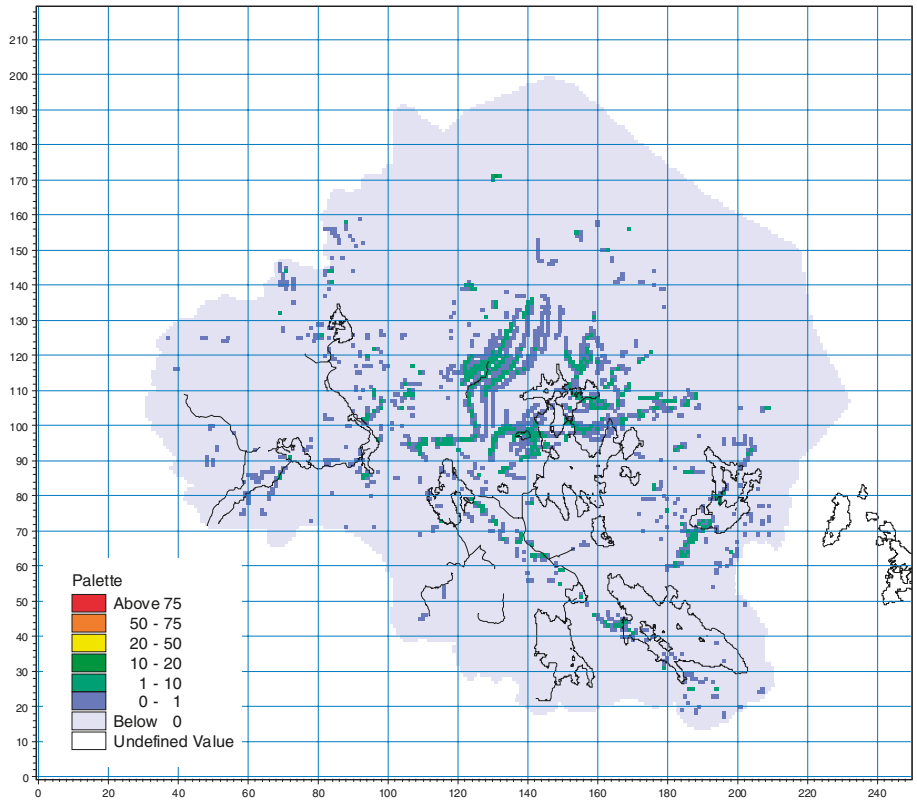

Figure 4-23. *Accumulated particle count after 300 years in layer 6 at c. 70 m.b.s.l. In this layer, the accumulated particles clearly illustrate where the deformation zones with high horizontal conductivities are situated. Locations of streams and lake shorelines are also marked in the figure.*

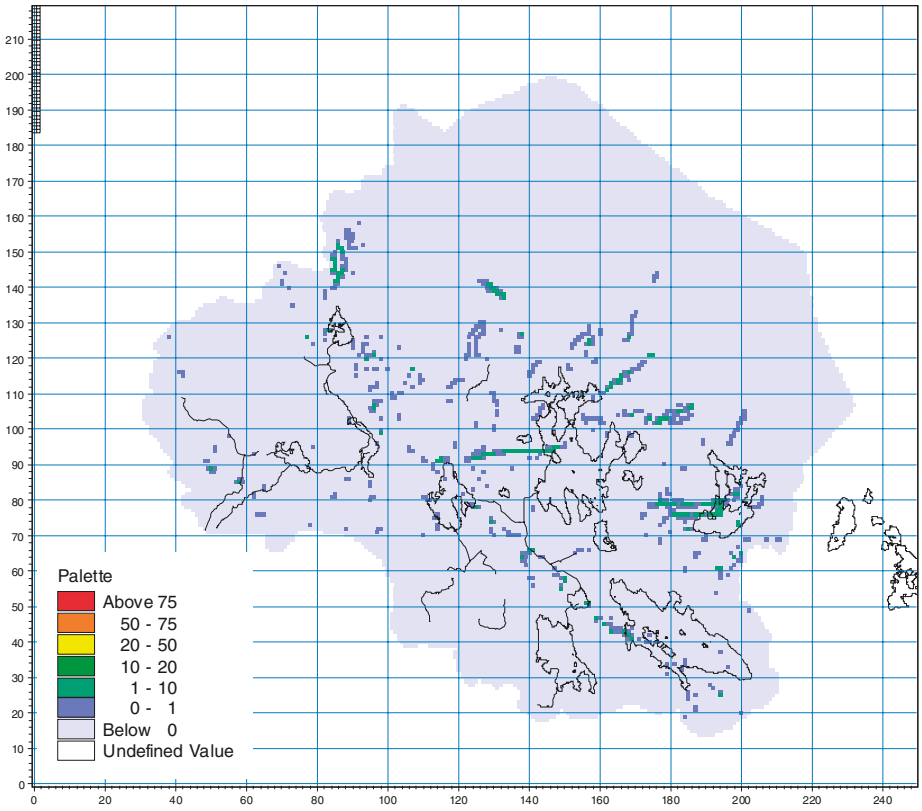

Figure 4-24. *Accumulated particle count after 300 years in layer 9 at c. 130 m.b.s.l. Locations of streams and lake shorelines are also marked in the figure.*

4.2.2 Advection-dispersion modelling

For the advection-dispersion transport modelling with an infiltration source, results are shown for the simulation case *AD10*. Figure 4-25 shows simulation results for three different layers after one year. The upper figure is from the Quaternary deposits. While the source is an infiltration source, discharge areas with no infiltration have no external source (e.g. at the lakes). Areas with higher amount of infiltration, being recharge areas over the whole year, consequently act as larger infiltration sources.

The middle figure is from a bedrock layer at 70 m.b.s.l. and indicates this pattern even clearer, with the solute concentration concentrated to recharge areas. Furthermore, in the figure it may be noted that because of the sheet joints that are located in bedrock layers further up under Lake Bolundsfjärden, the solute is transported horizontally towards the sea.

The lower figure, which is from a lower bedrock layer at 130 m.b.s.l., further indicates that the solute concentration is mainly concentrated to recharge areas. Furthermore, both in the middle and in the lower figure, the effect of the regional deformation zone in connection to Lake Eckarfjärden is clearly illustrated. The low concentrations in the deformation zones indicate that they are discharge areas from the deeper bedrock.

The vertical profile in Figure 4-10 is illustrated in Figure 4-26 for the case with the infiltration source. The figure shows the solute concentration along the profile at the end of the simulation. The figure confirms what is said above about the pattern of the source strengths. A horizontal solute transport from higher recharge areas to lower discharge areas (i.e. lakes etc) would be expected, but it seems like the littoral zones act as hydraulic barriers around some of the lakes, i.e. Lake Eckarfjärden (see Figure 4-27). This effect is not so clear around Lake Bolundsfjärden, see Figure 4-28, where the horizontal transport seems to spread the solute also under some parts of the lake. In both cases, however, the spreading through horizontal transport in the upper layers is less important than the effects of transport driven by vertical flow gradients.

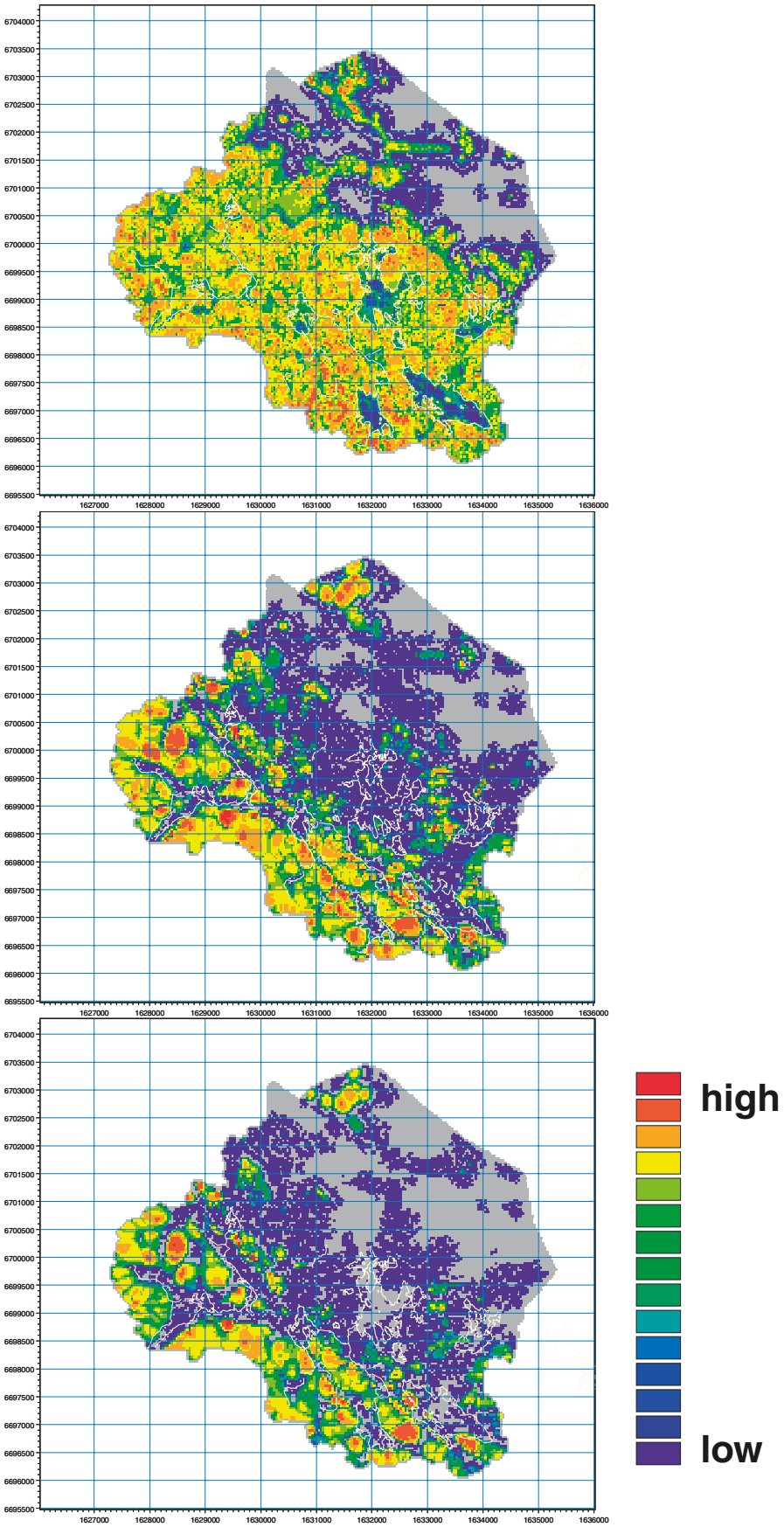

Figure 4-25. *Concentrations after one year in a simulation with an infiltration source. The upper figure is from the Quaternary deposits, the middle figure from a bedrock layer at 70 m.b.s.l. and the lower figure from a lower bedrock layer at 130 m.b.s.l.*

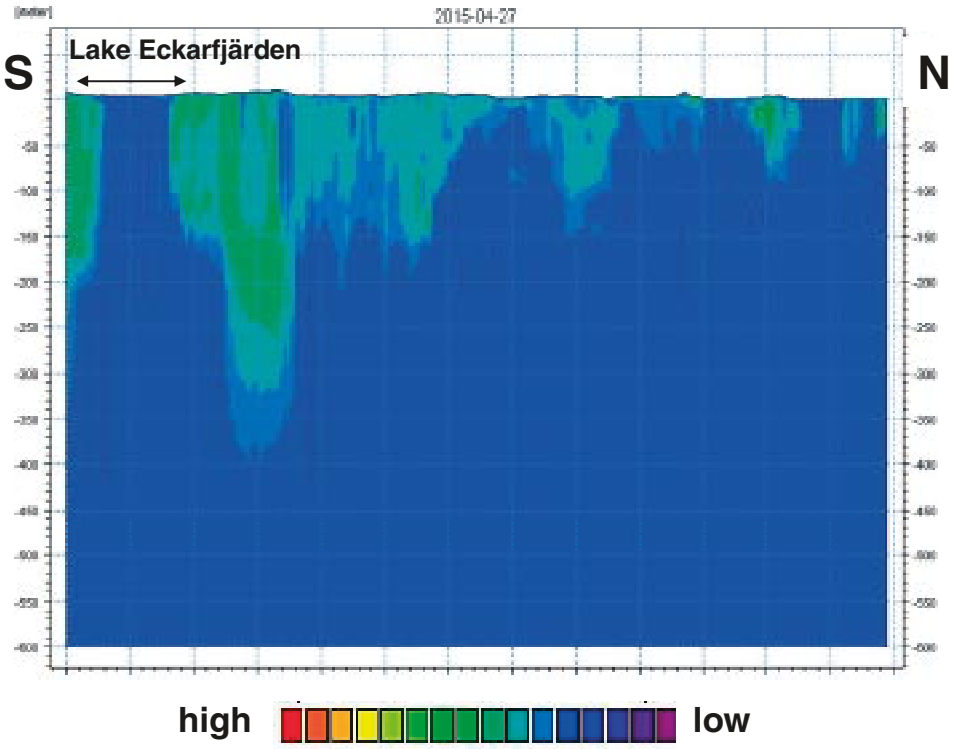

Figure 4-26. *Vertical profile taken according to Figure 4-10 from the transport simulation with an infiltration source. The figure shows the solute concentration after 10 years of simulation.*

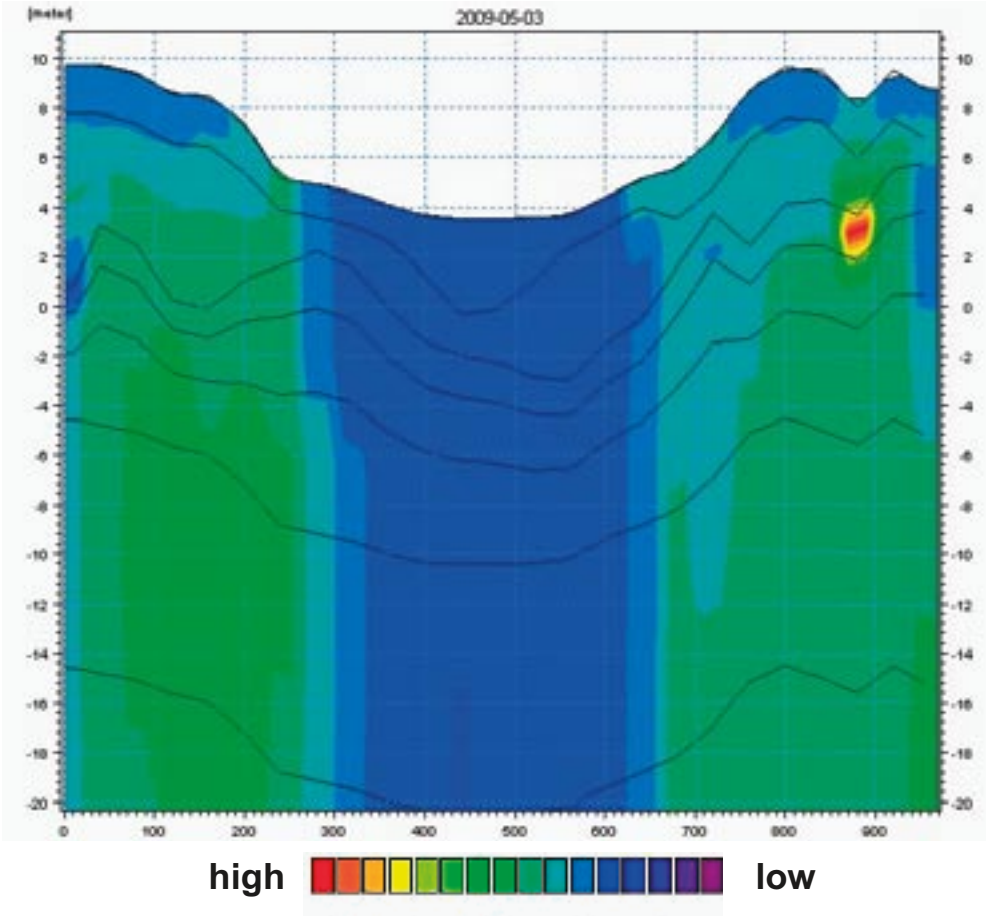

Figure 4-27. *Vertical profile through Lake Eckarfjärden for the transport simulation with an infiltration source. The figure shows the solute concentration after 5 years of simulation.*

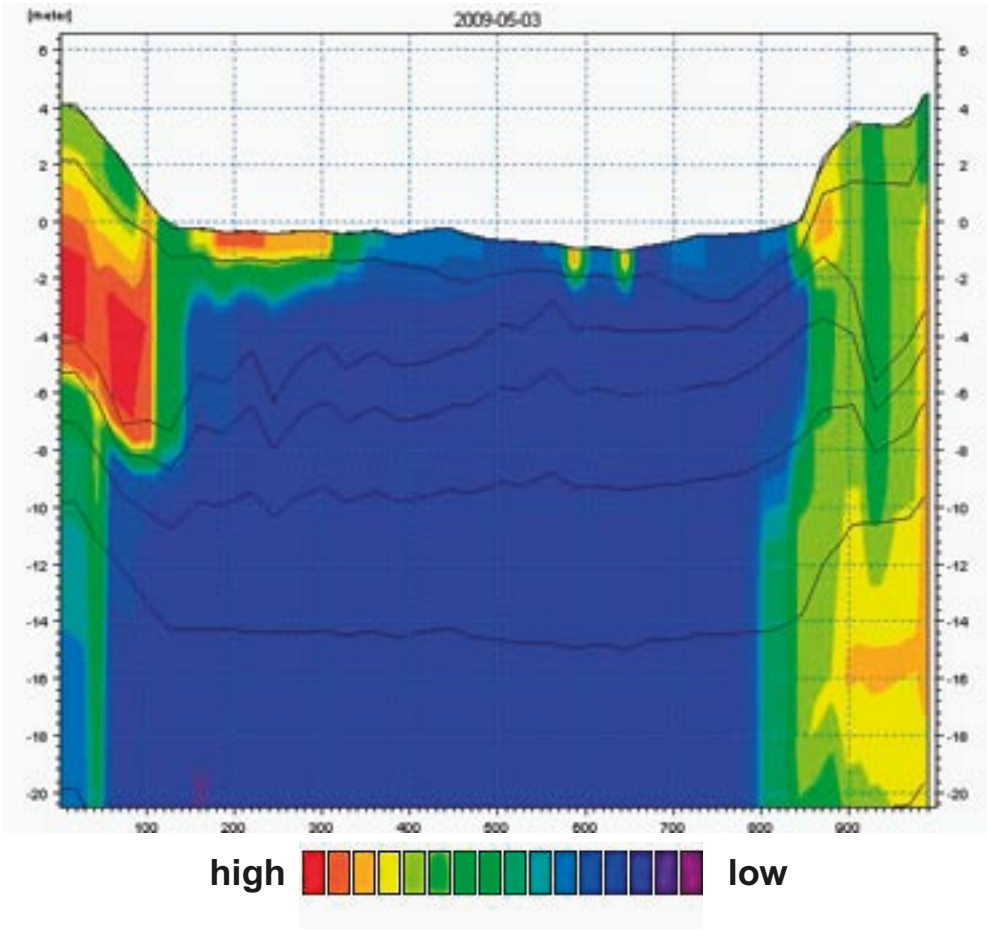

Figure 4-28. *Vertical profile through Lake Bolundsfjärden from the transport simulation with an infiltration source. The figure shows the solute concentration after 5 years of simulation.*

Table 4-5 shows a summary of sinks where the solute leaves the saturated zone. Each sink parameter is compared to the total saturated zone output at the time of the end of the simulation. The major part of the applied mass goes to the unsaturated zone, which is expected with an infiltration source. Evaluation of the continued transport from the different compartments demands that all flow components are included in the transport modelling; this was however not possible with the model version used for the present simulations.

Table 4-5. Summary of model sinks after 10 years of AD-simulation with an infiltration source.

	Cumulative mass in % of total output
Saturated zone storage	5.1
Saturated zone to unsaturated zone	83.6
Saturated zone baseflow to streams	1.9
Saturated zone drain to streams	3.6
Saturated zone flow to boundary	0.7
Saturated zone drain to boundary	5.1
Total source to saturated zone	100.0

5 Sensitivity analyses

This chapter presents results from the transport simulations made in order to evaluate the effect of changing the vertical grid and selected transport parameters. Specifically, the sensitivity to variations in dispersion and sorption coefficients is investigated.

5.1 Influence of the vertical model discretisation

A sensitivity analysis was made in order to evaluate whether the model was affected by so called numerical dispersion, i.e. dispersion although given dispersivities are zero. This phenomenon arises when the grid cells are too large in relation to the advective velocities. Three simulations with different vertical grid cell sizes were made. All other parameters were the same in the three simulations.

In *AD1* the number of calculation layers was 14, which is the number of layers used in the water movement simulations. In *AD2*, the number of vertical layers was increased to 30 layers (see Table 3-2). The increased number of layers was obtained by dividing layers L4 to L9 into three equally thick layers and by dividing layer L3 into 5 layers. The new layers in L3 were 10%, 15%, 20%, 25% and 30% of the original thickness. In *AD3*, the number of layers was 22. This number of layers was obtained by dividing each layer between L4 and L9 into 2 equally thick layers and by dividing layer L3 into 3 layers. The new layers in L3 were 20%, 30% and 50% of the original layer thickness.

Figures 5-1 to 5-3 shows different mass balance parameters in terms of time series for the three different simulations *AD1*, *AD2* and *AD3*. The figures indicate that the difference between any of the three simulation cases is not very large. However, in most cases the *AD1* simulation differs more, while *AD2* and *AD3* show more similar patterns.

An increase in the number of vertical layers also leads to a significant increase in computational times. It is therefore also desirable to limit the number of vertical layers. The small difference between *AD2* and *AD3* with regard to the mass balance parameters indicate that 22 layers are sufficient to ensure reliable simulation results.

Figure 5-1. *Mass balance time series for AD1 (green line), AD2 (red line) and AD3 (blue line). The uppermost figure shows the saturated zone storage, the middle figure the amount of solute transported from the saturated zone to the unsaturated zone, and the lower figure the amount of solute transported from the saturated zone to sinks.*

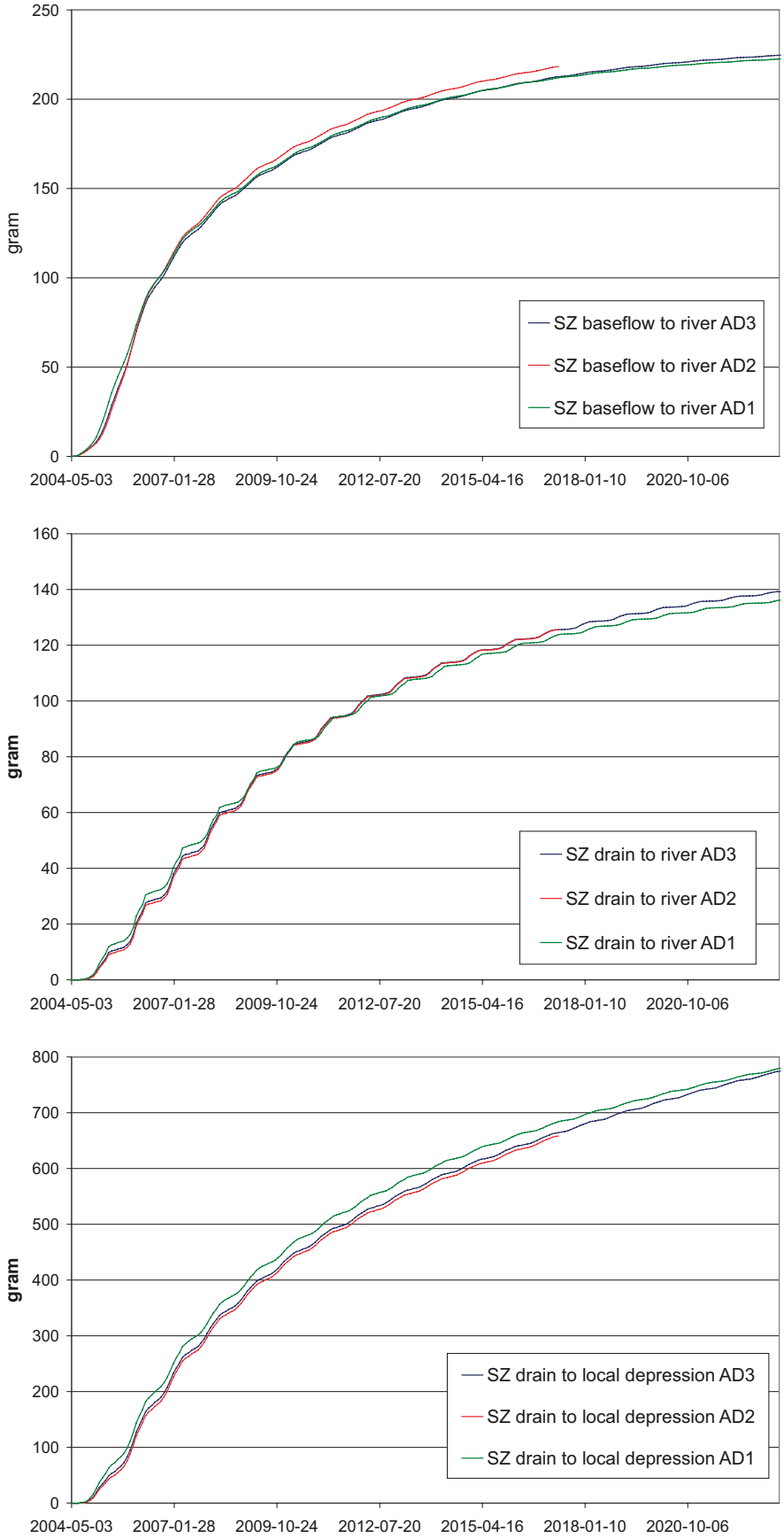

Figure 5-2. *Mass balance time series for AD1 (green line), AD2 (red line) and AD3 (blue line). The uppermost figure shows the amount solute transported by saturated zone baseflow to streams, the middle figure the transport by saturated zone drains to streams, and the lower figure the transport by saturated zone drains to local depressions.*

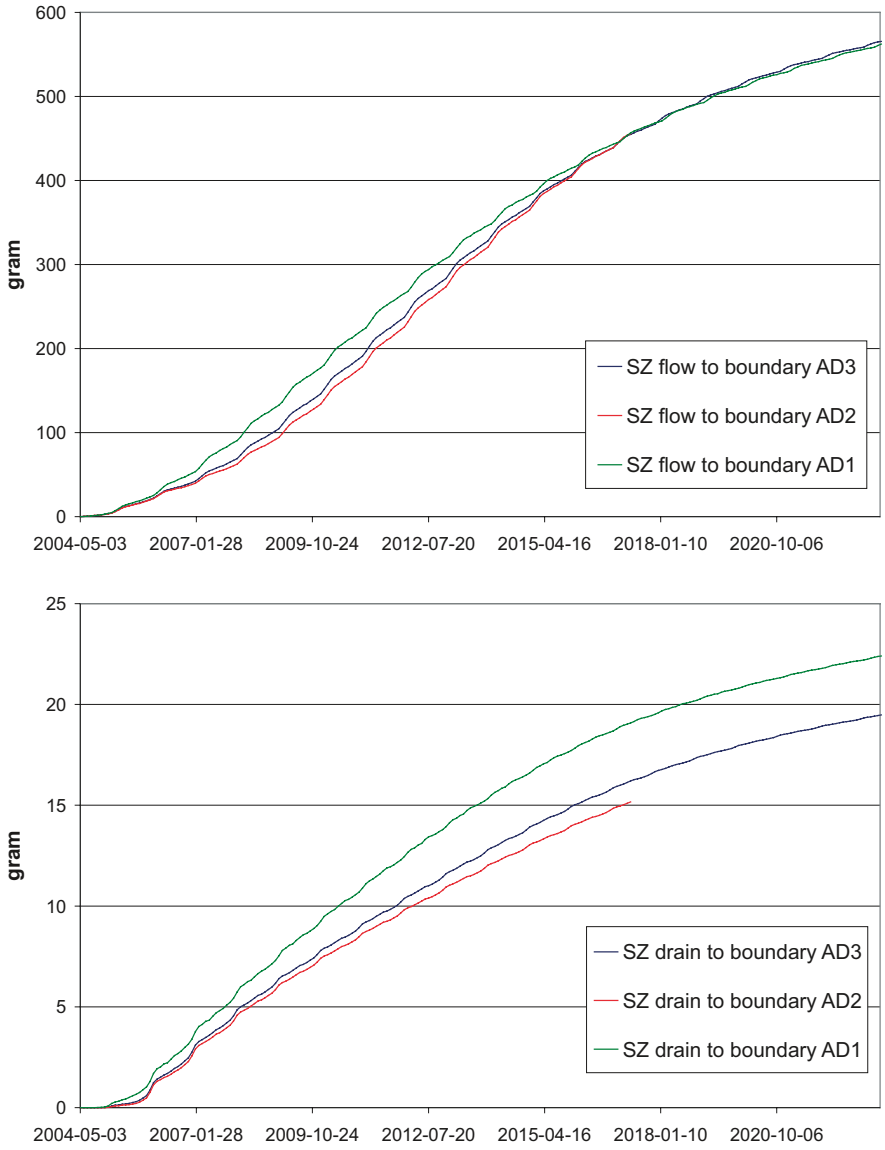

Figure 5-3. *Mass balance time series for AD1 (green line), AD2 (red line) and AD3 (blue line). The upper figure shows the amount of solute transported by saturated zone flow to boundaries, and the lower figure the transport by saturated zone drains to boundaries.*

To further illustrate the impact of the increase in number of calculation layers, two points were chosen from which time series in different layers were extracted and compared between *AD1*, *AD2* and *AD3*. Figure 5-4 shows the positions of the two cells for which time series were extracted. The layers between L3 and L9 in *AD2* and *AD3* were divided into several layers and in order to be able to compare the results between the different simulations, mean values were calculated for the divided layers.

Figures 5-5 and 5-6 show the extracted time series. Results were extracted for layers L9, which is just above the pollution source, L6, which is a layer with high values of the horizontal hydraulic conductivity, and L2, which is the lower layer with Quaternary deposits. The figures indicate that, in most graphs, the difference between *AD2* and *AD3* is smaller than the difference between *AD1* and *AD3*. Also, the pattern in *AD2* is better reflected in *AD3* than in *AD1*.

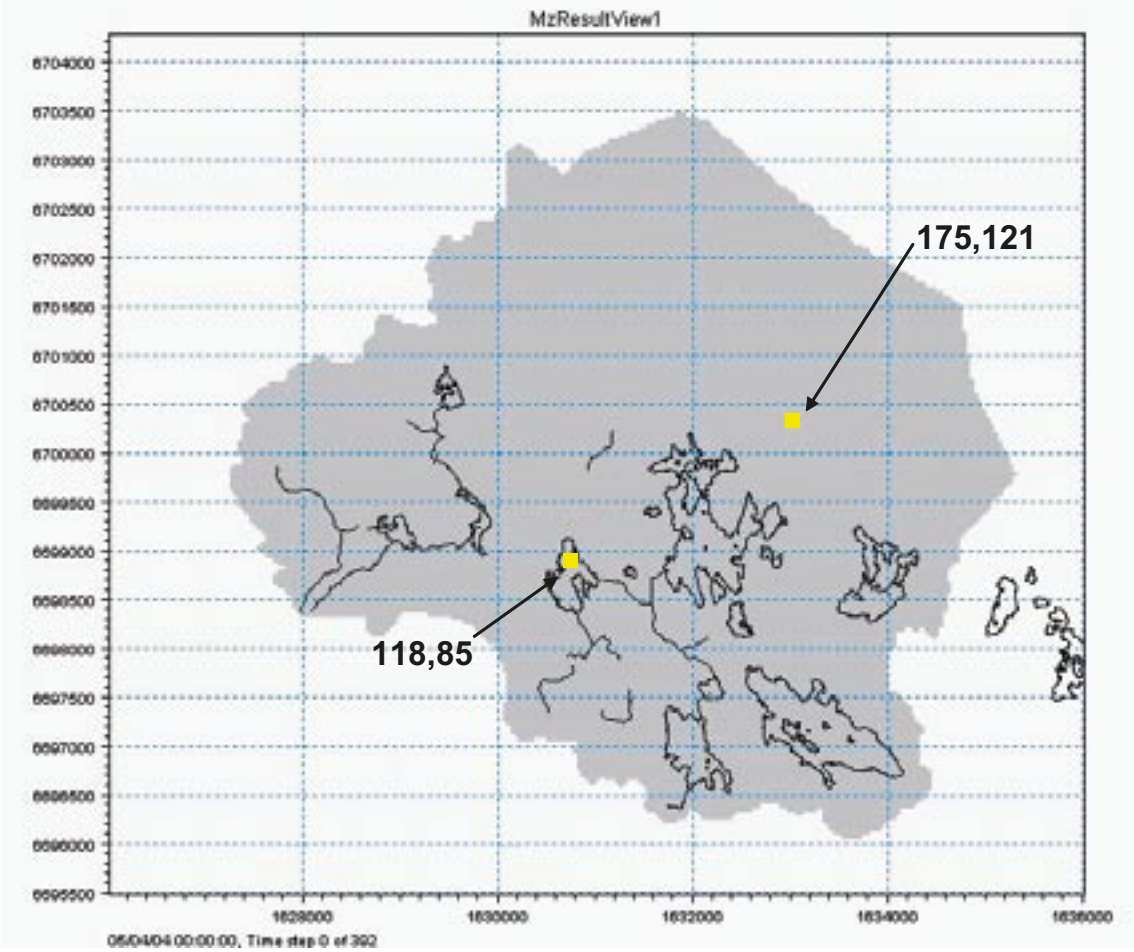

Figure 5-4. *Positions of cells for which time series were extracted in three different layers in the AD1, AD2 and AD3 simulations.*

Figures 5-7 to 5-9 show concentration plots for layer L6, which is located approximately 70 m.b.s.l., at three different times. Figure 5-7 shows concentrations after 2 months of simulations, Figure 5-8 show concentrations after 2 years and Figure 5-9 after 10 years of simulation. In each figure, the uppermost graph is from the *AD1* simulation case, the middle graph from *AD2*, and the lower one from *AD3*. The figure further confirms that the difference between the three simulations is in most areas very small. It is also confirmed that the *AD3* case gives a result closer to *AD2*. Based on the observation that presented results for *AD2* and *AD3* were similar, as well as the fact that computational time was significantly smaller for *AD3* than for *AD2*, it was decided to use the *AD3* simulation case as basis for further analysis and results.

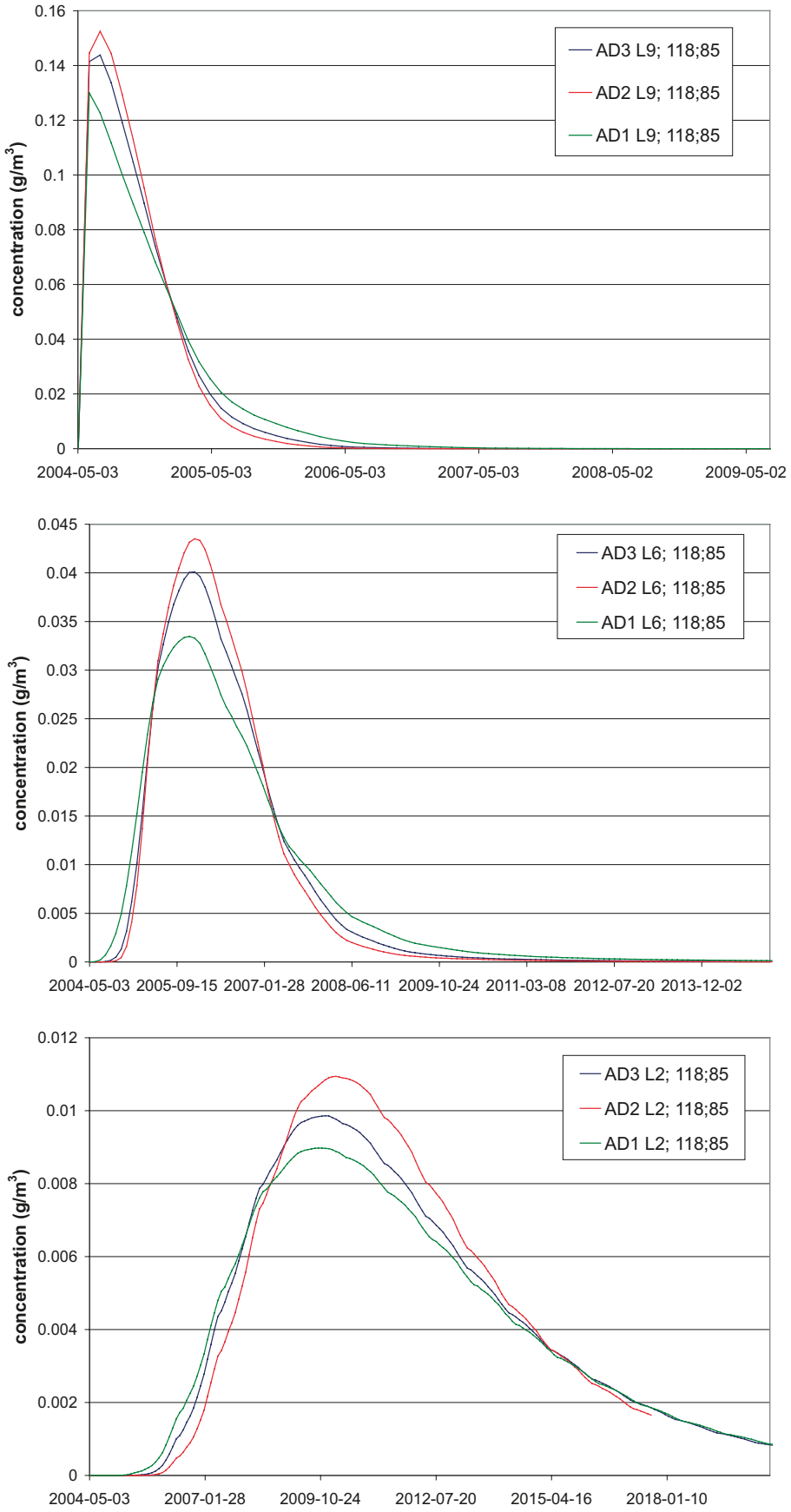

Figure 5-5. *Times series for cell (118,85) for AD1, AD2 and AD3. In the uppermost figure, the times series are extracted from layer L9, which is situated just above the solute source, in the middle figure the time series are from layer L6, and in the lower figure time series are from the lower layer in the Quaternary deposits, L2.*

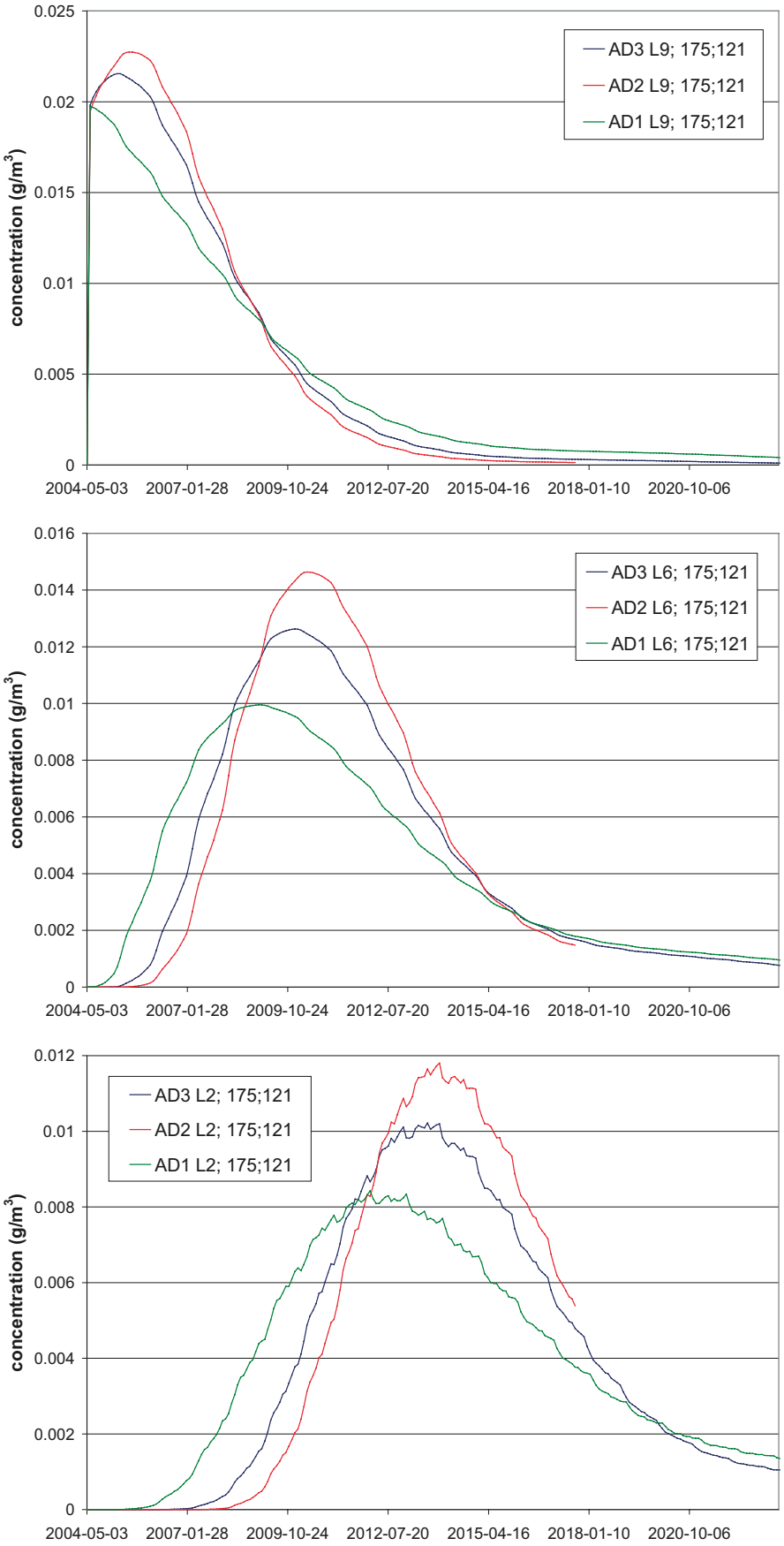

Figure 5-6. *Times series for cell (175,121) for AD1, AD2 and AD3. In the uppermost figure, the times series are extracted from layer L9, which is situated just above the solute source, in the middle figure the time series are from layer L6, and in the lower figure time series are from the lower layer in the Quaternary deposits, L2.*

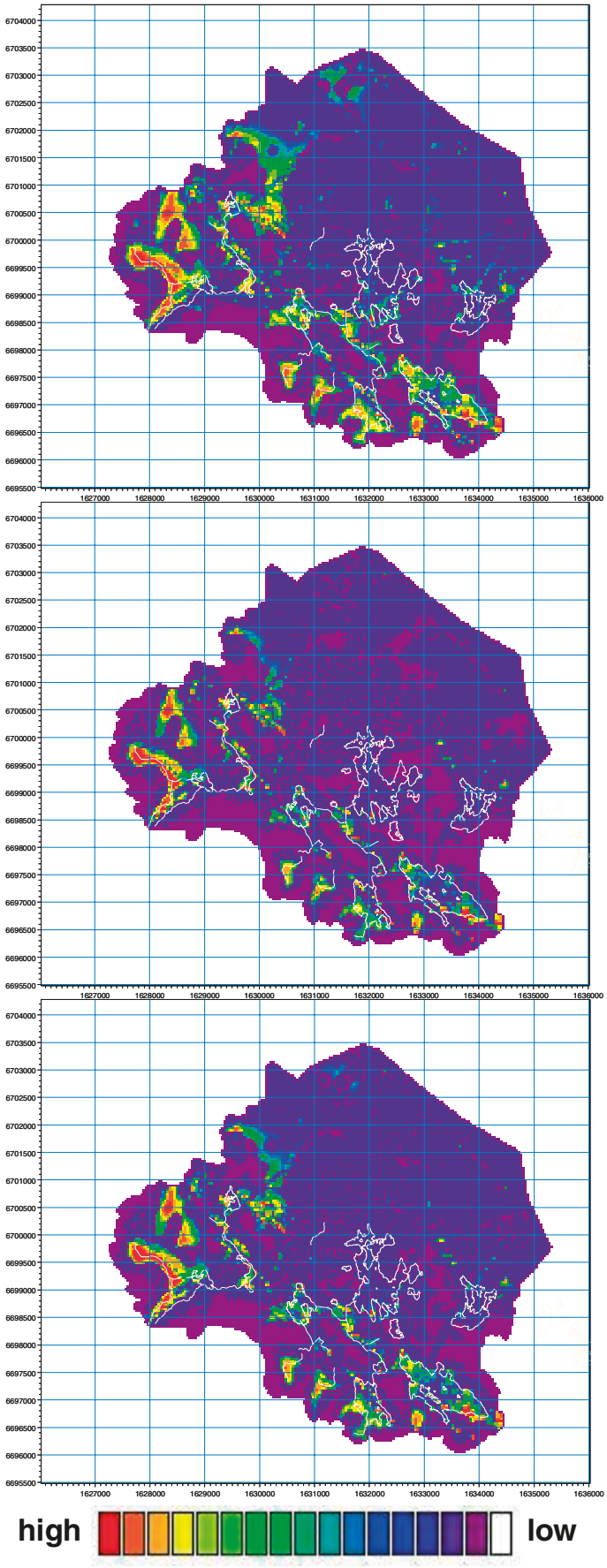

Figure 5-7. *Concentrations at approximately 70 m.b.s.l. in the bedrock after 2 months in AD simulations with a pulse source in the bedrock. The uppermost figure is from AD1, the middle figure from AD2 and the bottom figure from AD3. The shorelines of the lakes and the water courses are marked in the figure.*

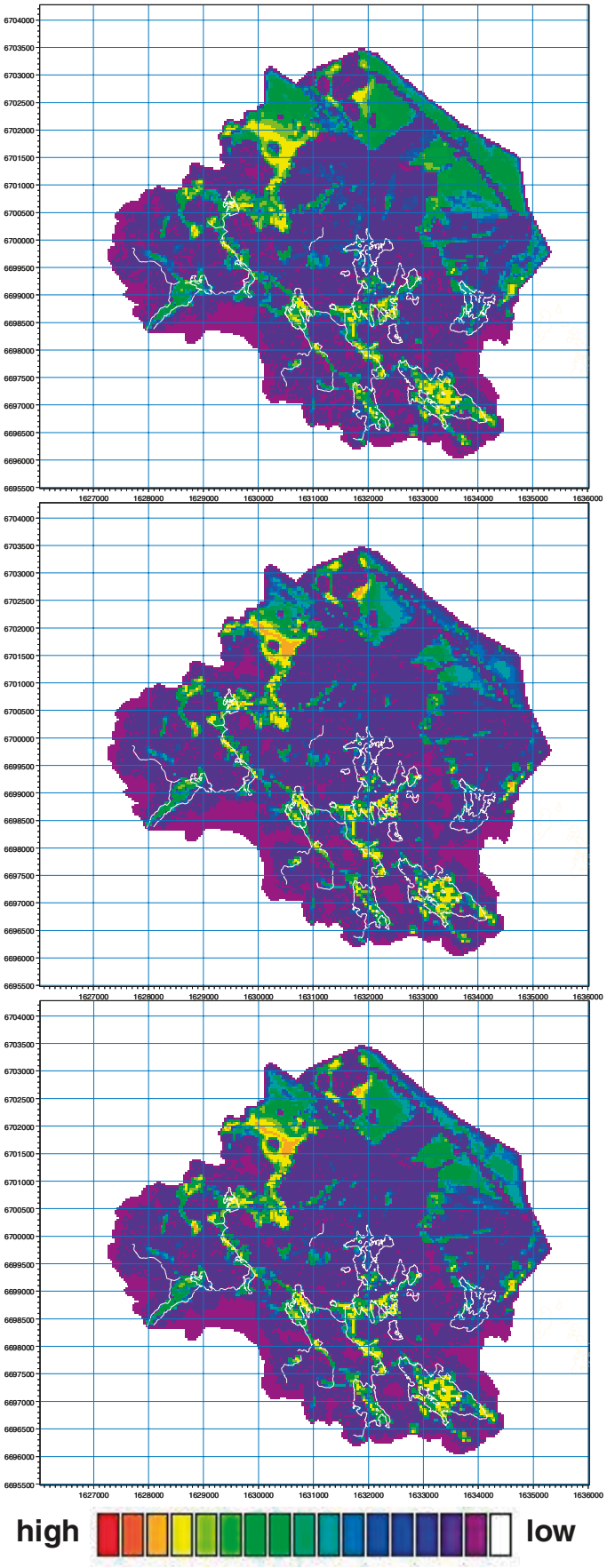

Figure 5-8. *Concentrations at approximately 70 m.b.s.l. in the bedrock after 2 years in AD simulations with a pulse source in the bedrock. The uppermost figure is from AD1, the middle figure from AD2 and the bottom figure from AD3. The shorelines of the lakes and the water courses are marked in the figure.*

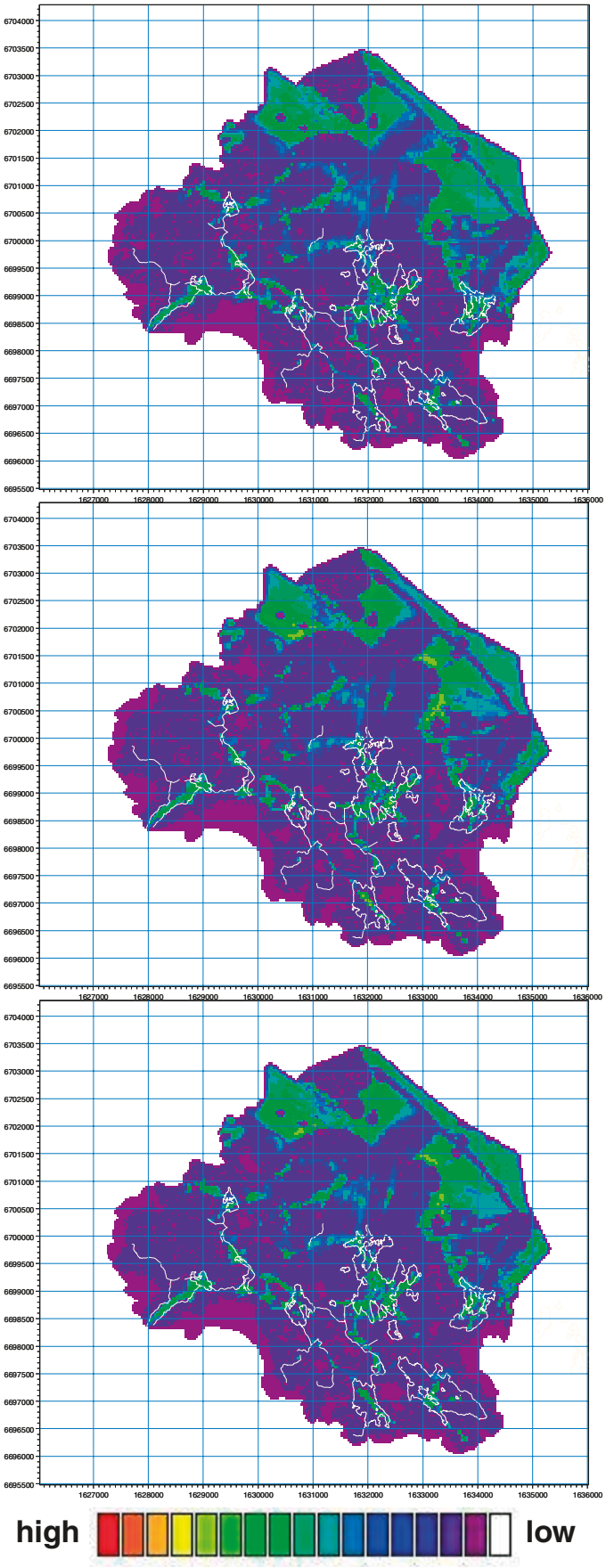

Figure 5-9. *Concentrations at approximately 70 m.b.s.l. in the bedrock after 10 years in AD simulations with a pulse source in the bedrock. The uppermost figure is from AD1, the middle figure from AD2 and the bottom figure from AD3. The shorelines of the lakes and the water courses are marked in the figure.*

5.2 Influence of saturated zone dispersion

Solute dispersion refers to the spreading of solute around its mean position. To investigate the influence of the saturated zone dispersion on the solute transport results for the Forsmark area, simulations were made with two different set-ups of dispersion coefficients and then compared to the results of particle tracking, which in MIKE SHE is a purely advective simulation. The influence of the dispersion is examined both for the bedrock source and the infiltration source.

Observe that, although the PT simulations are made with a completely equivalent source description in terms of introduced mass over time in the source layer at 140 m.b.s.l., the results are discrete because only integer numbers of particles are possible. When a particle reaches a certain cell, the concentration will take an immediate jump equivalent to the particle mass divided by the effective water volume in the actual cell. In the AD simulation on the other hand, the concentration is a continuous model variable. This is the explanation behind the somewhat saw-shaped PT results, compared to the smoother AD results. A smaller specified particle mass would produce more particles and smoother PT results, however with much longer simulation times.

5.2.1 Simulation with source in bedrock layer

Figures 5-10 to 5-14 show the results from simulations with the source in a bedrock layer at a level of approximately 140 m.b.s.l. Figures 5-10 and 5-11 show examples of the effect of including dispersion in transport modelling for two cells located according to Figure 5-4. In the figures, it is clearly illustrated that the dispersion is an important factor when estimating the time of the concentration peak. The higher the dispersion, the earlier the concentration break-through, but also the lower the concentration value at the peak. Also, the higher the dispersion, the longer the time before the concentration approaches zero again.

In the PT simulation, the intervals between storage of results were significantly longer than in AD, which may be seen in the figure. In the uppermost graph in Figure 5-10, the peak concentration in the PT curve is lower than in the AD curves. This is because the peak in the PT curve is missing due to the long storage intervals. In all graphs in Figures 5-10 and 5-11, concentrations are illustrated on separate y-axes for the AD- and PT-simulations.

In Figures 5-12 to 5-14, concentration plots are shown after a simulation time of 2 years for three different layers. In the upper figures, the concentration plot is from the particle tracking simulation, in the middle figure from the AD-simulation with low dispersion, and in the lower figure from the AD-simulation with higher dispersion. Figure 5-12 is from the layer situated just above the solute source. The figure clearly illustrates the effect of the dispersion. For the particle tracking simulation the solute is concentrated to small areas. The middle graph, with the low dispersion, shows that the dispersion results in solute spreading over much larger areas. The lower graph illustrates that the higher the dispersion, the larger the area covered by the solute. Figure 5-13 is from a layer at about 70 m.b.s.l. and Figure 5-14 from the Quaternary deposits. Both figures further illustrate the patterns from Figure 5-12.

All figures indicate that dispersion is an important factor to include if the transport simulation has other purposes than just to delineate solute flow paths. The figures also indicate that the difference between the simulation with a very low dispersion and the particle tracking simulations is larger than between the simulations with high and low dispersion. The times series illustrated in Figures 5-10 and 5-11 were selected with regard to the results from the particle tracking simulation. For most cells there is zero concentration in the particle tracking, but the time series were selected to illustrate the effect of dispersion.

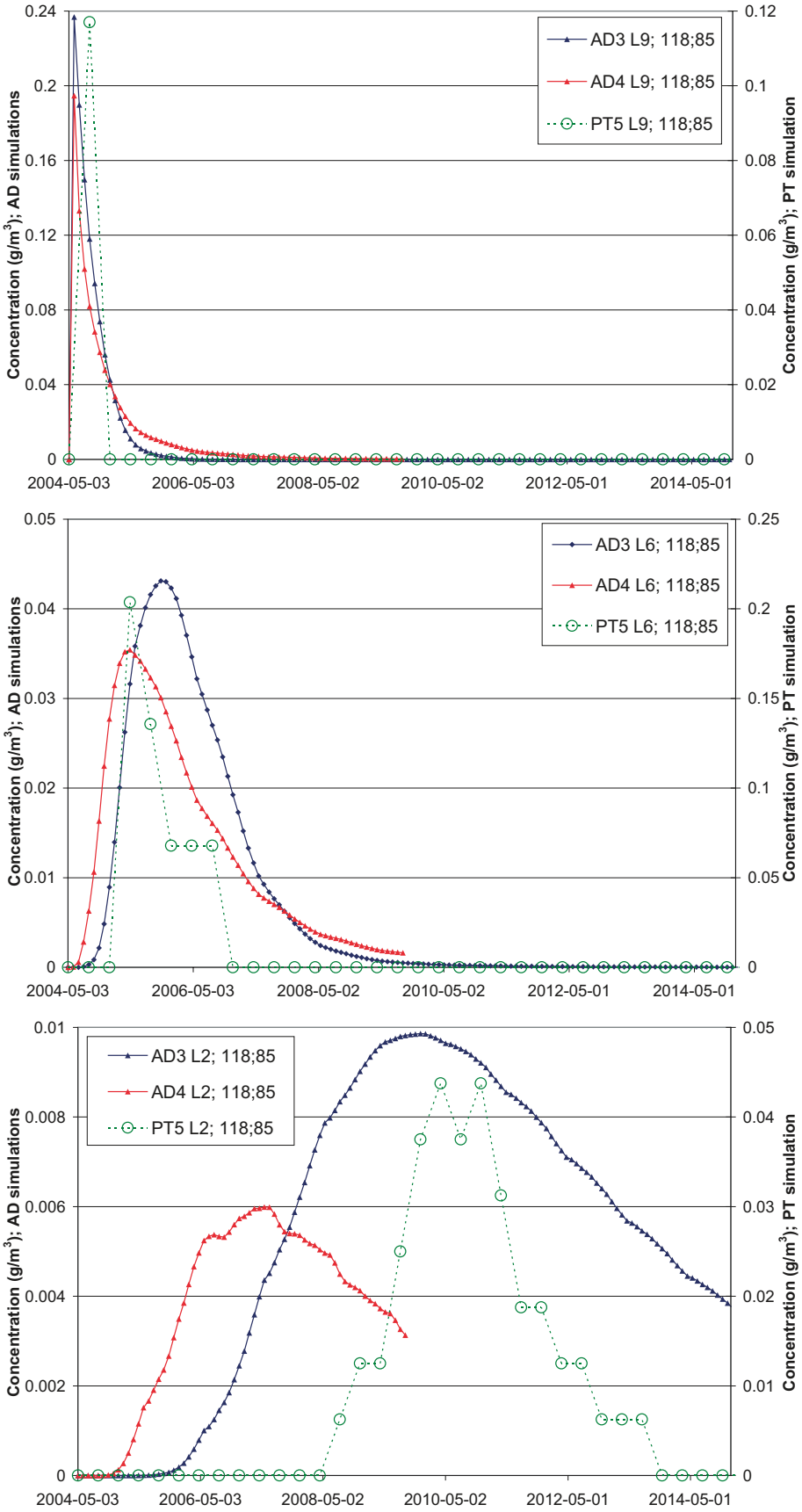

Figure 5-10. *Time series for cell (118,85), located in Lake Gällsboträsket, for AD3 (blue line), AD4 (red line) and PT5 (green line). In the uppermost figure the times series are extracted from layer L9, which is situated just above the solute source, in the middle figure the time series are from layer L6, and in the lower figure time series are from the lower layer in the Quaternary deposits, L2. Note the different y-axis scales for the AD- and PT-results.*

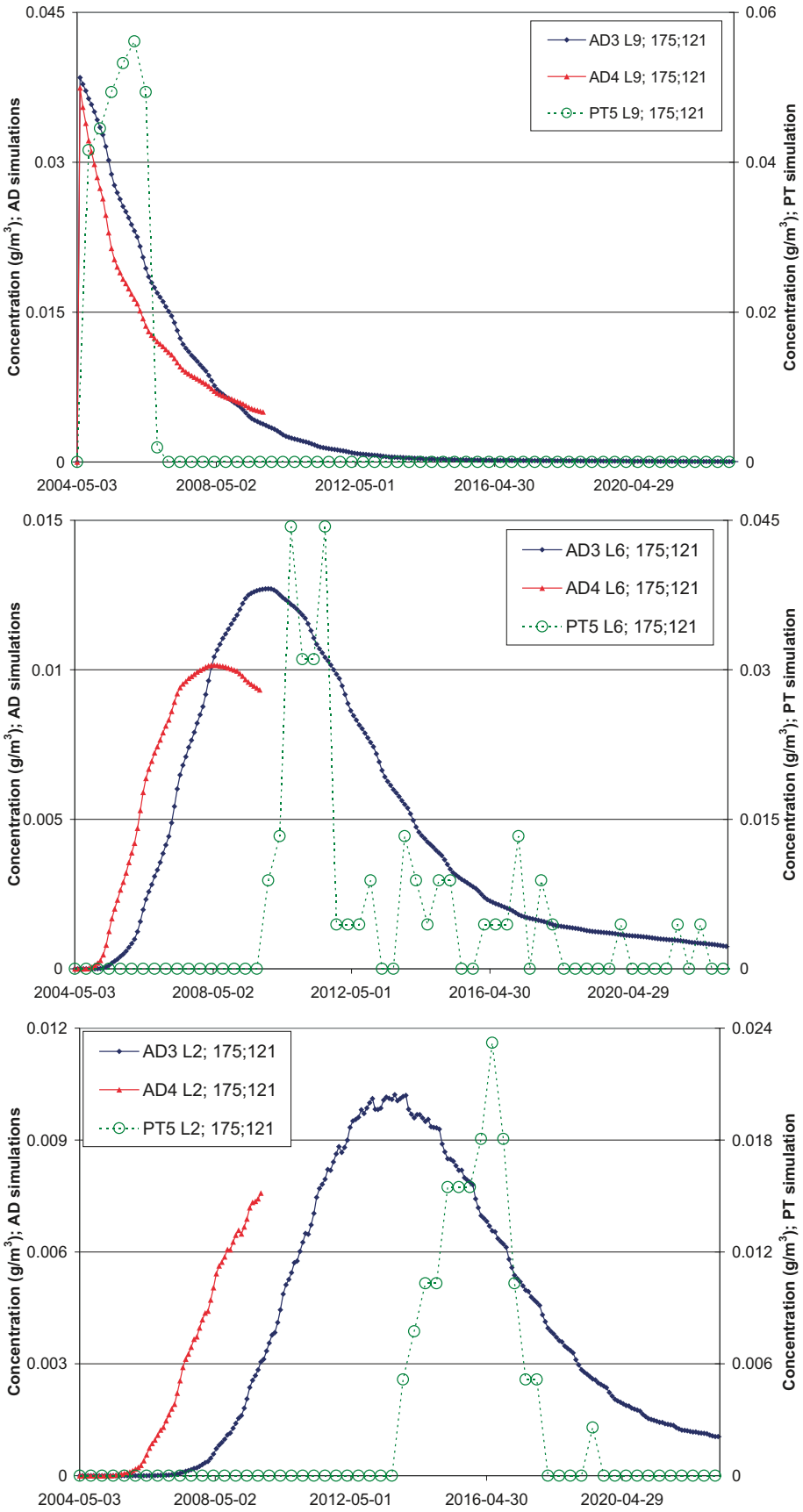

Figure 5-11. *Time series for cell (175,121), located in the sea, for AD3 (blue line), AD4 (red line) and PT5 (green line). In the uppermost figure the times series are extracted from layer L9, which is situated just above the solute source, in the middle figure the time series are from layer L6, and in the lower figure time series are from the lower layer in the Quaternary deposits, L2. Note the different y-axis scales for the AD- and PT-results.*

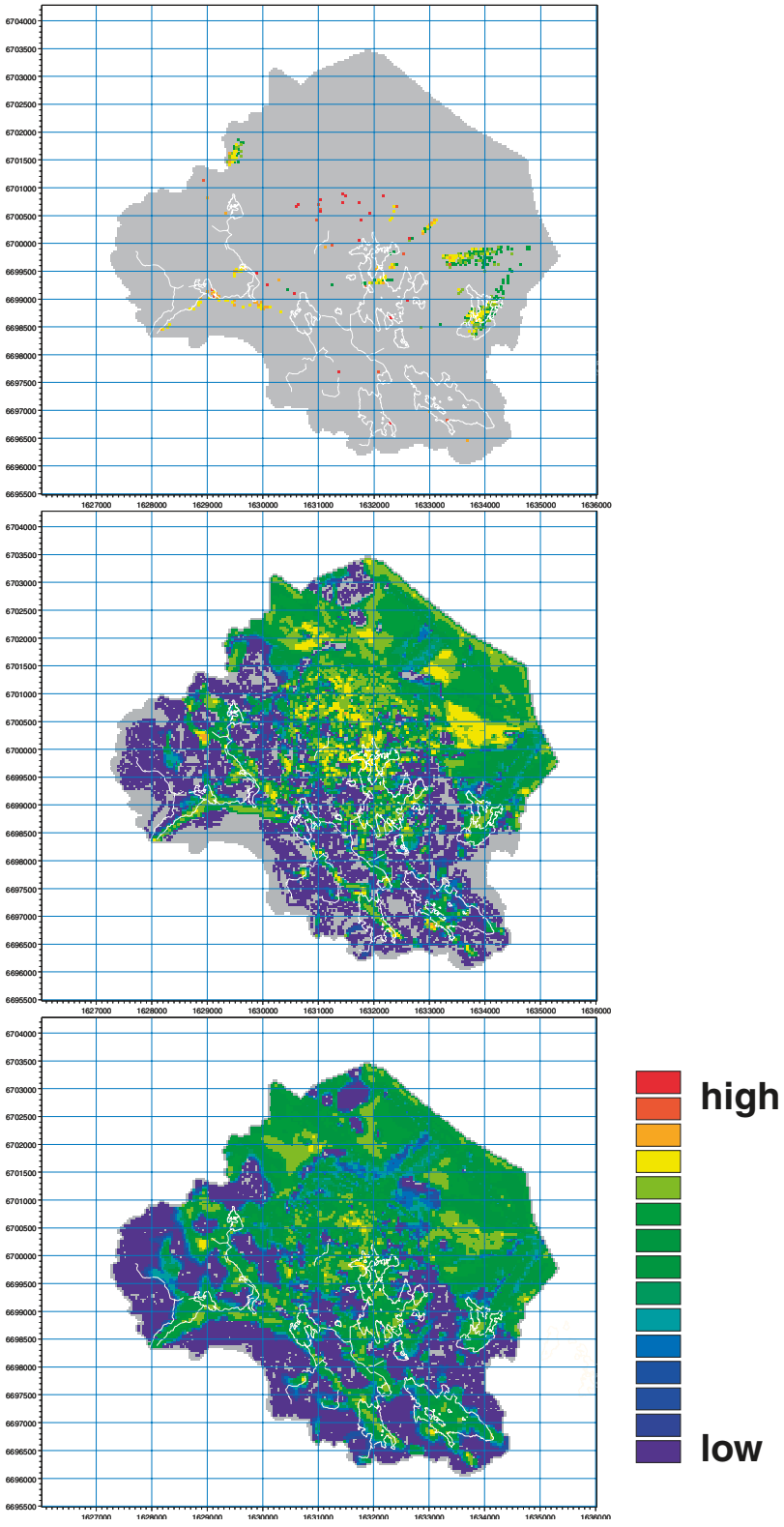

Figure 5-12. *Concentrations in the bedrock after 2 years at approximately 130 m.b.s.l., in simulations with source in the bedrock layer. The uppermost figure is from the PT5, the middle figure from the AD3 and the bottom figure from the AD4. As orientation, the shoreline of the lakes and the water courses are marked in the figure.*

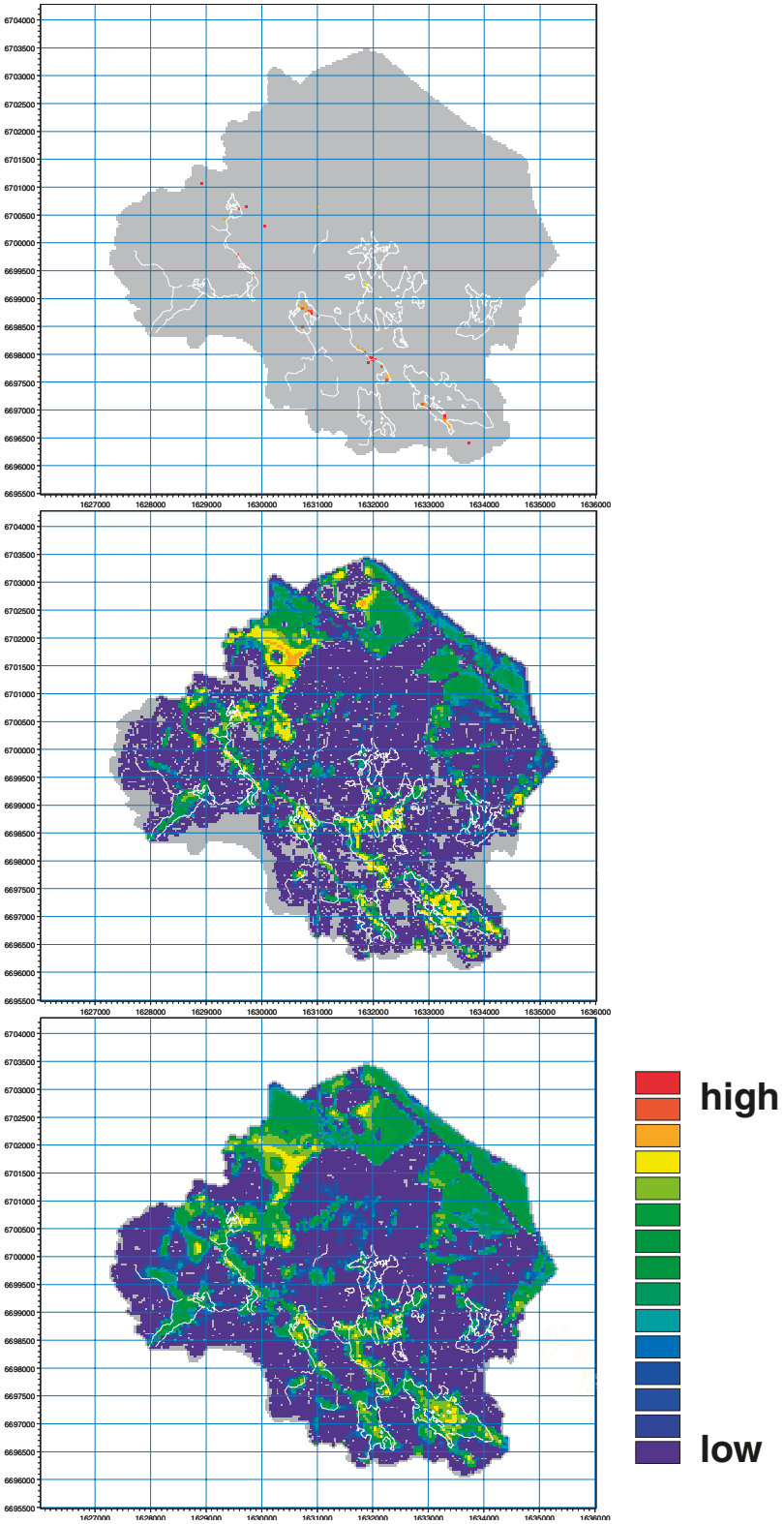

Figure 5-13. *Concentrations at approximately 70 m.b.s.l. in the bedrock after 2 years in simulations with a source in the bedrock. The uppermost figure is from PT5, the middle figure from AD3 and the bottom figure from AD4. The shorelines of the lakes and the water courses are marked in the figure.*

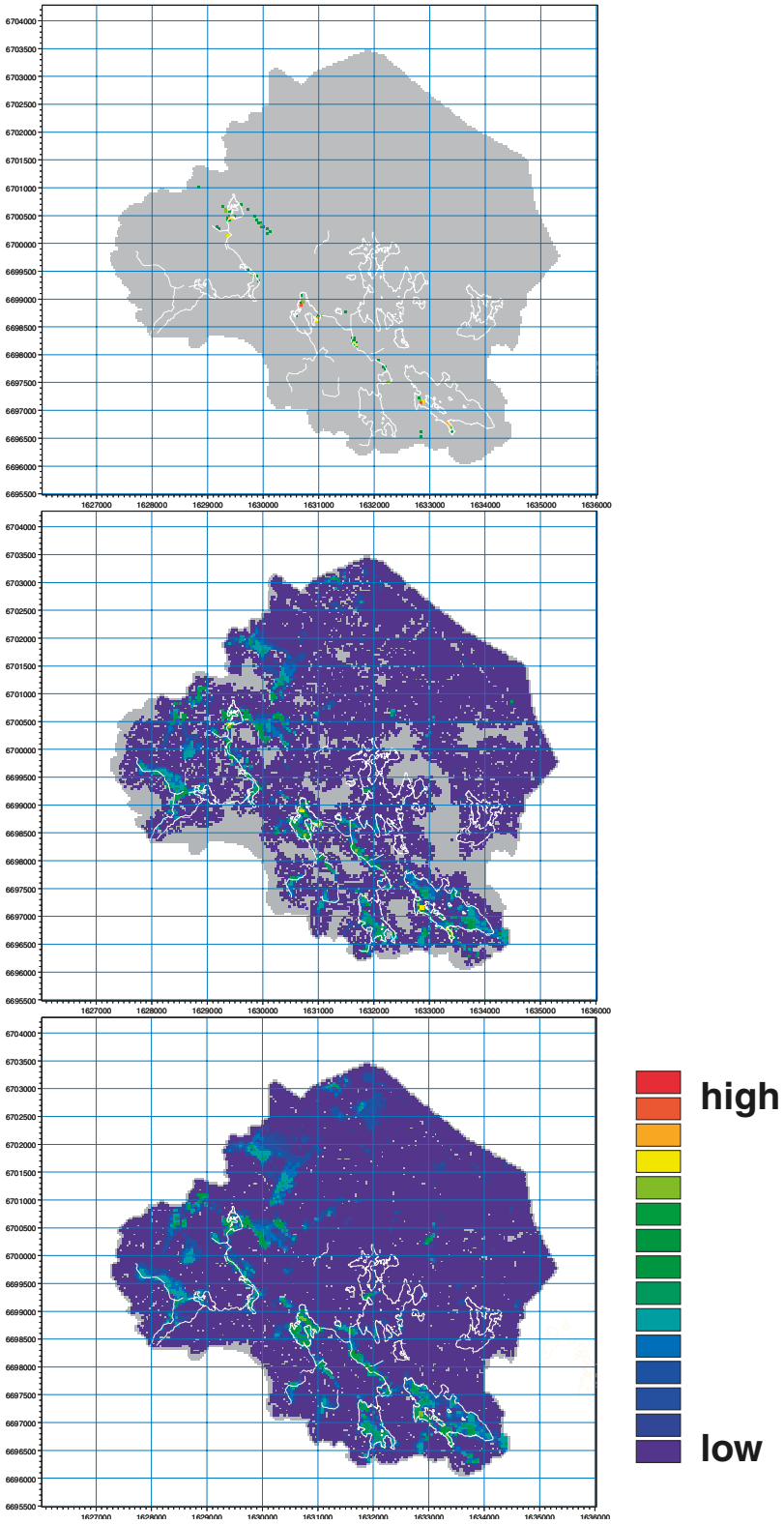

Figure 5-14. *Concentrations after 2 years in the Quaternary deposits in simulations with a source in the bedrock. The uppermost figure is from PT5, the middle figure from AD3 and the bottom figure from AD4. The shorelines of the lakes and the water courses are marked in the figure.*

5.2.2 Simulation with infiltration source

Figures 5-15 to 5-22 show the results from simulations with a constant-concentration infiltration source. Two AD-simulations with a constant-concentration source in the top layer were made: *AD10* with only the saturated zone component included and a low dispersion, and *AD11* also with only the saturated zone component but with a high dispersion. The results of these simulations are compared with results from *PT12*, which is a particle tracking simulation with a similar infiltration source.

Figures 5-16 to 5-19 show time series from selected model cells. Concentrations from AD- and PT-simulations are shown on different y-axes. Figure 5-15 shows the positions of the selected cells. In Figures 5-16 to 5-19, the upper graphs are from the lower layer, L9, the middle graphs from layer L6 and the lower graphs from the lower Quaternary deposit layer, L2. Since the source is constant, the solute mass is accumulated in the layers. From the figures it is seen that seasonal patterns affect the solute concentration, especially in layer L2 and for cells with a quick response.

For the PT simulation, the effect of the seasonal flow pattern is even more distinct. Since there is no dispersion in the PT simulation, the changes in concentration are more drastic, either there are particles in the cell or there are not. As a consequence, the concentrations vary significantly in many cells in the PT simulation due to seasonal variations, and when the concentration in the AD-simulation is low the concentration in the PT simulation is often zero. In the PT simulations, the time interval between storage of results is long, which is seen in the figures. This, together with the discrete nature of particle detection and the use of small observation volumes (single cells), are the reasons why only very few (in one case none) non-zero PT concentrations are displayed in some of the graphs in Figures 5-16 to 5-19.

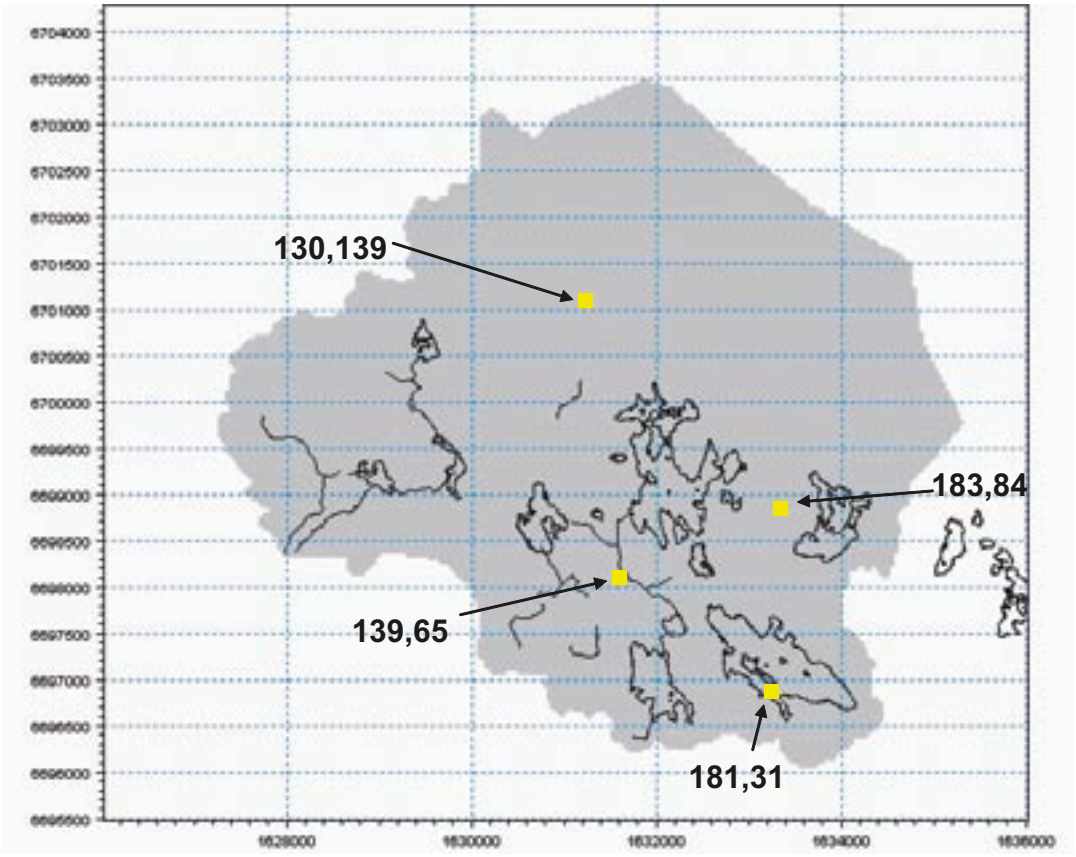

Figure 5-15. *Positions of cells for which time series were extracted in three different layers in simulations AD10, AD11 and PT12.*

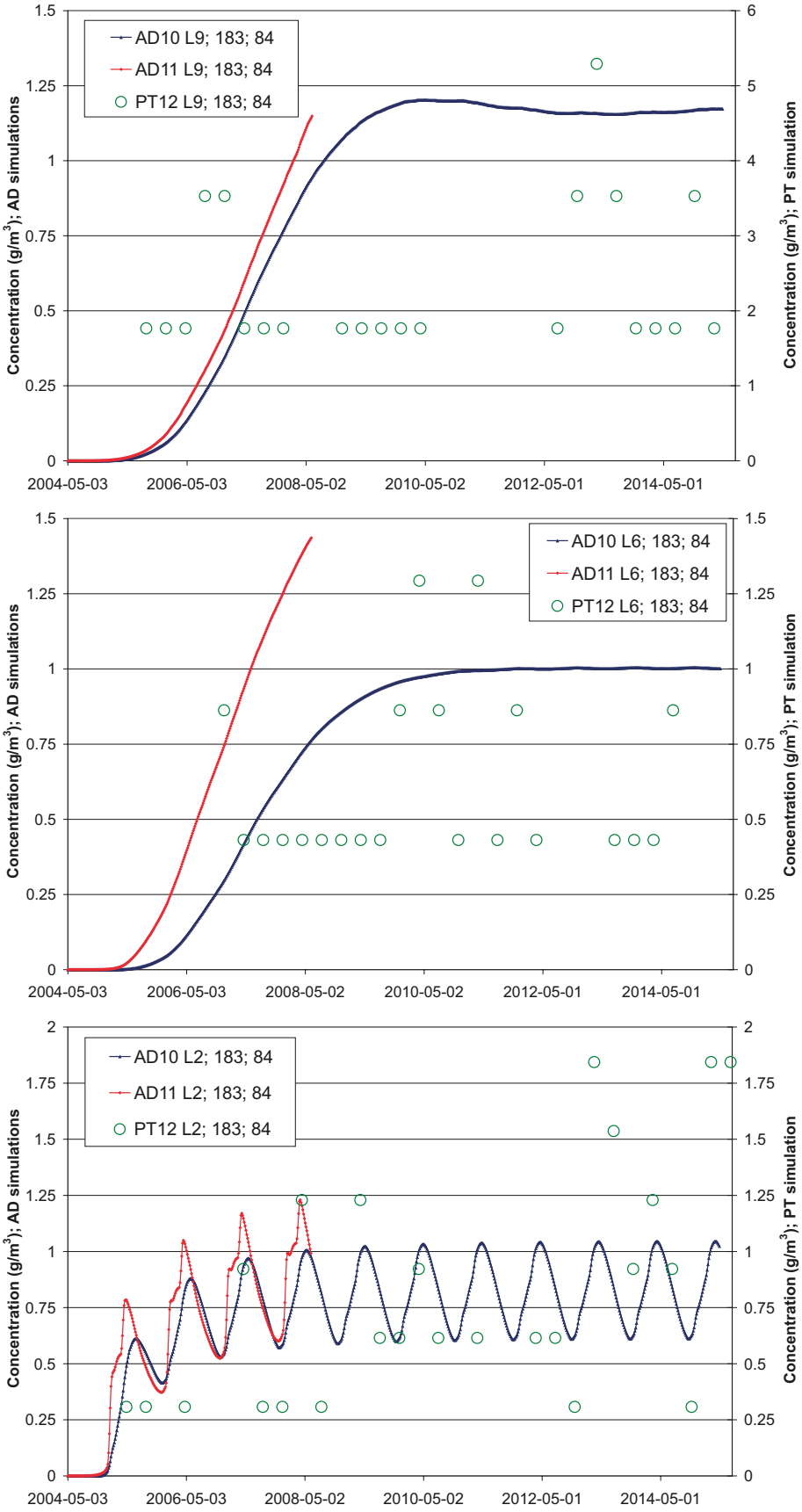

Figure 5-16. *Time series for cell (183,84) for AD10 (blue line), AD11 (red line) and PT12 (green symbols). In the uppermost graph the times series are extracted from layer L9, in the middle graph the time series are from layer L6, and in the lower one time series are from the lower layer in the Quaternary deposits, L2. Note the different y-axis scales for the AD- and PT-results in the uppermost graph.*

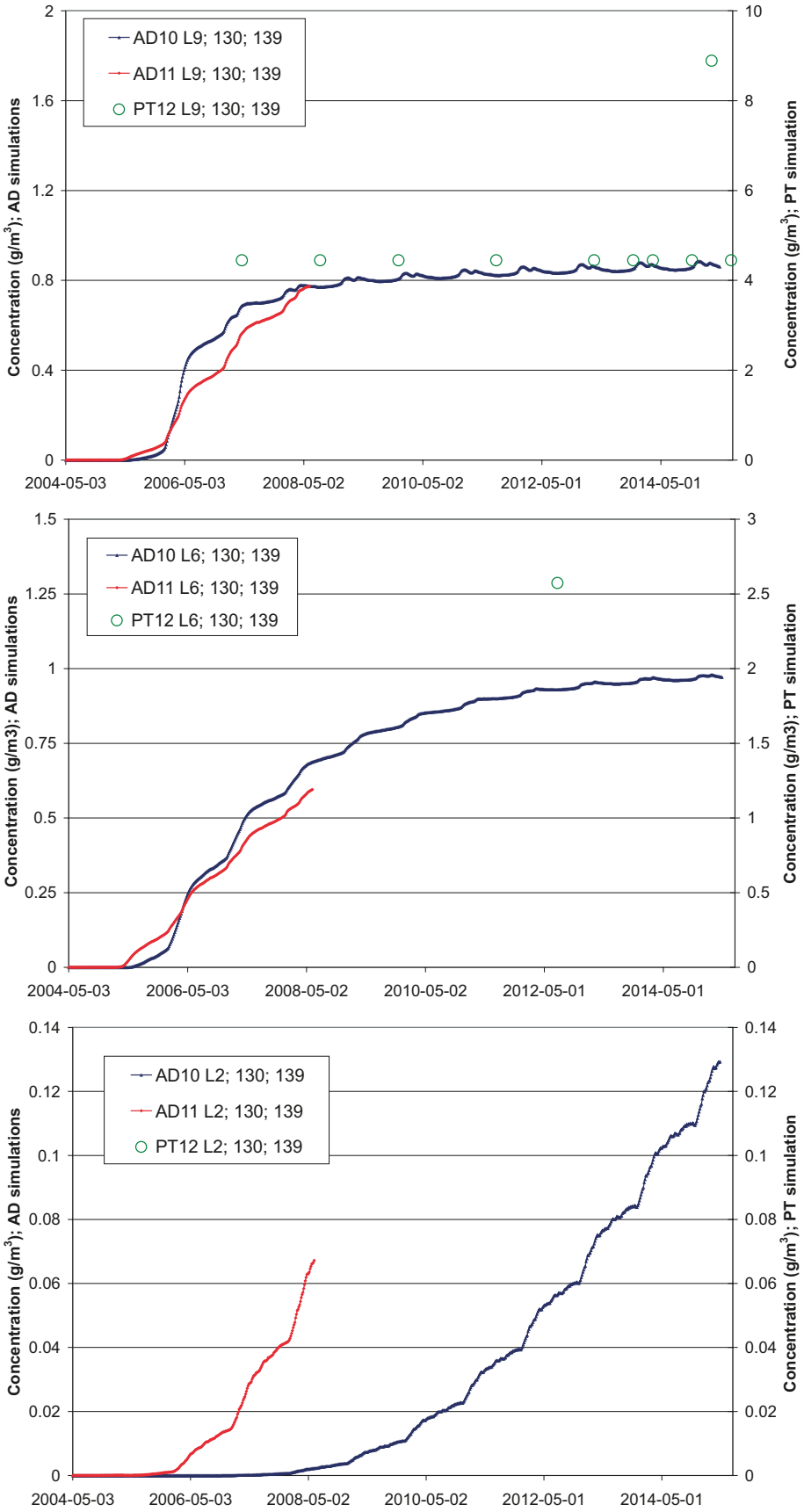

Figure 5-17. *Time series for cell (130,139) for AD10 (blue line), AD11 (red line) and PT12 (green symbols). In the uppermost graph the times series are extracted from layer L9, in the middle graph the time series are from layer L6, and in the lower one time series are from the lower layer in the Quaternary deposits, L2. Note the different y-axis scales for the AD- and PT-results in the upper graphs.*

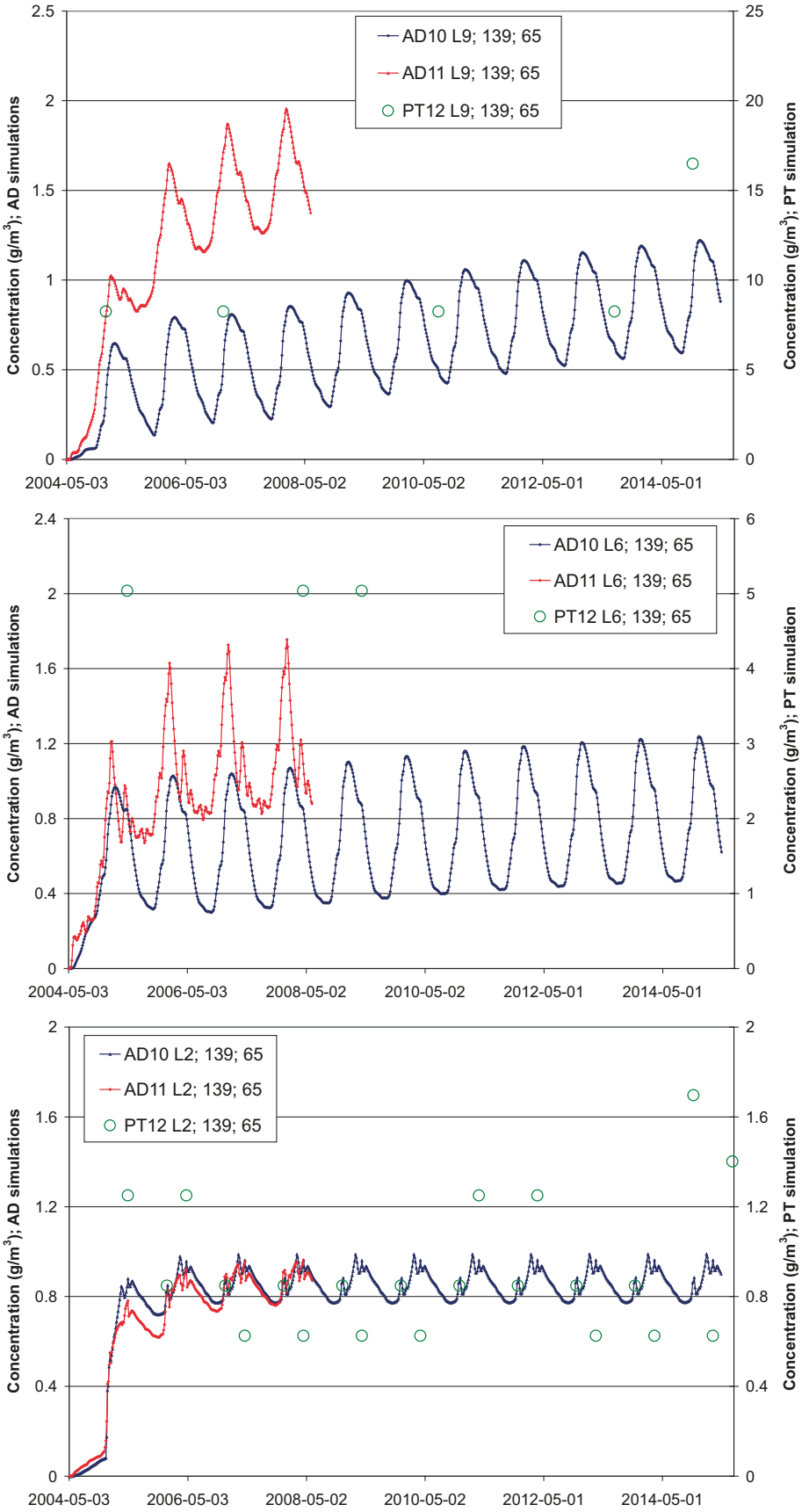

Figure 5-18. *Time series for cell (139,65) for AD10 (blue line), AD11 (red line) and PT12 (green symbols). In the uppermost graph the times series are extracted from layer L9, in the middle graph the time series are from layer L6, and in the lower one time series are from the lower layer in the Quaternary deposits, L2. Note the different y-axis scales for the AD- and PT-results in the upper graphs.*

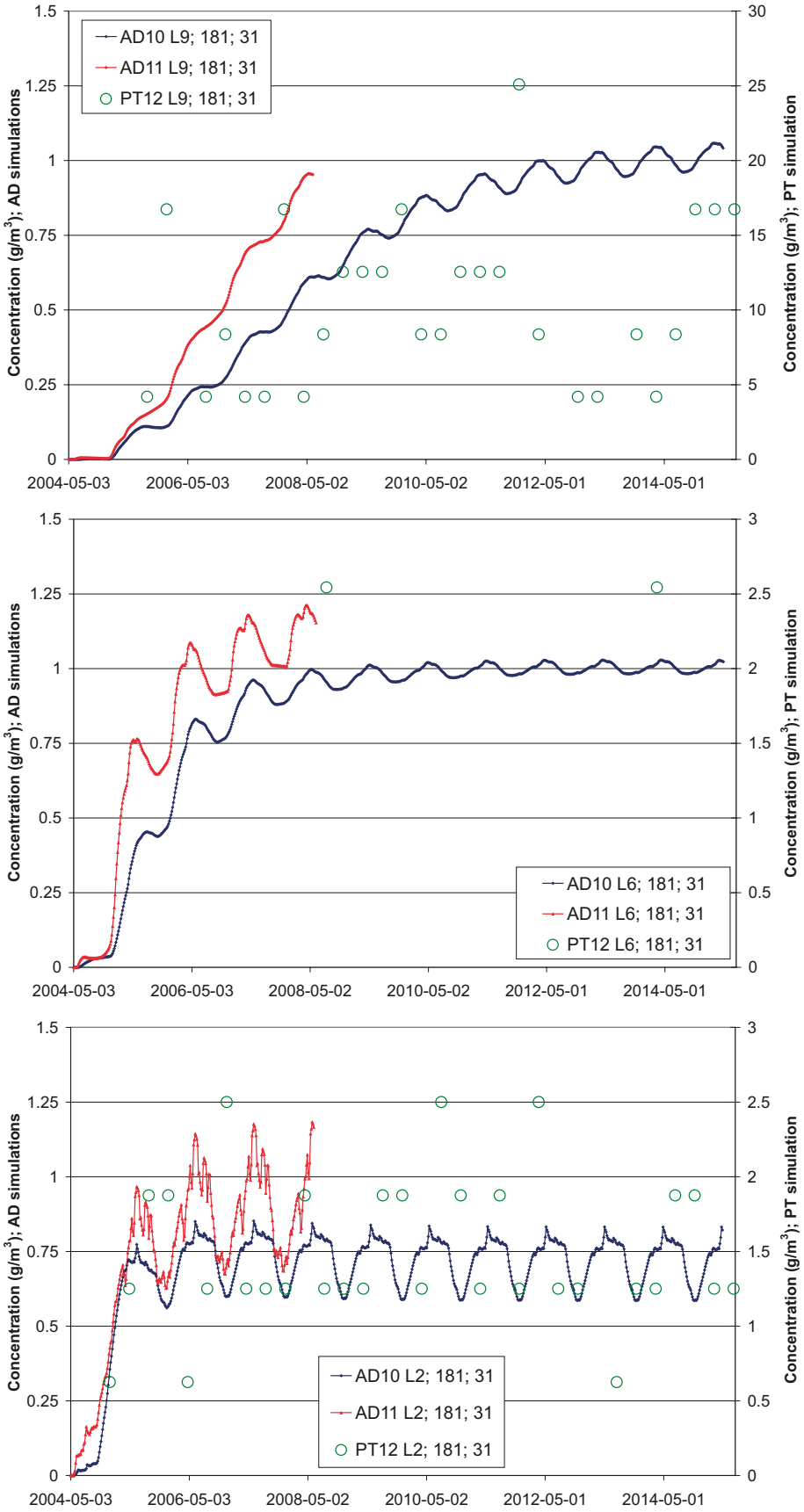

Figure 5-19. *Time series for cell (181,31) for AD10 (blue line), AD11 (red line) and PT12 (green symbols). In the uppermost graph the times series are extracted from layer L9, in the middle graph the time series are from layer L6, and in the lower one time series are from the lower layer in the Quaternary deposits, L2. Note the different y-axis scales for the AD- and PT-results.*

The time series show that the concentration in simulations with dispersion included is lower than for the purely advective simulation. The reason is that the dispersion leads to losses from the advective transport to neighbouring cells. The cells for which the time series are presented were selected with regard to where the particle tracking simulation showed non-zero solute concentrations. In the particle tracking simulation, however, most cells have zero concentration.

Figures 5-20 to 5-22 are surface plots from the three layers L2, L6 and L9. The figures show that the particle tracking simulation have very few cells with non-zero solute concentrations in the lower layers, In Figure 5-20, which is from the Quaternary deposits in layer L2, it is seen that with a higher dispersivity more solute is transported in under the lakes. Figures 5-21 and 5-22 show that the higher the dispersion, the deeper the solute is transported.

5.3 Influence of sorption in the saturated zone

The influence of sorption on the transport results is studied by comparing results from two simulations with different values of the sorption coefficient K_d (*AD6* and *AD7*) with results from *AD3* (no sorption). In *AD6* the K_d-value in the Quaternary deposits (QD) is $1.0 \cdot 10^{-7}$ m^3/g and $1.0 \cdot 10^{-10}$ m^3/g in the bedrock. In *AD7* the K_d-value is zero in the bedrock and $1.0 \cdot 10^{-7}$ m^3/g in the QD, i.e. the same as for *AD6* in the QD.

Figures 5-24 to 5-27 show times series with comparisons between *AD3*, *AD6* and *AD7*. In the figures, the upper graph is from layers L9, the middle graph from L6 and the lower graph from layer L2. The positions of the cells where the time series are extracted are shown in Figure 5-23. Since there is no sorption in the bedrock for *AD7*, the *AD3*-graph and the *AD7*-graph are identical in the bedrock layers L9 and L6. The graphs for the *AD6* simulation show that the effect of including sorption in the bedrock differs between the cells. For example, the effect in cell (149,40) is large, while in cell (175;121) it is small. With sorption included, the solute transport is slower, with a later peak time and lower maximum concentrations. In the QD layer, L2, the effect of including sorption in transport simulations is seen also for *AD7*.

The plots illustrated in Figures 5-28 and 5-29 show the concentration in layer L9 at two different times, after 2 months and after 10 years, for the three simulations *AD3* (top figure), *AD6* (middle figure) and *AD7* (lower figure). It is illustrated that for *AD6*, with sorption included in the bedrock layers, the concentration is lower after 2 months but higher after 10 years, which is consistent with the results from the time series, i.e with sorption included the peak arrival is later. Figures 5-30 to 5-31 indicates the same patterns.

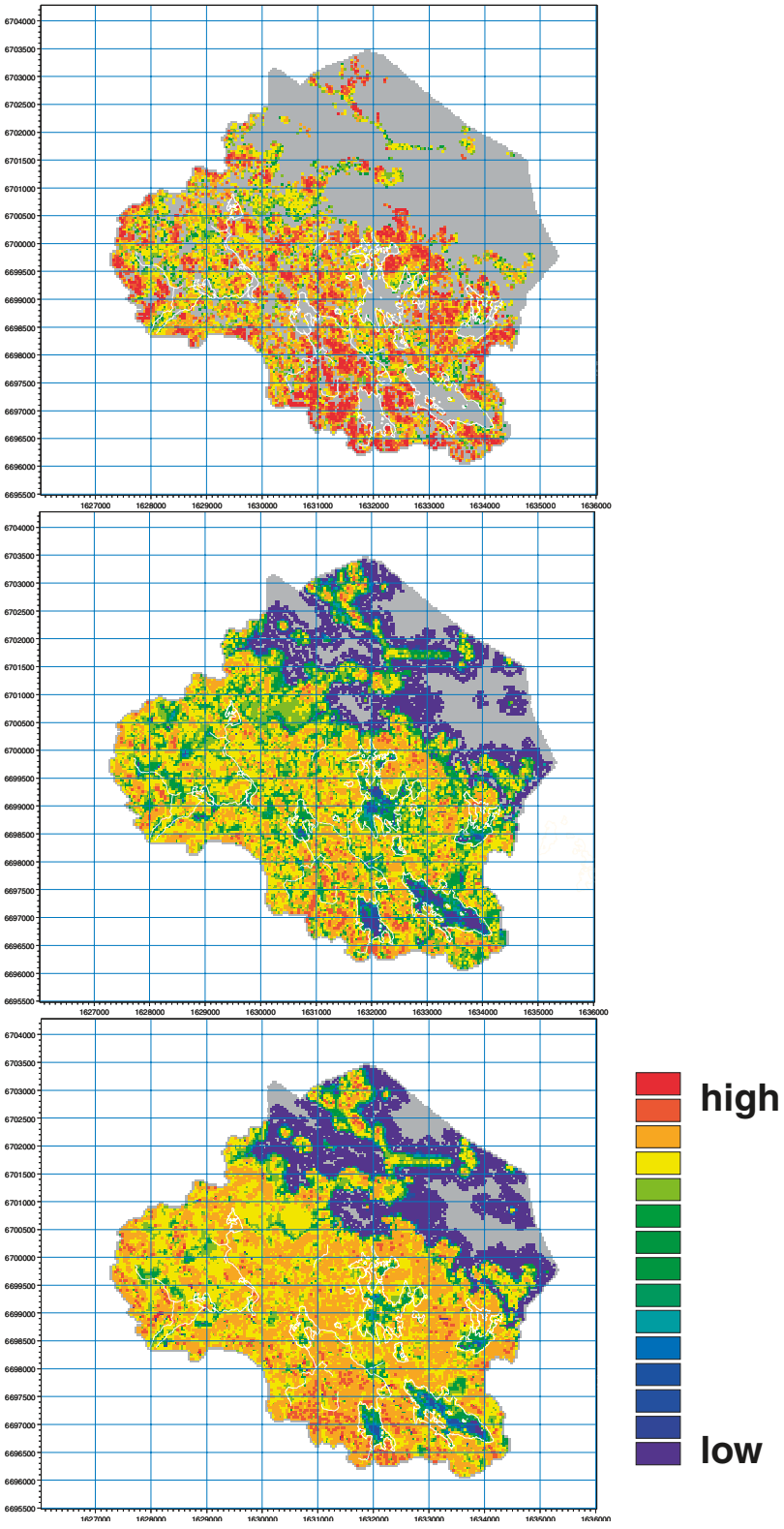

Figure 5-20. *Concentrations after 1 year in the Quaternary deposits in simulations with an infiltration source. The uppermost graph is from PT12, the middle graph from AD10 and the bottom graph from AD11. The shorelines of the lakes and the water courses are marked in the graphs.*

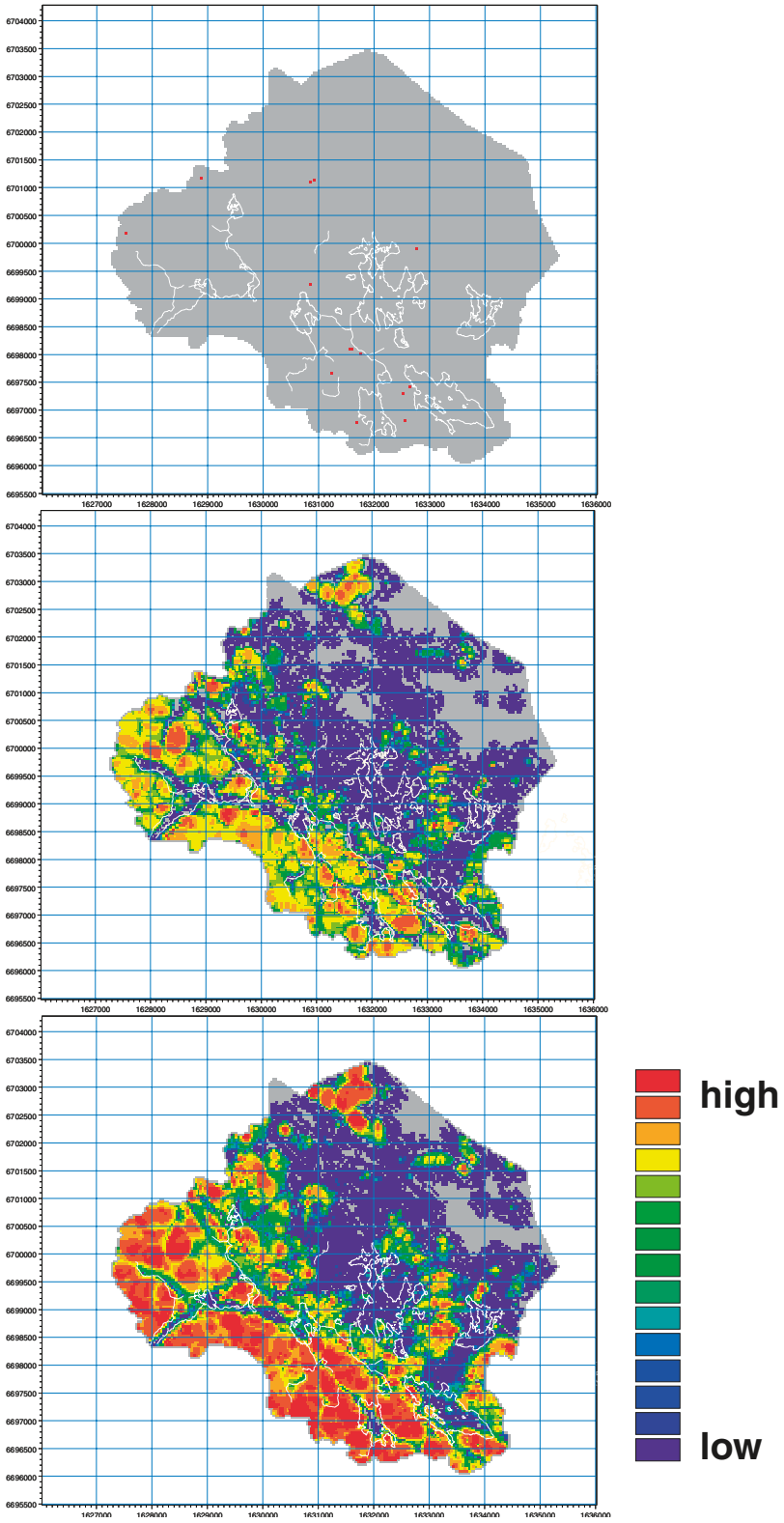

Figure 5-21. *Concentrations after 1 year in a bedrock layer at approximately 70 m.b.s.l. in simulations with an infiltration source. The uppermost graph is from PT12, the middle graph from AD10 and the bottom graph from AD11. The shorelines of the lakes and the water courses are marked in the graphs.*

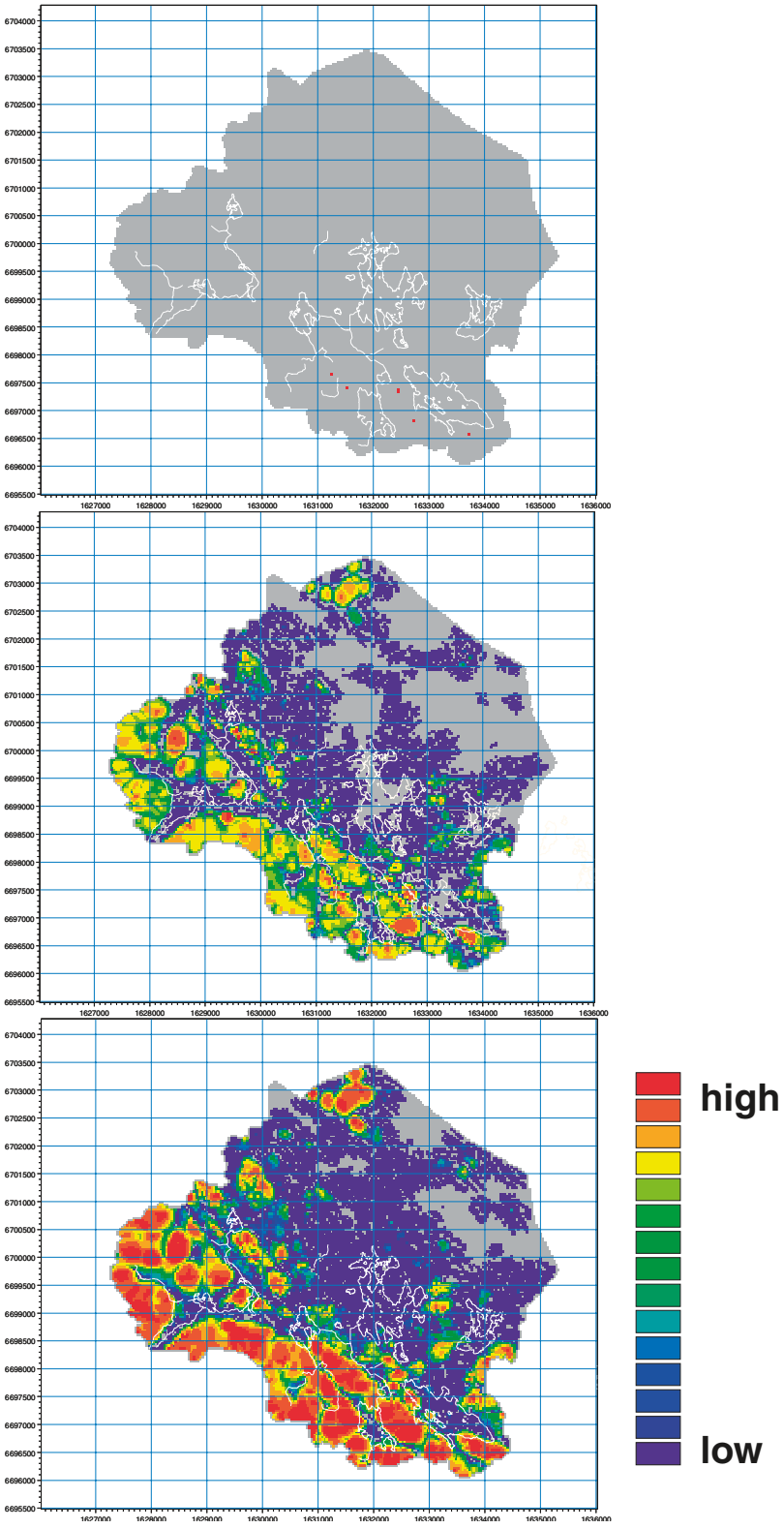

Figure 5-22. *Concentrations after 1 year in a bedrock layer at approximately 130 m.b.s.l. in simulations with an infiltration source. The uppermost graph is from PT12, the middle graph from AD10 and the bottom graph from AD11. The shorelines of the lakes and the water courses are marked in the graphs.*

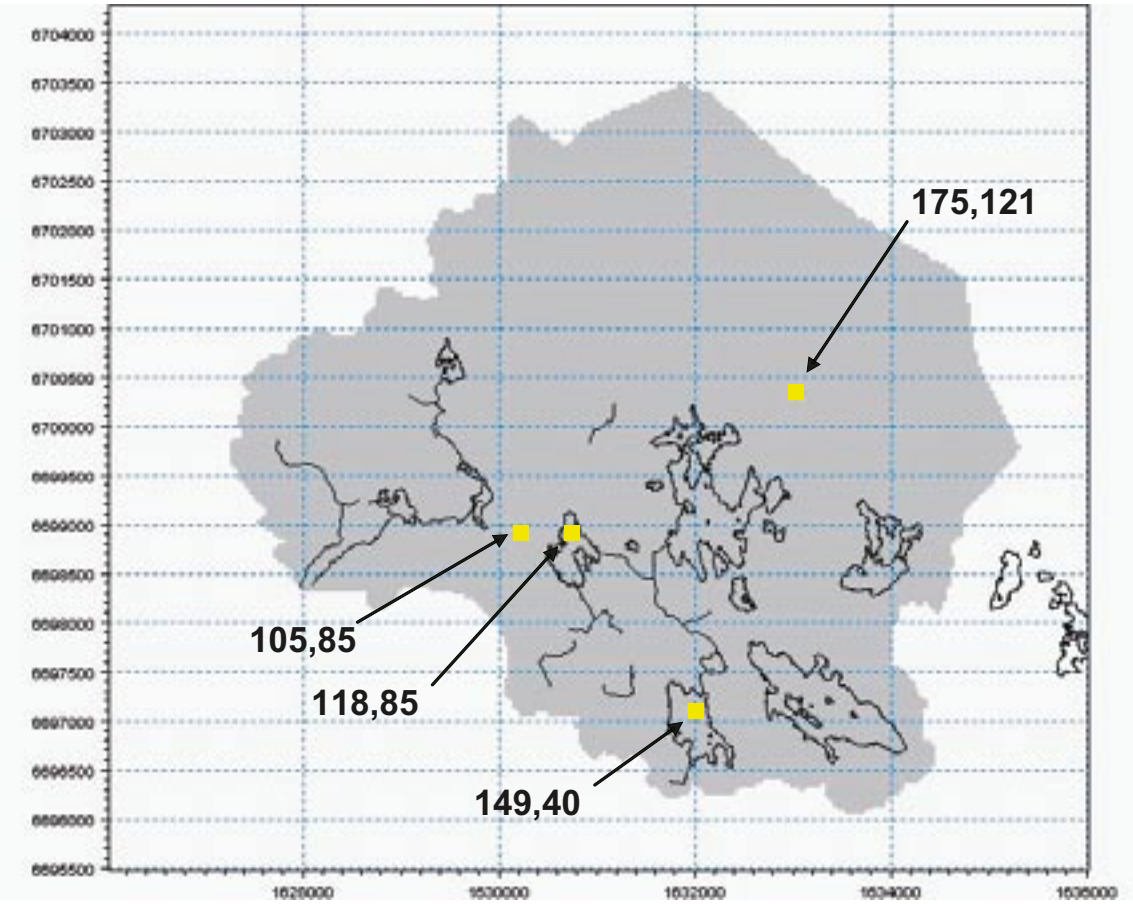

Figure 5-23. *Positions of cells for which time series were extracted in three different layers in simulation cases AD3, AD6 and AD7.*

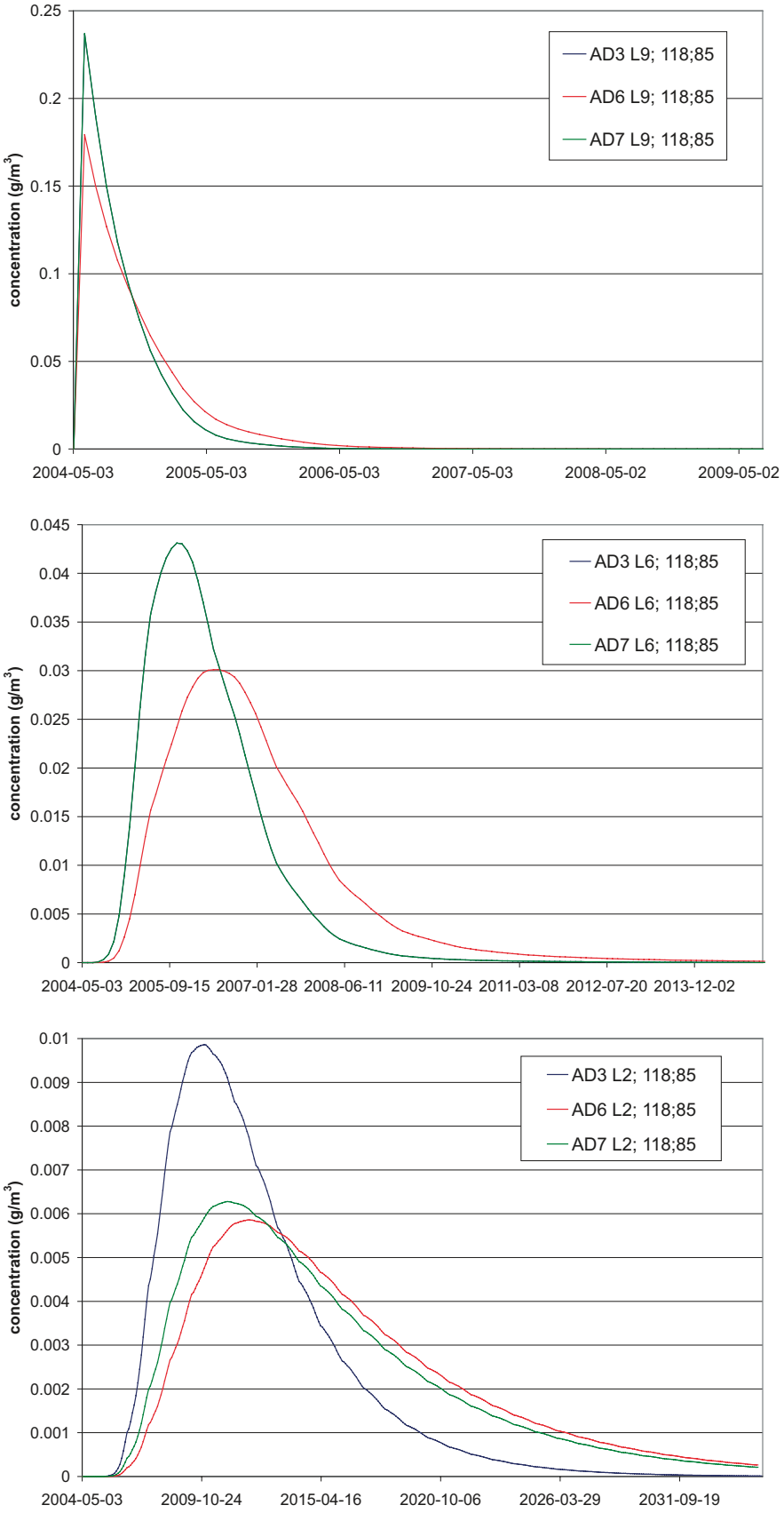

Figure 5-24. *Times series for cell (118,85) for AD3 (blue line), AD6 (red line) and AD7 (green line). In the uppermost graph the times series are extracted from layer L9, which is situated just above the solute source, in the middle graph the time series are from layer L6, and in the lower graph time series are from the lower layer in the Quaternary deposits, L2.*

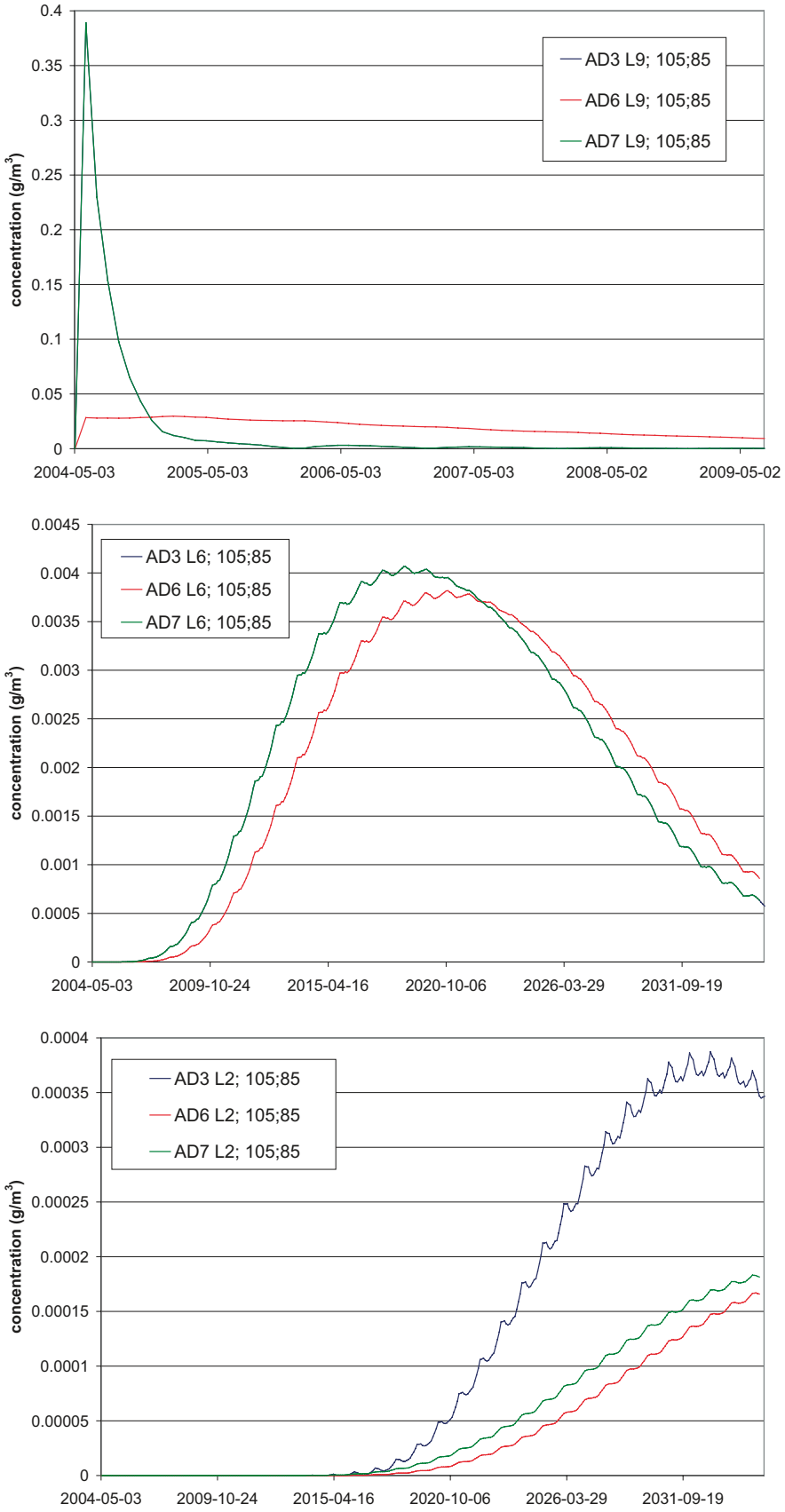

Figure 5-25. *Times series for cell (105,85) for AD3 (blue line), AD6 (red line) and AD7 (green line). In the uppermost graph the times series are extracted from layer L9, which is situated just above the solute source, in the middle graph the time series are from layer L6, and in the lower graph time series are from the lower layer in the Quaternary deposits, L2.*

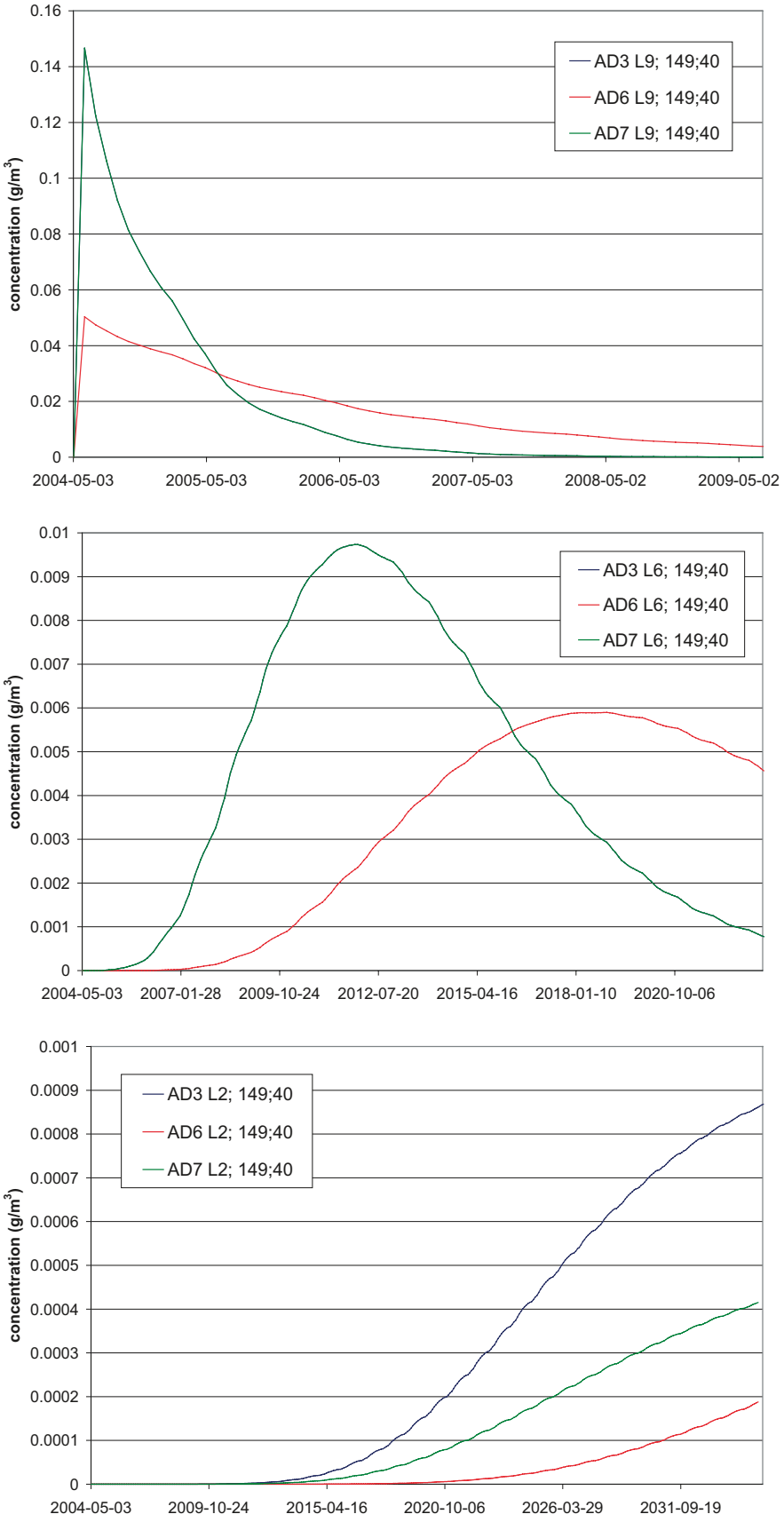

Figure 5-26. *Times series for cell (149,40) for AD3 (blue line), AD6 (red line) and AD7 (green line). In the uppermost graph the times series are extracted from layer L9, which is situated just above the solute source, in the middle graph the time series are from layer L6, and in the lower graph time series are from the lower layer in the Quaternary deposits, L2.*

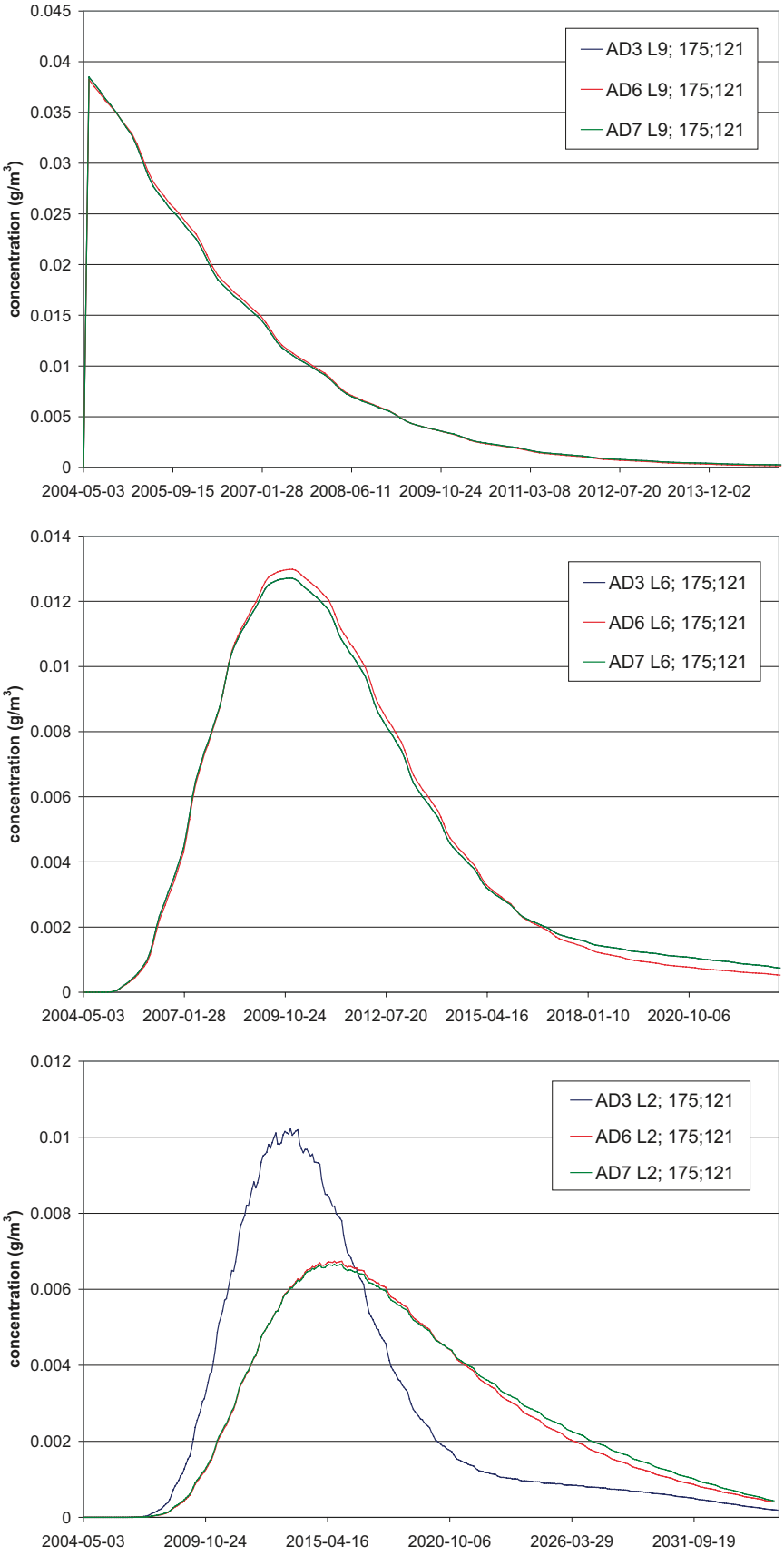

Figure 5-27. *Times series for cell (175,121) for AD3 (blue line), AD6 (red line) and AD7 (green line). In the uppermost graph the times series are extracted from layer L9, which is situated just above the solute source, in the middle graph the time series are from layer L6, and in the lower graph time series are from the lower layer in the Quaternary deposits, L2.*

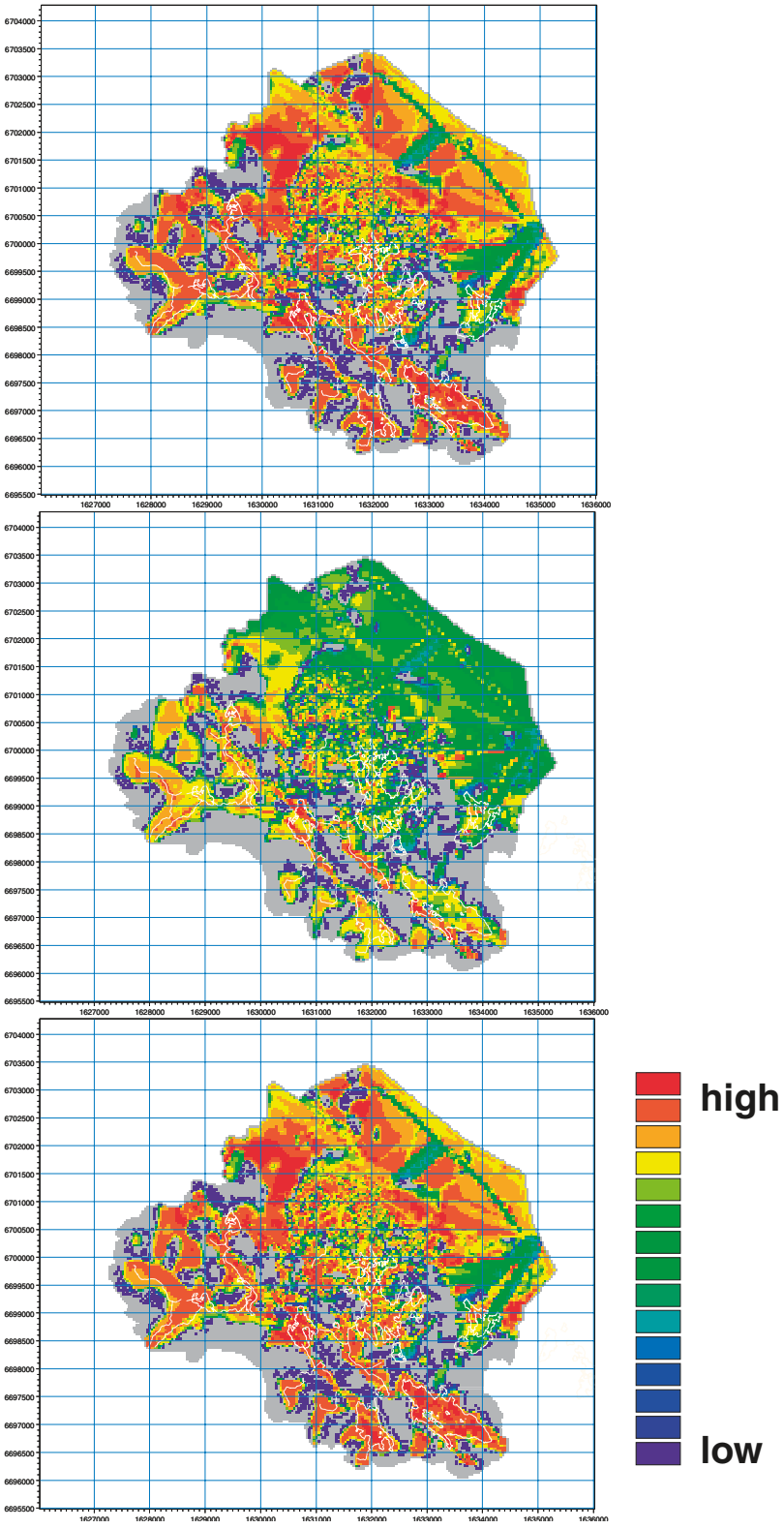

Figure 5-28. *Concentrations in the bedrock after 2 months at approximately 130 m.b.s.l. in simulations with a source in the bedrock. The uppermost graph is from AD3, the middle graph from AD6 and the bottom graph from AD7. The shorelines of the lakes and the water courses are marked in the graphs.*

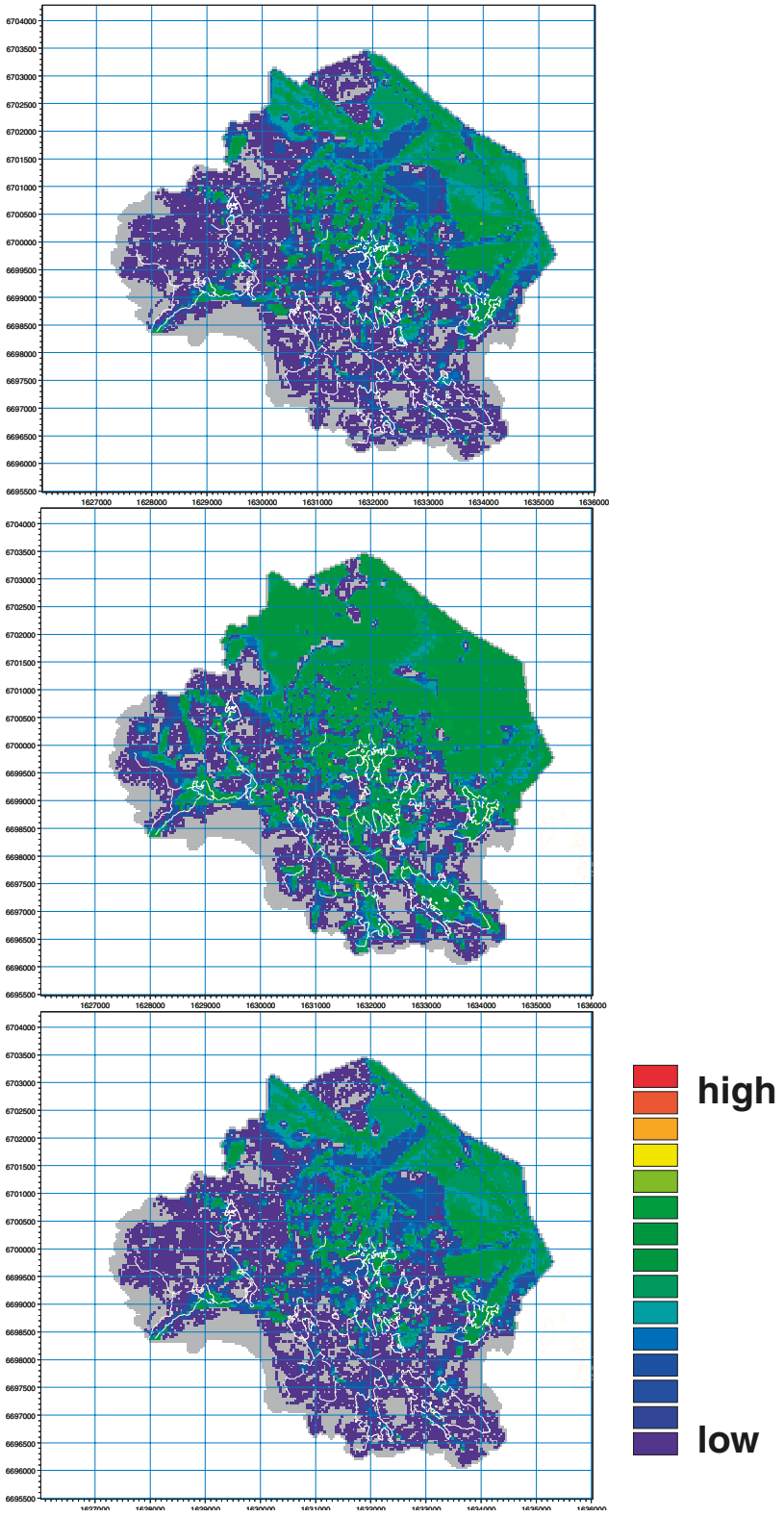

Figure 5-29. *Concentrations in the bedrock after 10 years at approximately 130 m.b.s.l. in simulations with a source in the bedrock. The uppermost graph is from AD3, the middle graph from AD6 and the bottom graph from AD7. The shorelines of the lakes and the water courses are marked in the graphs.*

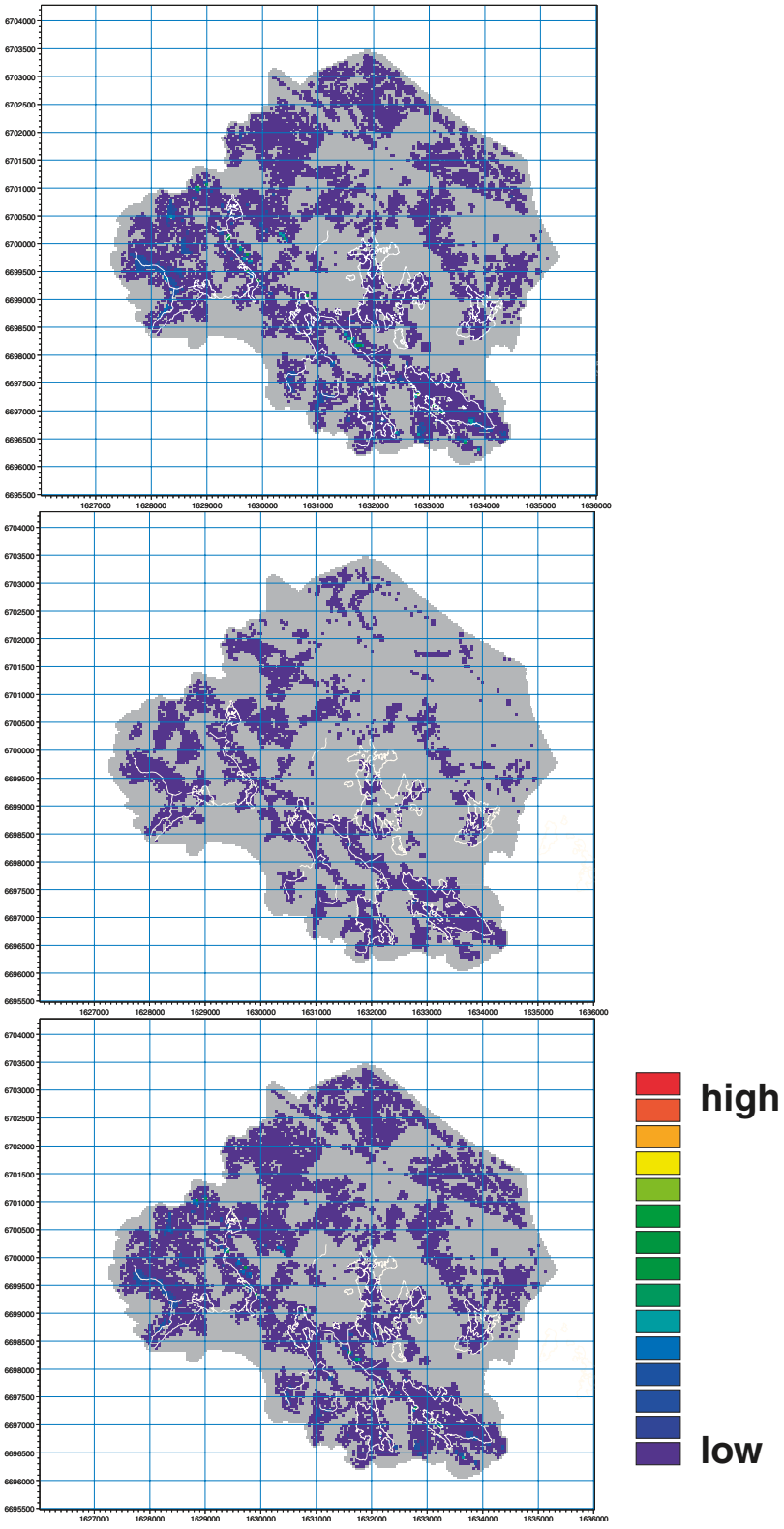

Figure 5-30. *Concentrations in the Quaternary deposits after 2 months in simulations with a source in the bedrock. The uppermost graph is from AD3, the middle graph from AD6 and the bottom graph from AD7. The shorelines of the lakes and the water courses are marked in the graphs.*

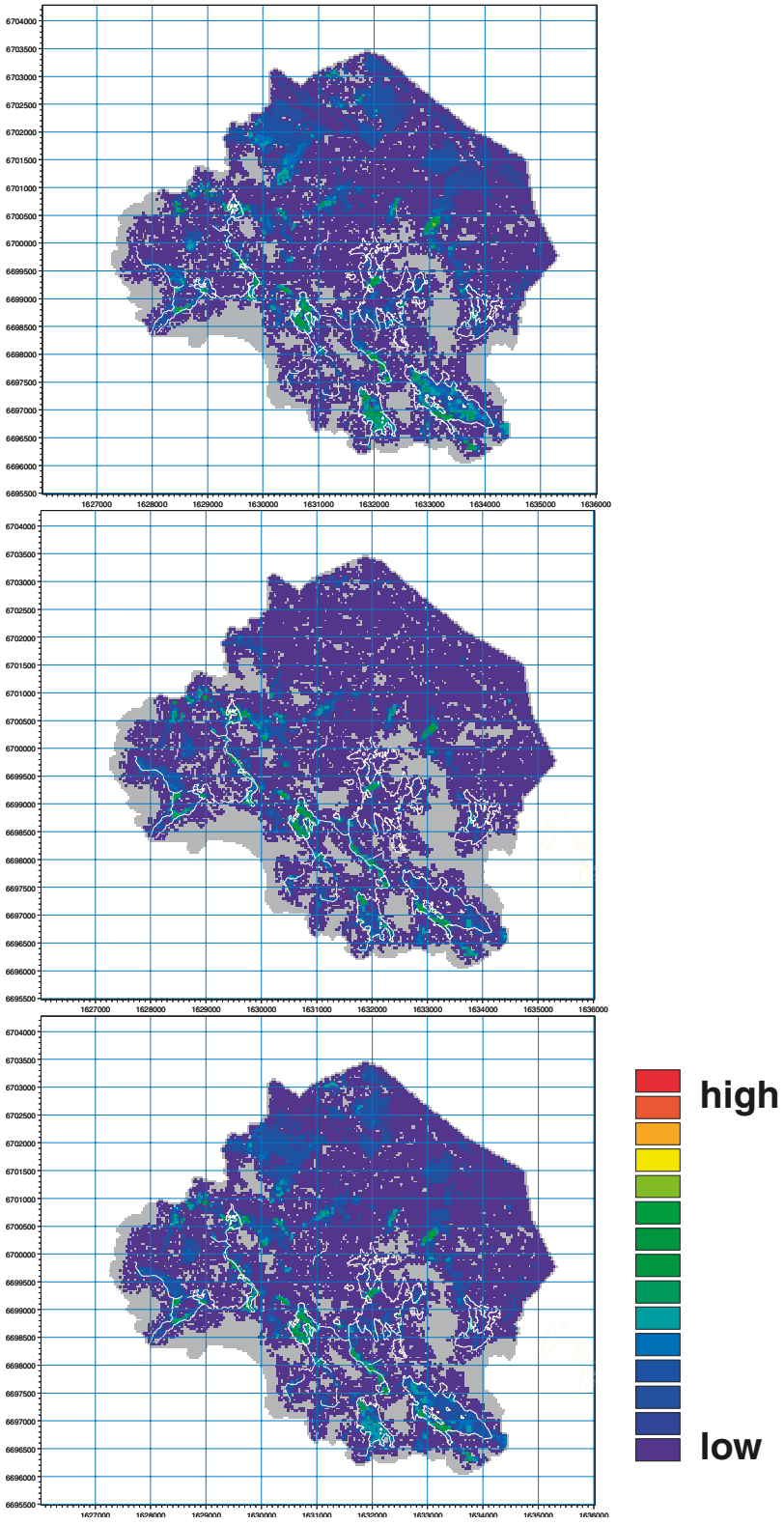

Figure 5-31. *Concentrations in the Quaternary deposits after 10 years in simulations with a source in the bedrock. The uppermost graph is from AD3, the middle graph from AD6 and the bottom graph from AD7. The shorelines of the lakes and the water courses are marked in the graphs.*

6 Simulations based on the final flow model

The simulations presented in Chapters 4 and 5 were all performed based on the "*Final calibrated model*" described in /Bosson et al. 2008, Chapter 4/. However, after these transport simulations were made, the water flow model was re-calibrated and some of the transport simulations were repeated using the updated flow model. Furthermore, additional PT simulations with particle injections within the intended repository area only were made. The results of these repeated and complementary simulations are reported in this chapter.

6.1 Particle tracking results

Two particle tracking simulation cases were performed based on the re-calibrated flow model described in /Bosson et al. 2008, Chapter 6/, each with and without pumping at the SFR facility. The following cases were considered:

- ***PT5-allover:*** One particle was introduced in each cell at 140 m.b.s.l. The particle injection was the same as in the *PT0-bedrock* case discussed in Chapter 4 above.
- ***PT5-repository:*** One particle was introduced in each cell within the area corresponding to the planned repository. Also in this case, the particles were introduced at 140 m.b.s.l. (even though the repository is planned to be built at c. 450 m.b.s.l.). This simulation case was not modelled with the previous version of the flow model.

The simulation period was 300 years in all four simulations, using the calculated transient flow modelling results obtained for the simulated one-year period from October 2003 to October 2004 as input. This means that the model results from the transient MIKE SHE Water movement calculation for this one-year period were cycled 300 times. A similar 5,000-year simulation was also performed with the *PT5-repository* model.

The present results show that many more particles are left in the model after 300 years compared to the Chapter 4 results. This is an effect of the changes in the hydraulic parameters of the rock relative to the previous model, primarily the reduction of the vertical hydraulic conductivity of the upper 200 m of the bedrock. Also, the horizontal hydraulic conductivities have been increased by a factor of ten in the area corresponding to the horizontal fractures/sheet joints in the upper rock /Follin et al. 2007, Johansson 2008/. This has an effect on the horizontal transport of particles in these specific layers, i.e. horizontal transport distances tend to increase. The results for *PT5-allover* with and without pumping in the SFR facility are summarised in Table 6-1. Again, they are expressed in terms of where the particles left the saturated zone, i.e. to which other model compartments or boundaries they went.

The dominating sink without the SFR pumping is the combined Overland flow-Unsaturated zone compartment. It is not possible to separate these two sinks. A large fraction, 65%, of the particles are still left in the model volume at the end of the simulation, which implies that it takes less than 300 years for 35% of the flow paths to reach the ground surface from 140 m depth. When pumping at SFR, the sink "particles removed by wells" is the dominating sink. Specifically, 15% of the particles left the model volume through the drainage in SFR. Only 5% of the particles moves to the sea when pumping in SFR, compared to 14% when the SFR pump is not activated. When pumping in the SFR facility 66% of the particles are left in the model volume after 300 years. However, it should also be noted that the travel times are longer than the time SFR will be in operation, implying that this is not a realistic case to assess.

Table 6-1. Distribution of particles on different sinks for particle tracking based on the re-calibrated MIKE SHE flow model with and without pumping in the SFR facility.

Sink	PT5-allover, no SFR Number of particles	%	PT5-allover, with SFR Number of particles	%
Particles removed to OL-UZ*	3,460	15	2,480	11
Particles removed directly to streams	817	4	468	2
Particles removed by drain to streams	415	2	352	1
Particles gone to the sea	3,349	14	1,149	5
Particles removed by wells (SFR)	0	0	3,404	15
Particles left in model	14,826	65	15,014	66
Sum	22,867	100	22,867	100

*OL-UZ is the combined Overland flow-Unsaturated zone sink.

Illustrations of the numbers in Table 6-1 are shown in Figures 6-1 and 6-2. The figures show the position of each particle where it left the saturated zone and moved to a specific sink; results are shown both for the case with and for that without SFR. The different sinks are marked with different colours. The blue dots represent the particles that moved to the combined Overland flow-Unsaturated zone sink. Since the majority of the blue dots are situated in the lakes and close to water courses, i.e. in water-saturated areas, it is concluded that the majority of the particles registered in this sink have moved to the Overland flow compartment. When pumping at SFR, the majority of the particles that have gone to sinks outside the land part of the model area have been removed by the pump in SFR.

Figure 6-3 shows the accumulated particle counts for each cell in the layers with their lower boundaries at 150, 130, 110 and 90 m.b.s.l. at the end of the simulation. To the left the case without the SFR drainage is presented and the case with the SFR drainage is presented to the right. The accumulated particle count is a way to present the density of the flow paths. Each time a particle passes a cell the accumulated particle count of that cell is increased by one. This means that the higher the value for a cell the more particles have travelled along flow paths going through that specific cell. The particle count reflects both horizontal and vertical transport, and since flow is transient a particle can pass the same cell several times.

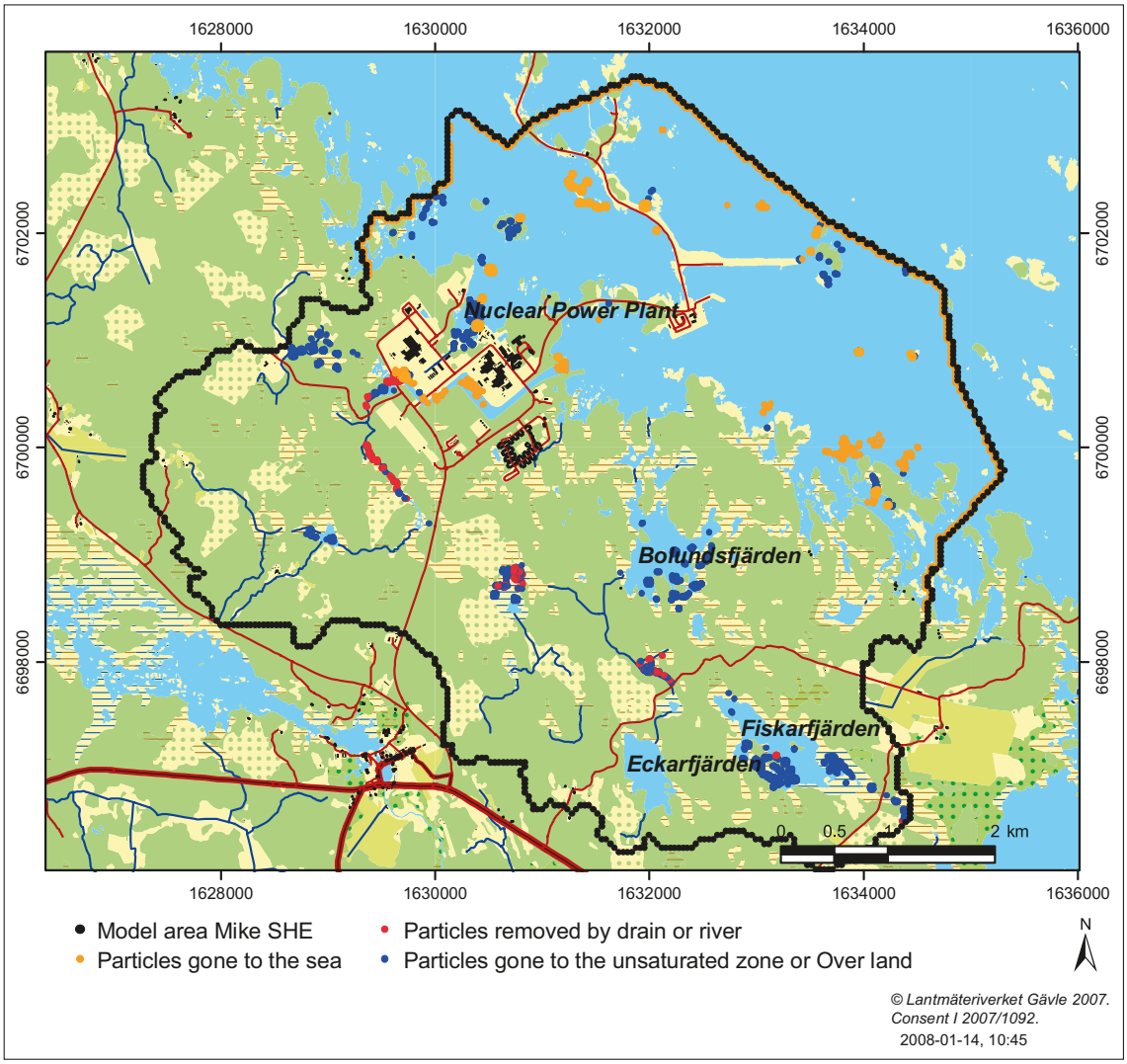

Figure 6-1. *Sinks for the particles in case PT5-allover. The figure presents the results obtained without the SFR drainage in the model.*

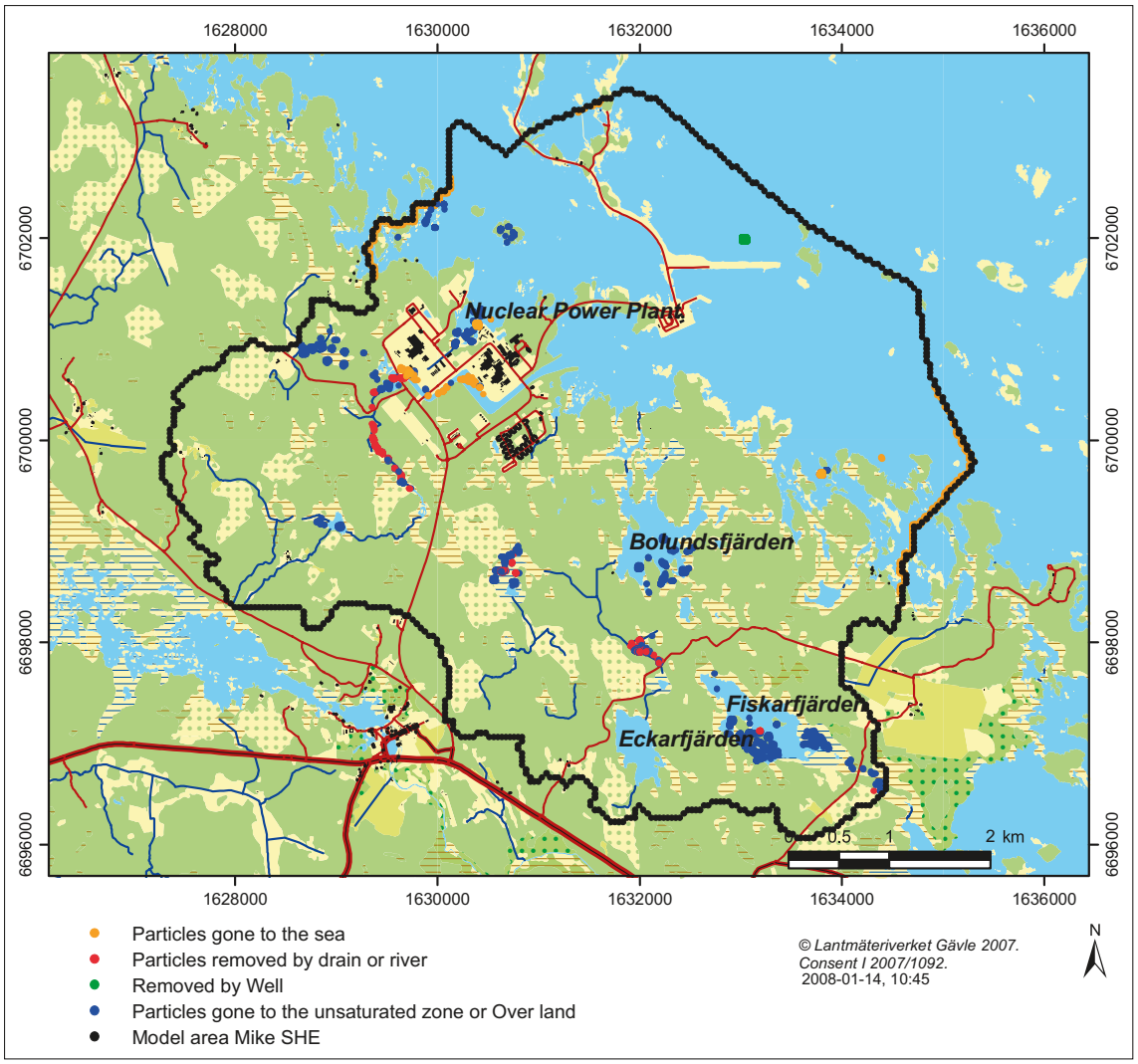

Figure 6-2. *Sinks for the particles in case PT5-allover. The figure presents the results obtained with the SFR drainage activated in the model.*

The particles were introduced in the layer extending from 130 to 150 m.b.s.l. Since one particle has been introduced in each cell at this level, the minimum accumulated particle count in this layer is 1 (see the uppermost graphs in Figure 6-3). Pink colour indicates cells where no particles have passed. As shown in Figure 6-3, the flow paths concentrate to specific areas on their way towards the surface. At 110 m.b.s.l. one layer of horizontal fractures/sheet joints are represented in the model. It is seen that the particles concentrate there, as indicated by the red areas in the figure. The same pattern is seen for both cases, with and without the SFR facility included. When pumping in SFR, particles released in the north-eastern part of the model area move towards SFR. The majority of the particles move towards SFR in the layer at 110 m.b.s.l. Above this level only 40% of the cells that received a particle at 110 m.b.s.l. are hit by a particle.

In case *PT5-repository*, 1,501 particles were released at 140 m.b.s.l. inside the area corresponding to the planned repository. After the 300-year simulation period only 10% of the particles have left the model volume; all the particles that have left the model volume have gone to the sea. When pumping at SFR, 18% have left the model volume through the pumping in SFR.

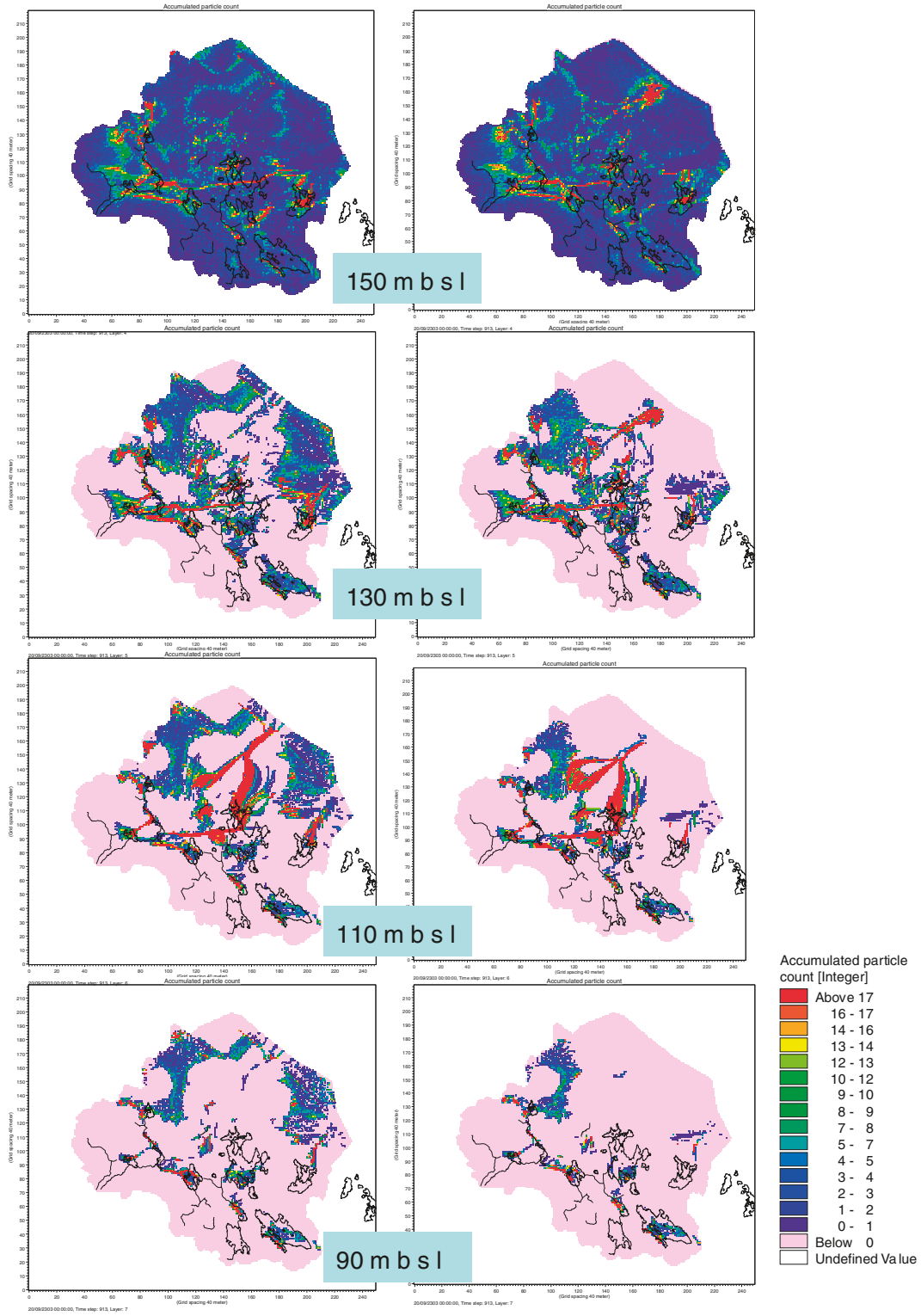

Figure 6-3. *Accumulated particle counts in layers with lower boundaries at 150 (injection layer), 130, 110 and 90 m.b.s.l. The particles move towards the fractures/sheet joints in the layer at 110 m.b.s.l. The figure to the left presents the PT5-allover results without the SFR drainage, and the figure to the right the results from the PT5-allover case with the SFR drainage was activated.*

The remaining 82% of the particles are still left in the model volume. For both cases, with and without SFR, the major part of the particles moves toward the sea at 110 m.b.s.l., see Figures 6-4 and 6-5. The particles concentrate to the sheet joint areas and the horizontal transport is dominating. Above this level only a few cells are passed by a particle. When pumping in SFR, no particles reach higher than 70 m.b.s.l. Thus, there are no exit points at the surface after 300 years simulation time when pumping at SFR. In the case where the pumping in SFR is not activated, a few particles reach the sea. These exit points are located close to the shoreline.

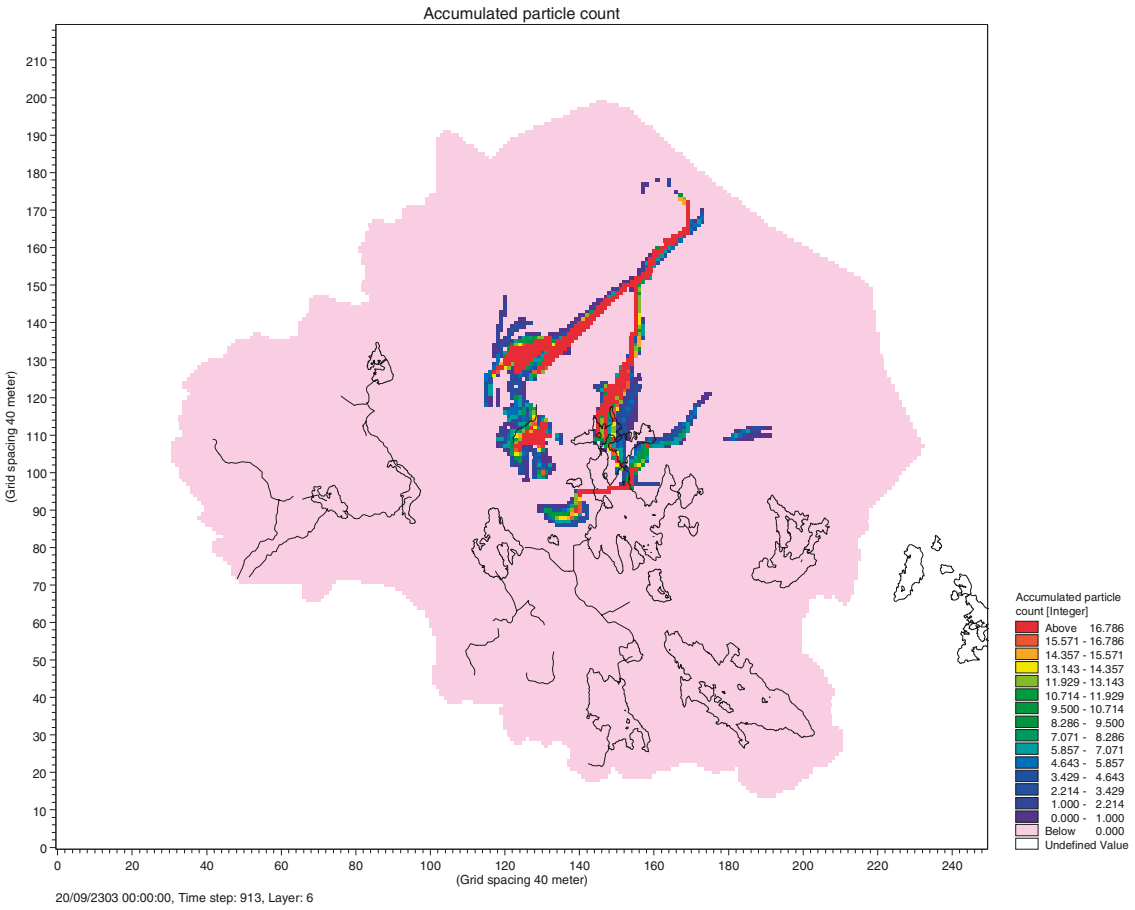

Figure 6-4. *Accumulated particle count at 110 m.b.s.l. for the PT5-repository model without the SFR pumping included in the model.*

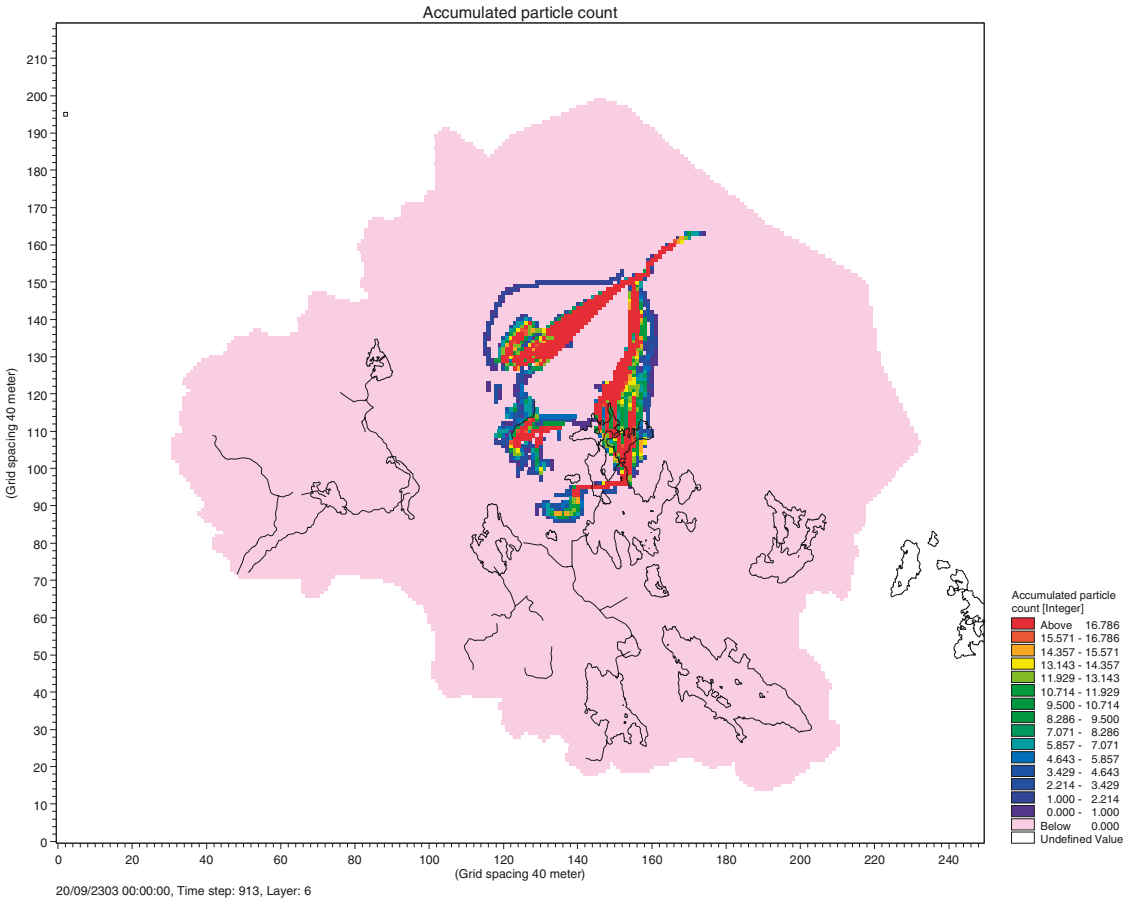

Figure 6-5. *Accumulated particle count at 110 m.b.s.l. for the PT5-repository model with the SFR pumping included in the model.*

Since so many particles were still left in the model volume after 300 years, an additional longer simulation was run using the *PT5-repository* setup. This particle tracking simulation was run for a period of 5,000 years. The exit points at the surface after 5,000 years are shown in Figure 6-6. As a comparison the exit points after 300 years are also shown in the same figure. The transport times are very long and even after 5,000 years the majority, 81%, of the particles are still left in the model volume. Still no exit points are found in the land part of the model area. All the particles exit the model volume to the sea. The results show that 79 particles, 5% of the total number of particles introduced, are stuck in the marine sediments. Apart from them, no particles are found in the upper calculation layers. All the other particles that are left in the model after 5,000 years are found in the deeper bedrock between layer 8 at 110 m.b.s.l. and layer 14 at 600 m.b.s.l.

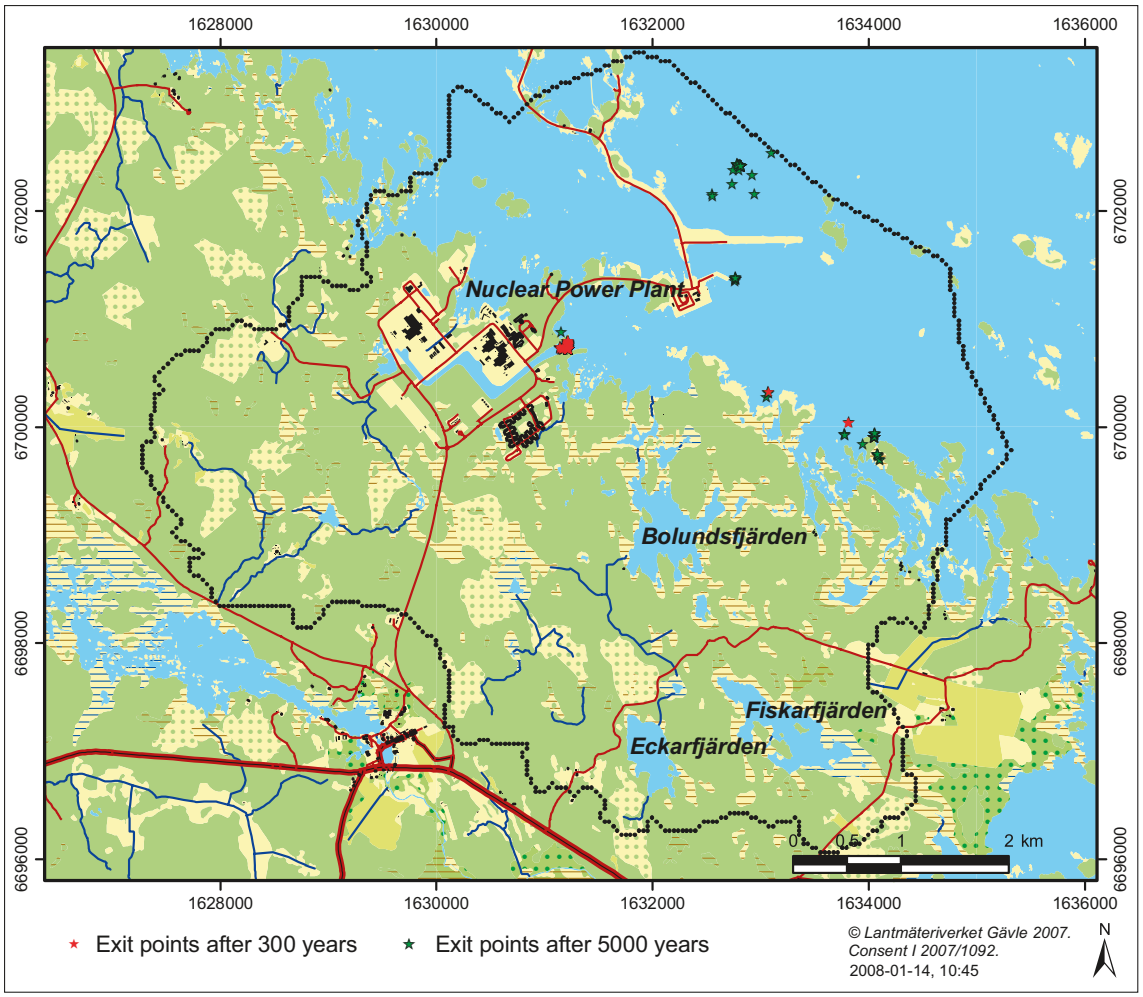

Figure 6-6. *Exit points at the surface or sea bottom after 5,000 years. As a comparison, the exit points after 300 years are also marked in the figure.*

6.2 Advection-dispersion modelling results

Two of the AD transport simulations discussed in Chapter 3, *AD3* and *AD10*, were performed also with the re-calibrated flow model. In both these simulations, only solute transport in the saturated zone was considered. The advective transport was modelled by use of the flow field from the re-calibrated flow model where SFR was not included. The results from the MIKE SHE Water movement calculations are used by cycling the calculated flow for one year, from May 2004 to May 2005.

In the first simulation, *AD3*, the solute source is located in a bedrock layer at a level of approximately 140 m.b.s.l. The source is applied all over the model area with a concentration of 1 g/m^3. The initial concentration in the model is 0 g/m^3. The source is applied for one month, starting at the time of the simulation. The solute dispersion is isotropic with a longitudinal dispersivity of 0.2 m and a transverse dispersivity of 0.01 m. The dispersion coefficients correspond to a very low degree of solute dispersion.

Figures 6-7 to 6-9 show simulation results for three different layers at six different times each. Two of the layers are bedrock layers and one is a layer in the Quaternary deposits. The figures show concentrations after 2 months, and 2, 10, 20, 100 and 200 years of simulation time.

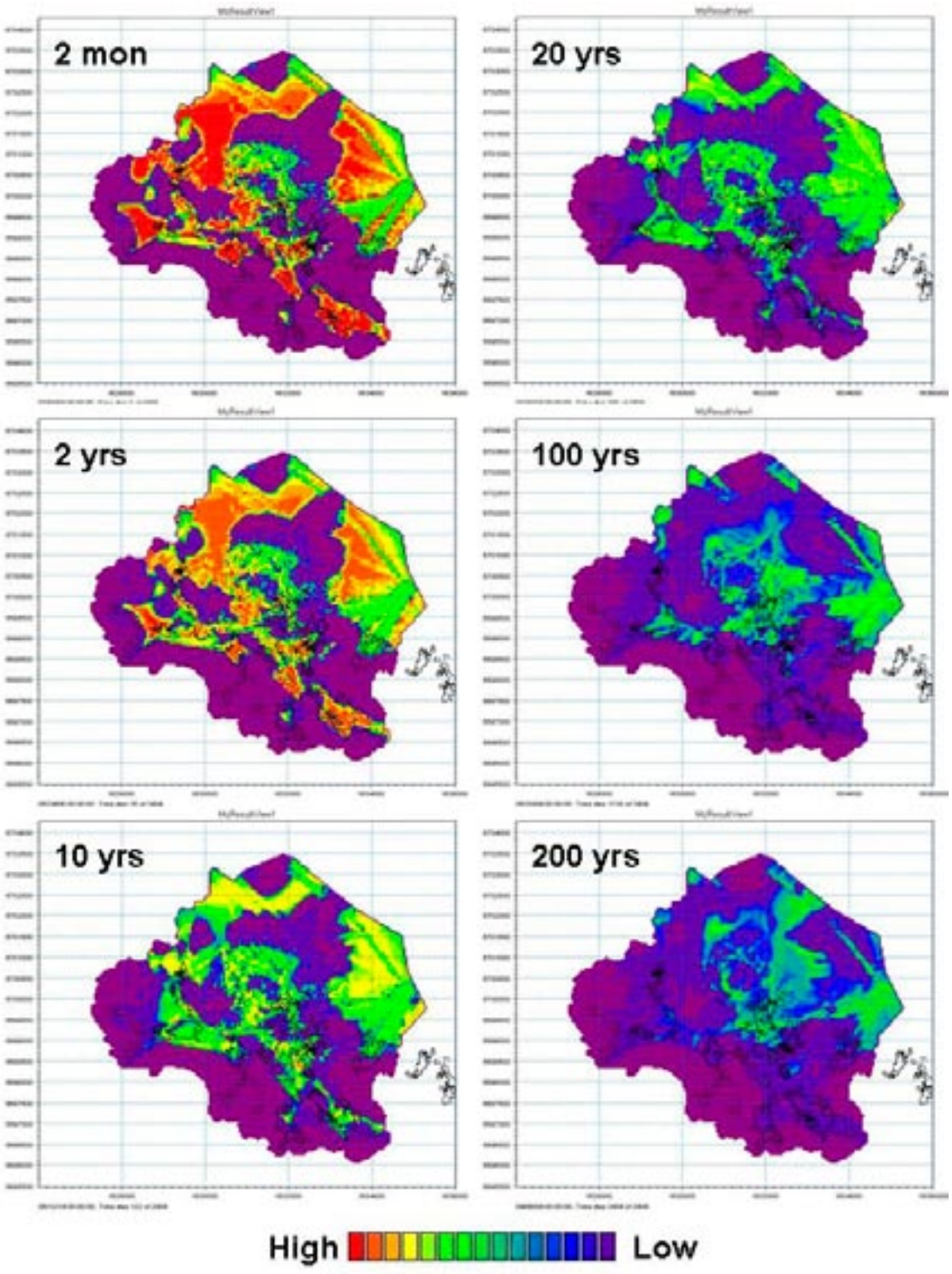

Figure 6-7. *Results of advection-dispersion simulation with a uniform pulse solute source in the bedrock showing concentrations in the bedrock at approximately 130 m.b.s.l. at different times after solute injection.*

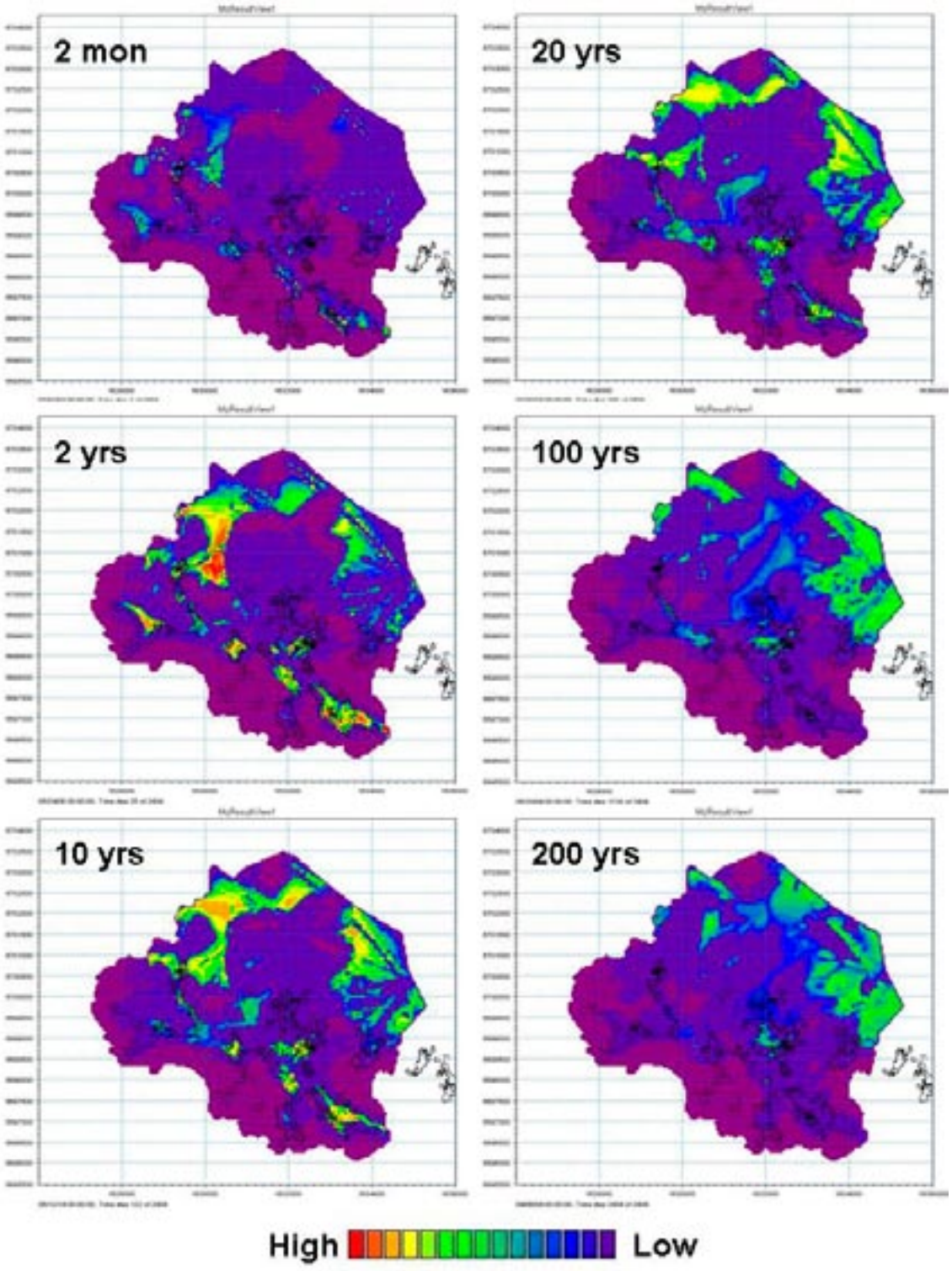

Figure 6-8. *Results of advection-dispersion simulation with a uniform pulse solute source in the bedrock showing concentrations in the bedrock at approximately 70 m.b.s.l. at different times after solute injection.*

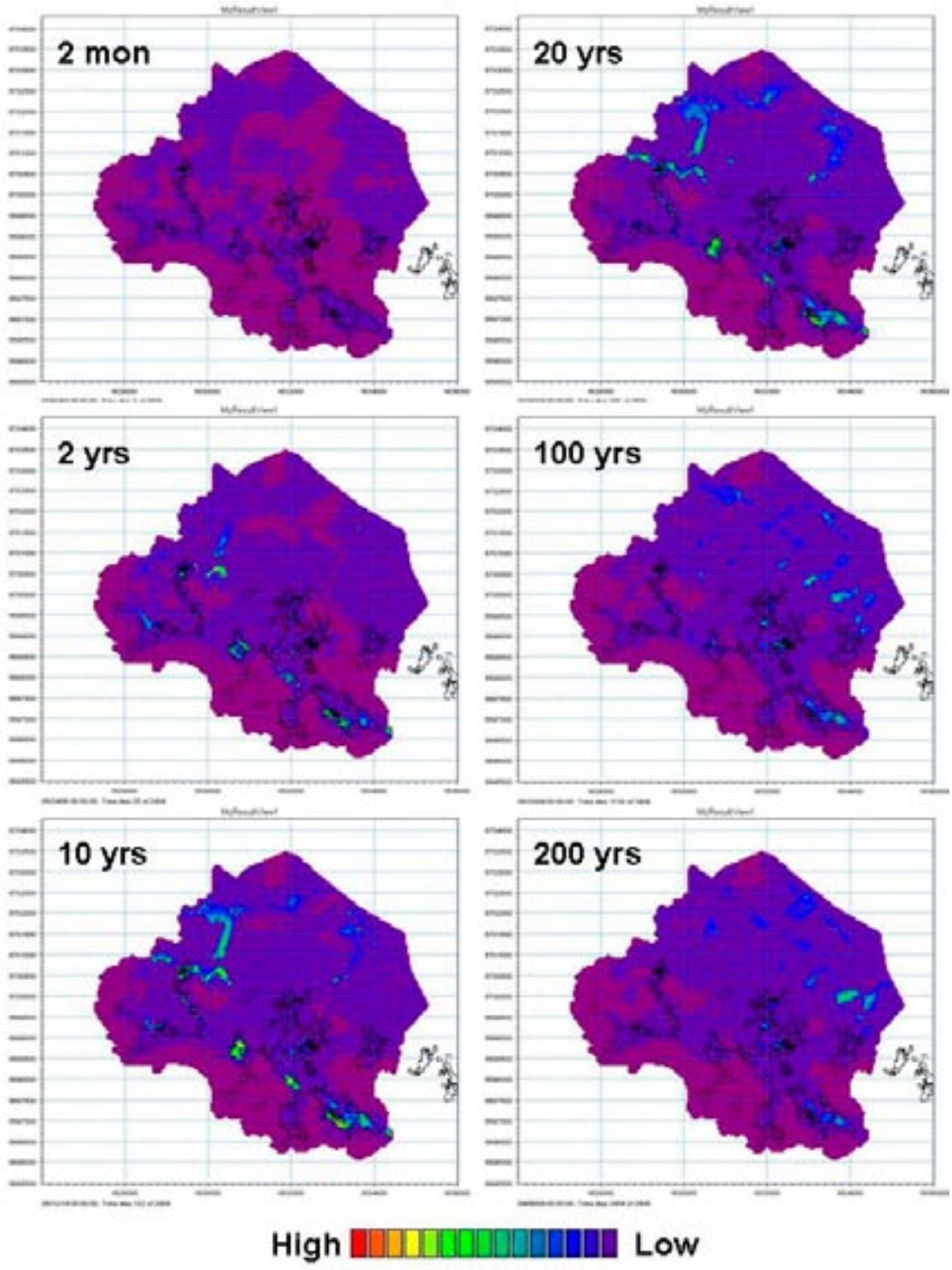

Figure 6-9. *Results of advection-dispersion simulation with a uniform pulse solute source in the bedrock showing concentrations in the Quaternary deposits at different times after solute injection. The purple colour is zero concentration and the dark blue colour indicates a very low concentration.*

The scale of the solute concentration is the same in all figures. Figure 6-7 shows concentration plots from a bedrock layer at approximately 130 m.b.s.l. The layer is situated just above the layer with the hypothetical solute source. The figure illustrates that the solute concentration is high in the beginning of the simulation but then decreases as the pollution is transported away from the layer. It is also seen that the concentration initially is high in connection to the more conductive zones in the bedrock. As time progresses, the concentration in the conductive zones decreases and instead the concentration is higher in connection to the sea.

Figure 6-8 shows concentration plots from a bedrock layer at an elevation of approximately 70 m.b.s.l. containing areas with high horizontal hydraulic conductivities north west of Lake Bolundsfjärden and towards the sea. The figure illustrates that initially the concentration is high in the fracture zones under the lakes and watercourses. After 20 years the concentrations in the most conductive zones have decreased, whereas concentrations have increased in areas covered by the sea. After 200 years, the concentration pattern is concentrated to the sea areas.

Figure 6-9 shows concentration plots from calculation layer 2, which is the lower layer in the Quaternary deposits containing sea bottom sediments. The figure shows that after two months almost no solute has yet reached the Quaternary deposits. It can be seen that the solute has reached the upper part of the model after two years. The figure shows that the solute is mainly transported upwards through the fracture zones that are connected to the lakes and water courses. This is further established in the plots showing concentrations after 10 and 20 years, where it is also seen that the lake areas are solute recipients. After 100 years the concentrations are decreasing.

A comparison between results from simulations with the PT module and the AD module shows that the overall pattern is the same. In Figure 6-3 the accumulated particle count at a level of 130 m.b.s.l. is illustrated. The left figure is based on the flow results without the SFR drainage included. Figure 6-7 show results from the AD simulation based on the same flow results and at approximately the same depth. The figures illustrate that the patterns are very similar.

To further illustrate the solute transport pattern, a vertical concentration profile through the model area is analysed. The profile is taken according to Figure 6-10. Figure 6-11 shows the vertical profile at six different time steps, i.e. 2 months and 2, 10, 20, 100 and 200 years. The white band at a level of about 140 m.b.s.l. is the layer in which the solute source is applied. It is illustrated in the figure that parts of the applied solute mass are transported downwards. The areas in which the solute is transported downwards are located in topographically relatively higher areas, which act as recharge areas. The solute mass moving upwards is mainly transported towards the sea and the lake areas.

Figure 6-12 is the same figure as Figure 6-11 but looking only at the upper part of the model, above the pollution source. The figure further shows that the solute transport mainly takes place towards the sea and the lake areas. It also illustrates that some solute is transported rapidly while some is moving slowly, which reflects the heterogeneity of the flow field.

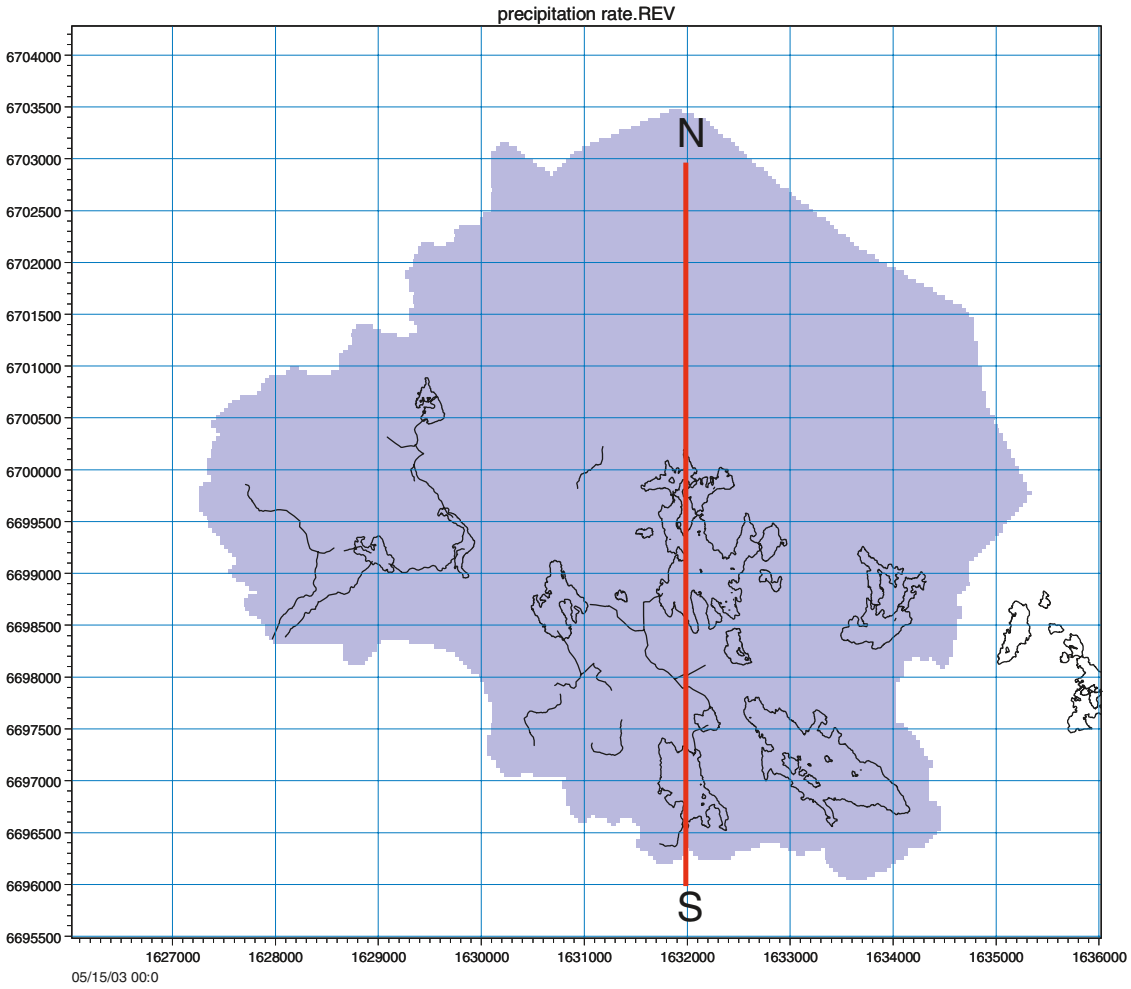

Figure 6-10. *Position of profile through the model area in the north-south (N-S) direction.*

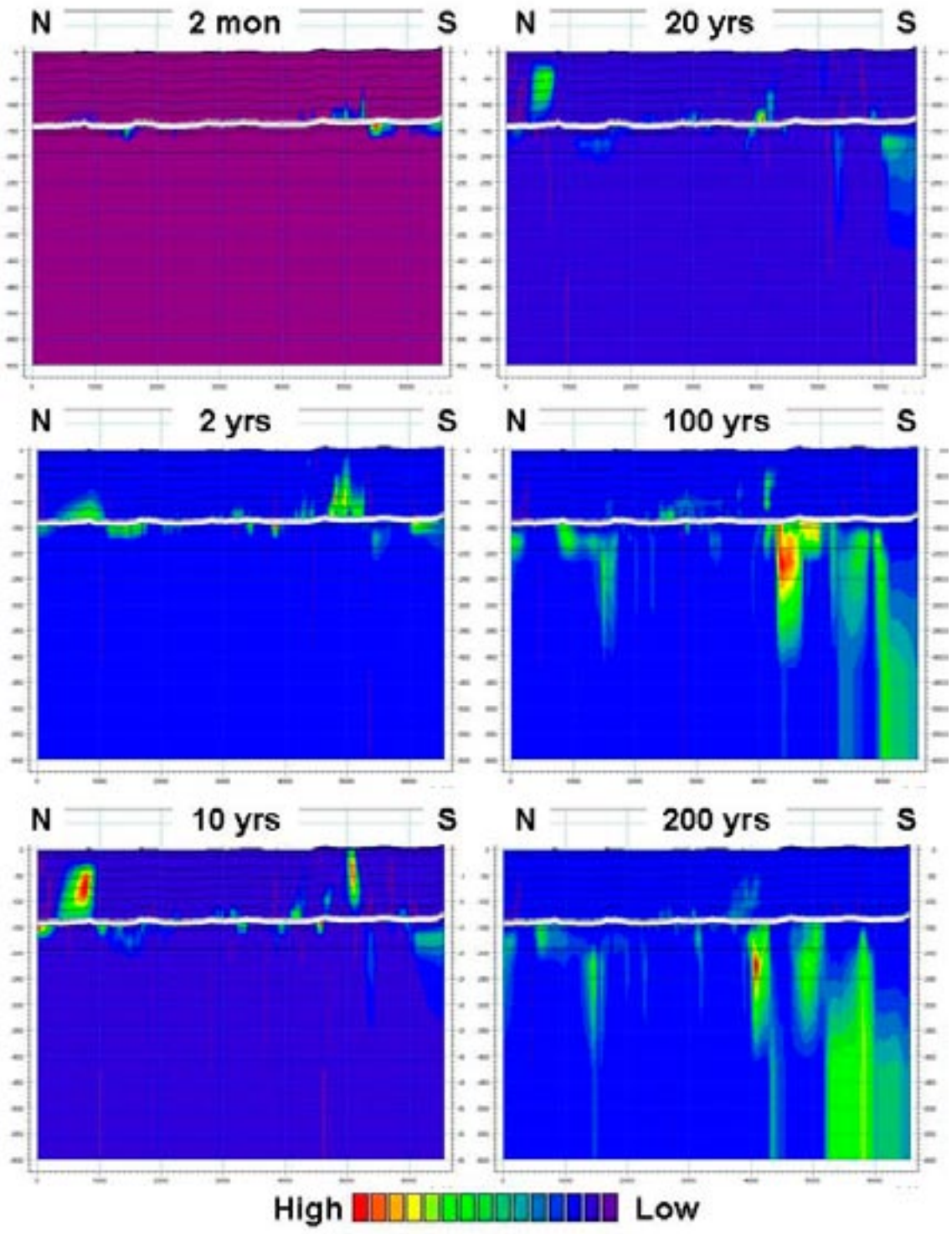

Figure 6-11. *Profile through the model area (location indicated in Figure 6-10) showing the advection-dispersion solute concentrations at six different times during the simulation.*

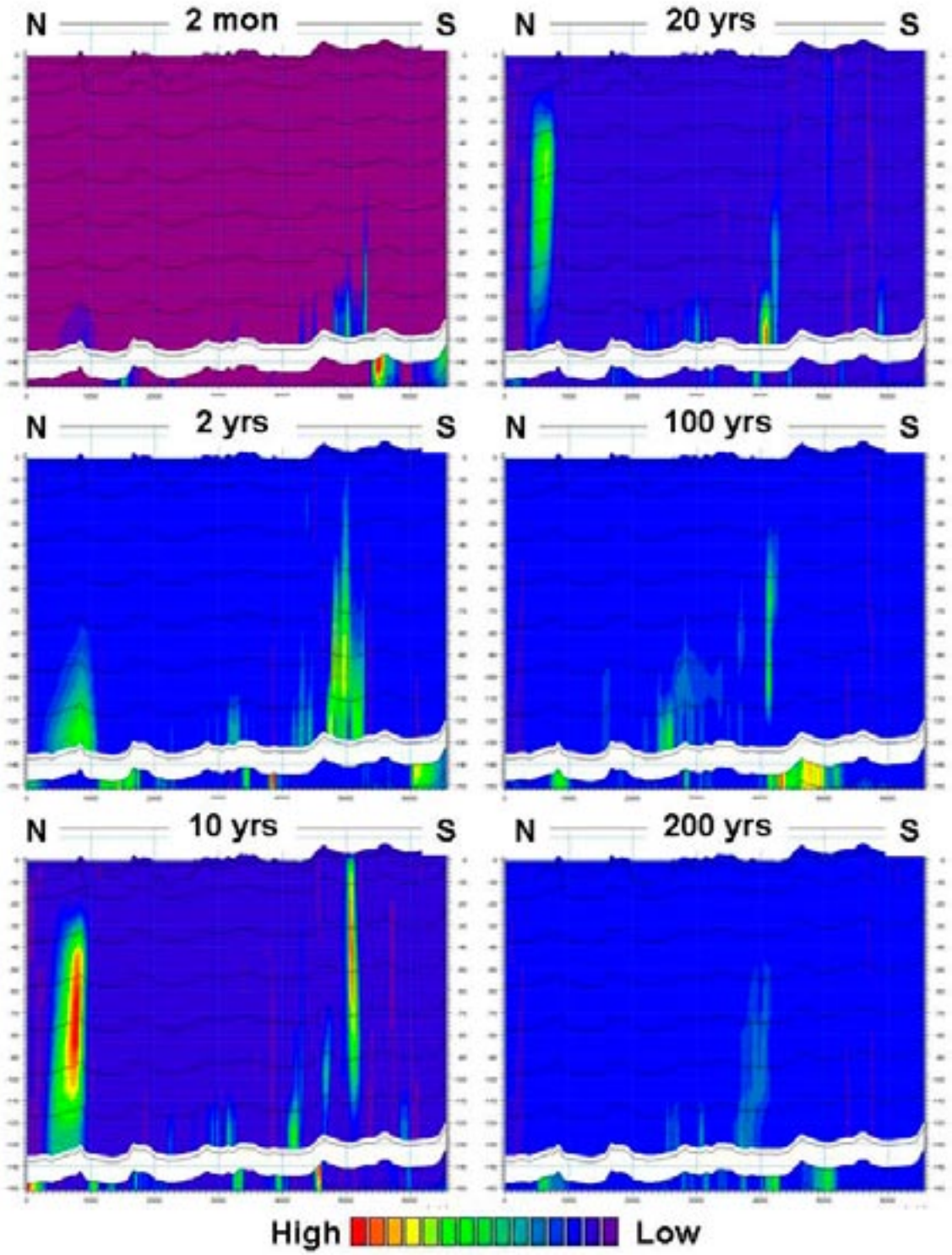

Figure 6-12. *Profile through the model area (location indicated in Figure 6-10) showing the advection-dispersion solute concentrations in the upper 150 m at six different times during the simulation.*

As discussed in /Bosson et al. 2008, Section 3.2.1 and Figure 3-5/, zones with high horizontal hydraulic conductivities in the bedrock exist within the model area. In these areas, solute transport is mainly directed horizontally towards the sea. Figure 6-13 shows the position of the profile for which concentrations are displayed in Figure 6-14. In this profile, there are zones with high horizontal conductivities at levels of approximately 70 and 100 m.b.s.l. In Figure 6-14, concentrations along the profile are illustrated for simulation times 10, 20, 50, 100, 150 and 200 years. The horizontal transport towards the sea is clearly seen in the results.

The figures illustrate that solute is moving mainly in the vertical direction until it reaches the area with the higher horizontal conductivity, located at approximately 100 m.b.s.l. The solute is then transported mainly in the horizontal direction. After about 100 years, parts of the solute mass are transported to the upper layer with high horizontal conductivity, located at a level of approximately 70 m.b.s.l., and at that level it starts moving towards the sea.

The differences in transport velocity between different sub-areas within the model area are illustrated by examples of time series in Figures 6-16 and 6-17. Figure 6-15 shows the positions of the four points for which time series are illustrated. Each figure presents time series in seven different calculation layers in the model. The uppermost layer is situated in the Quaternary deposits while the other layers are in the bedrock. Cell (107,147) is situated close to the coastline in the northern part of the model area, cell (104,128) is situated in the cooling water intake channel of the power plant, cell (176, 121) is in the sea close to the coastline, and cell (155,87) is situated in Lake Bolundsfjärden.

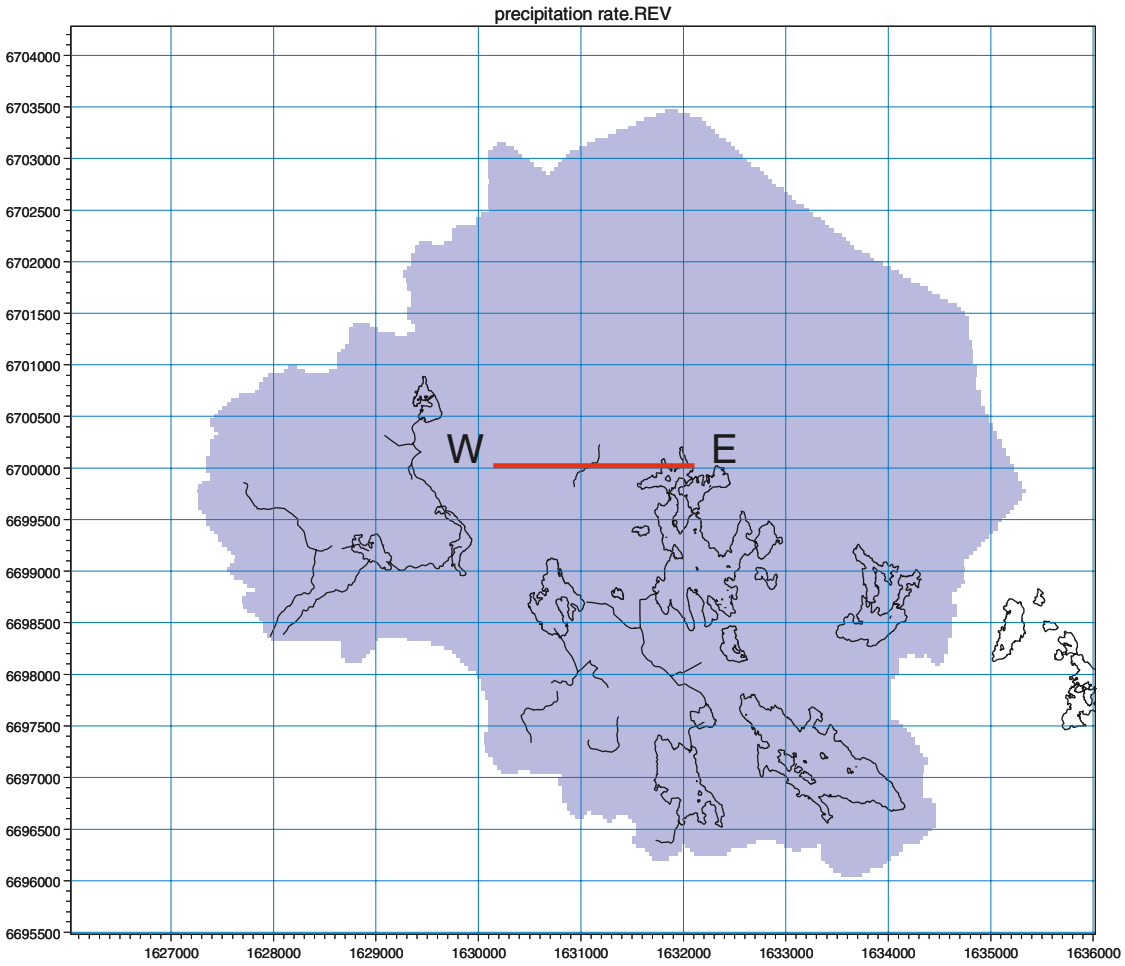

Figure 6-13. *Position of profile through an area of high horizontal conductivity in the west-east (W-E) direction.*

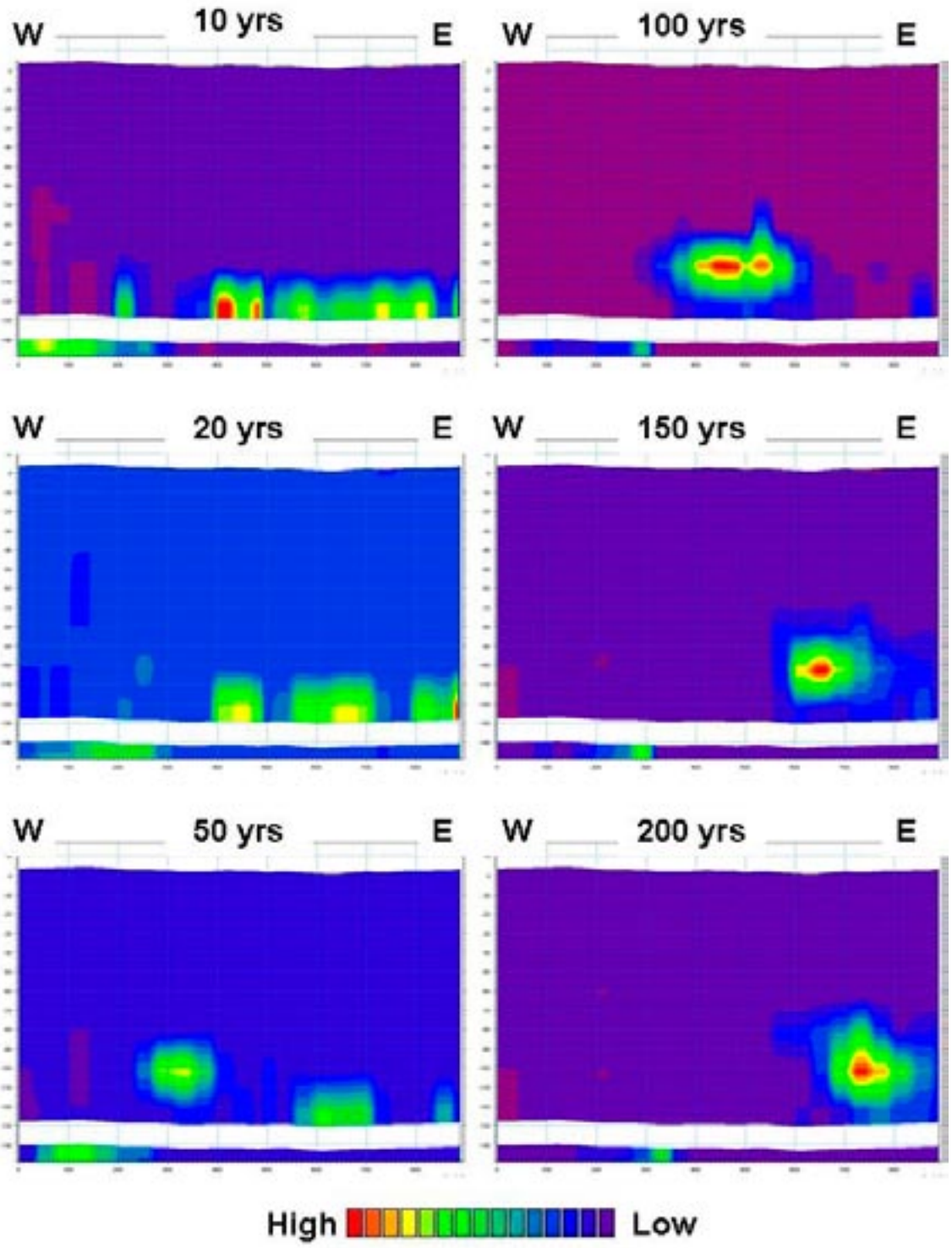

Figure 6-14. *Profile through the model area (location indicated in Figure 6-13) showing the advection-dispersion solute concentrations at six different times during the simulation.*

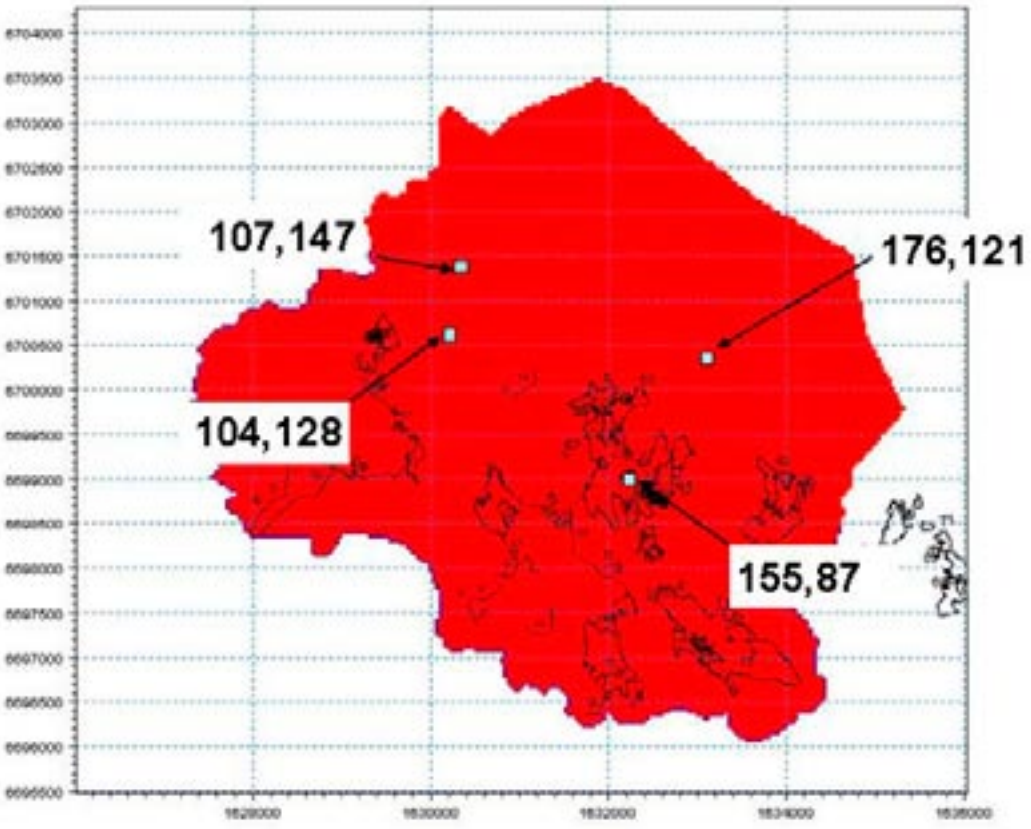

Figure 6-15. *Cells for which time series are illustrated in Figures 6-16 and 6-17.*

Figure 6-16 shows the time series in cell (107,147) and cell (104,128). Both figures show a relatively fast solute breakthrough; the maximum concentration is reached within a few years in all layers. Furthermore, in both figures it is seen that the concentrations in the upper layers are affected by seasonal variations, especially in cell (107,147).

Figure 6-17 illustrates time series from a point in the sea, cell (176,121). The solute transport is slower than for the previous two points; maximum concentrations are reached after about 10 years in the lower layer and after about 20 years in the upper layers. Furthermore, in all layers the solute concentration decreases for about 70–80 years after the maximum value but then increases to a new maximum which is reached after approximately 100 years of simulation. The reason for this is probably that a part of the solute mass is moving in areas with higher transport velocity, whereas the rest travels in parts where lower velocities prevail.

In the fourth time series figure, also in Figure 6-17, the solute transport is significantly slower. The maximum concentration is reached after approximately 150 years. The cell is situated under Lake Bolundsfjärden, where also measurements indicate that water movement is slow.

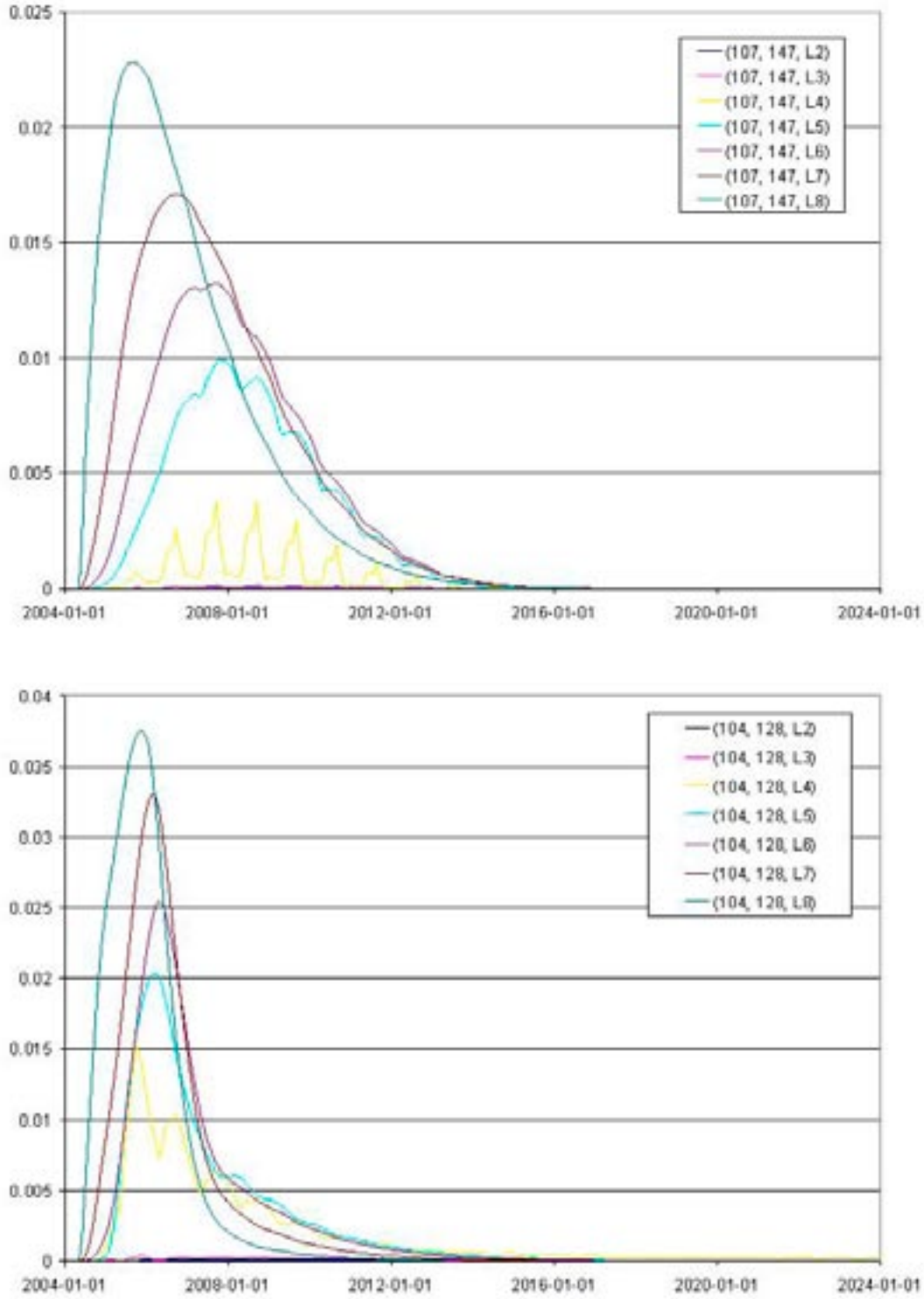

Figure 6-16. *Solute concentrations in different layers (L2 is layer 2, L3 layer 3, etc), in the upper figure from cell (107,147) and in the lower figure from cell (104,128).*

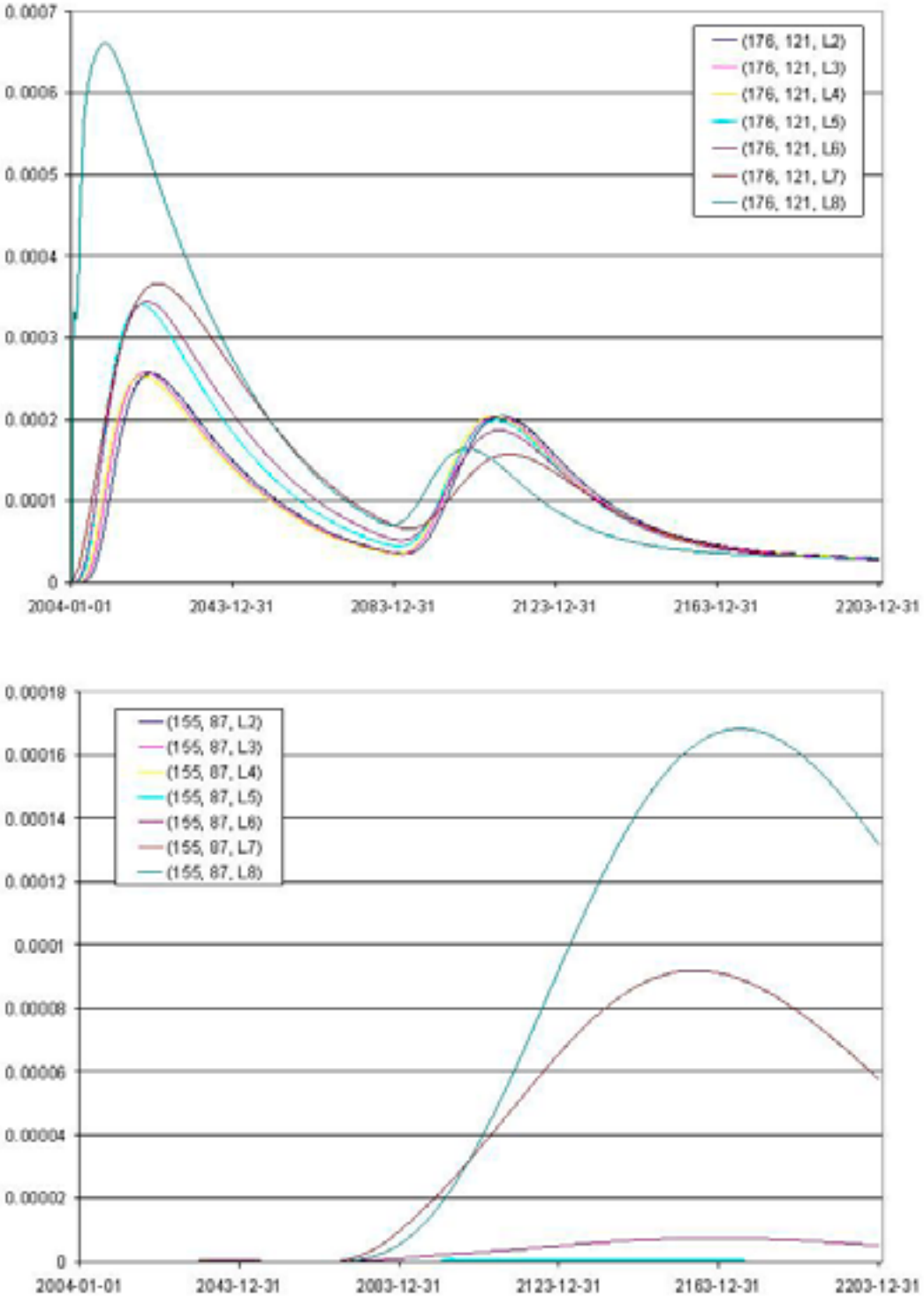

Figure 6-17. *Solute concentrations in different layers (L2 is layer 2, L3 layer 3, etc), in the upper figure from cell (176, 121) and in the lower figure from cell 155,87).*

A profile is drawn between the two cells (176,121) and (155,87), in order to further illustrate the flow pattern from Lake Bolundsfjärden and towards the sea, see Figure 6-18. In the bedrock layers along the profile, two of the layers with high horizontal conductivities are present at approximately 70 m.b.s.l. and 110 m.b.s.l. Figure 6-19 shows the concentrations along the profile at six different times. The figures show that after 20 years only the fast transport close to cell (176,121) has reached the upper layers. As time goes, solute starts spreading upwards also closer to cell (155,87), and after 40 years it is seen that solute that has reached a level of 110 m.b.s.l. starts moving horizontally towards the sea. After 50 years, solute has also reached the layer at about 70 m.b.s.l. and the figures show that the solute transport at that level is also towards the sea.

Table 6-2 shows a summary of model sinks where the solute left the saturated zone. The amount in each sink is compared to the total amount applied in the source. After 200 years, almost half of the applied source mass (48.9%) is still left in the saturated zone. The major part of the applied mass that has left the saturated zone goes to the sea. Also, a large part of the applied mass goes to the unsaturated zone.

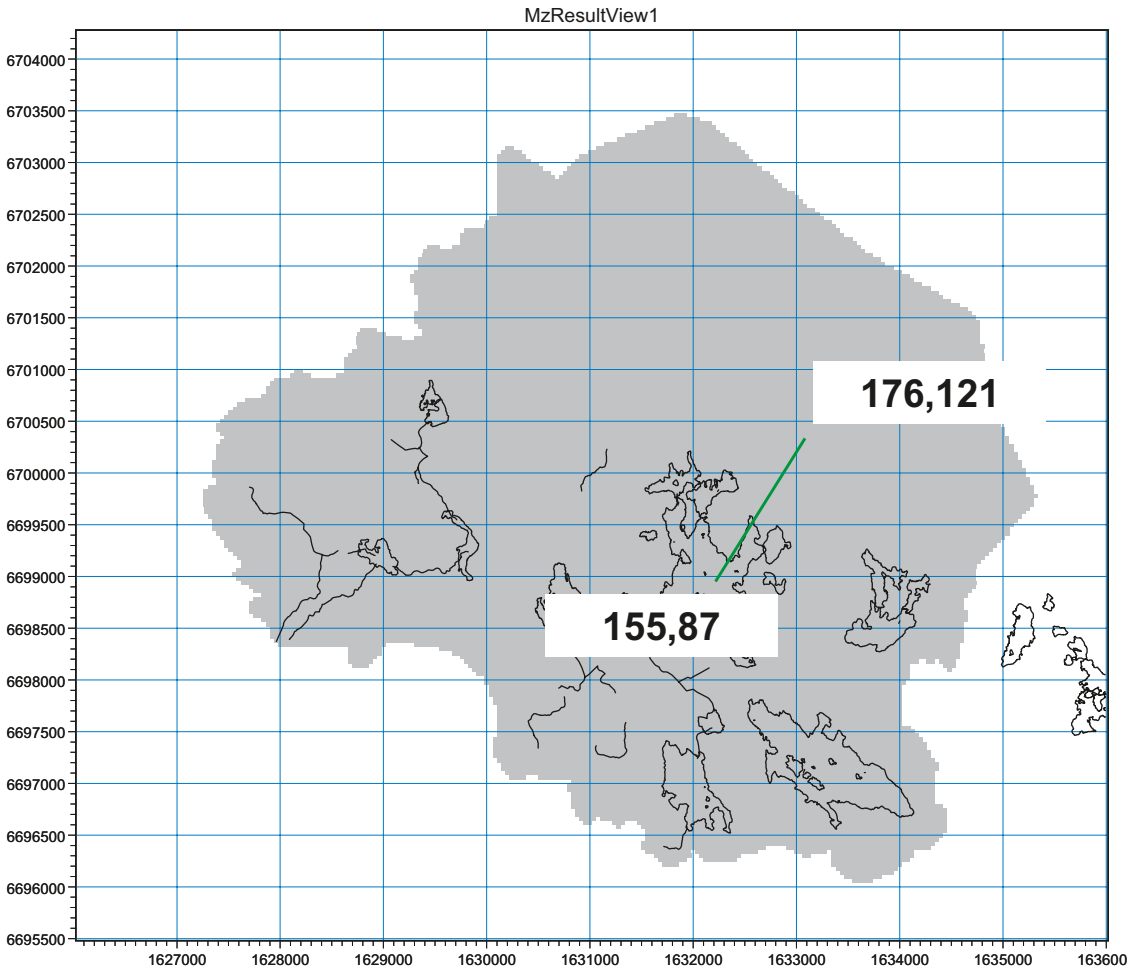

Figure 6-18. *Position of profile between cells (176,121) and (155,87).*

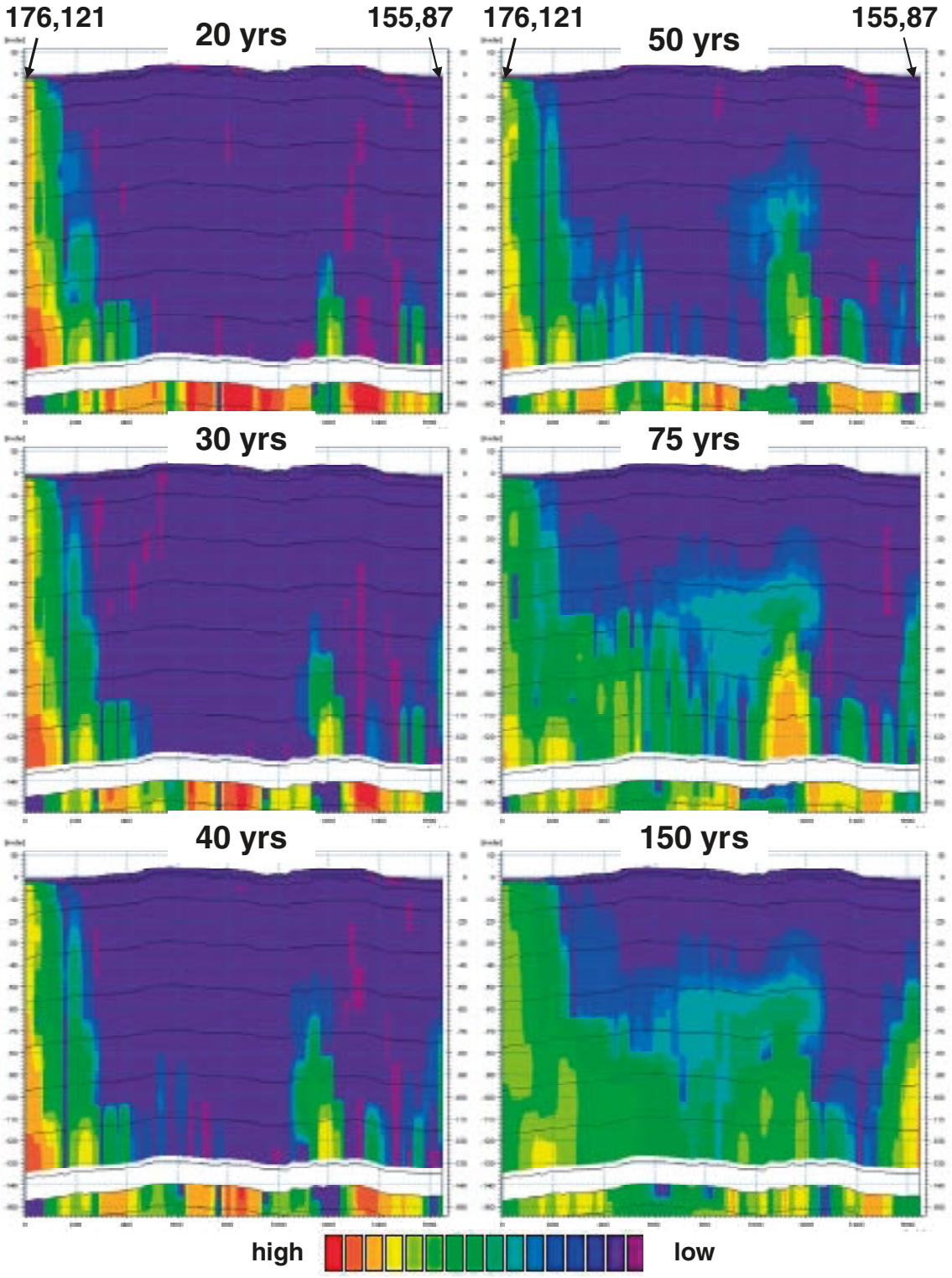

Figure 6-19. *Solute concentrations in a profile between cells (176,121) and (155,87) at six different times during the advection-dispersion simulation.*

Table 6-2. Summary of model sinks after 200 years advection-dispersion simulation with a source at a level of 140 m.b.s.l.

	Accumulated mass in % of total applied source mass after 200 years
Saturated zone storage	48.9
Saturated zone to unsaturated zone	16.9
Saturated zone baseflow to streams	1.2
Saturated zone drain to streams	1.8
Saturated zone to the sea	19.7
Saturated zone flow to boundaries	10.6
Saturated zone drain to boundaries	0.9
Total source to saturated zone	100.0

In the second simulation, the solute source is applied as a continuous infiltration source, i.e. the source is infiltrated to the model by the precipitation. As a consequence, the amount of solute infiltrated to the model depends on the amount of precipitation. The source is continuous with a concentration of 1 g/m^3. The initial concentration is zero and the dispersion coefficients are the same as in the case with a bedrock source. In cells with a fixed head the concentration is always zero.

Figure 6-20 shows simulation results in three different layers after 5 years. The upper figure is from the Quaternary deposits. Whereas the source is an infiltration source, discharge areas with no infiltration have no external source. This is the case with, for example, the lake areas. Areas with larger amount of infiltration, being recharge areas over the whole year, consequently act as larger infiltration sources.

The middle figure is from a bedrock layer at 70 m.b.s.l. and indicates this pattern even clearer, with the solute mass concentrated to recharge areas. Furthermore, in the figure it may be noted that because of the horizontal fractures/sheet joints that are located in bedrock layers further up under Lake Bolundsfjärden, the solute is transported horizontally towards the sea.

The lower graph in Figure 6-20, which is from a lower bedrock layer at 130 m.b.s.l., further indicates that the solute concentration is mainly concentrated to recharge areas. Furthermore, both in the middle and in the lower figure, the effect of the regional fracture zone in connection to Lake Eckarfjärden (see /Bosson et al. 2008, Figure 3.2/) is clearly illustrated. The low concentrations in the fracture zones indicate that they are discharge areas from the deeper bedrock.

Results for the vertical profile in Figure 6-10 are illustrated in Figure 6-21 for the case with the infiltration source. The figure shows the solute concentration along the profile after 10 years of simulation. The figure confirms what is said above about the pattern of the source strengths. However, a horizontal solute transport from higher recharge areas to lower discharge areas (i.e. lakes etc) would be expected, but the littoral zones appear to act as hydraulic barriers around some of the lakes, as exemplified by Lake Eckarfjärden in Figure 6-22. This effect is not so obvious around Lake Bolundsfjärden, see Figure 6-23, where the horizontal transport seems to spread the solute also under some parts of the lake. In both cases, however, the spreading through horizontal transport in the upper layers is much smaller than the effects of transport along vertical flow directions.

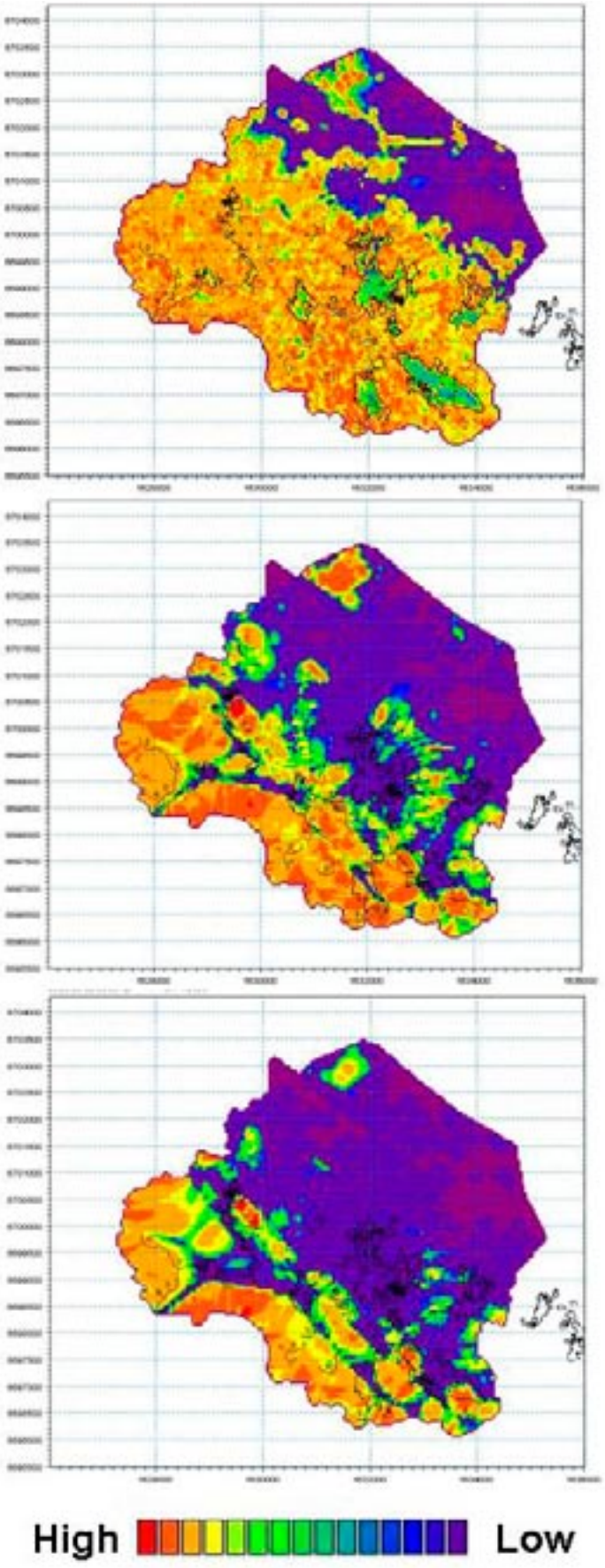

Figure 6-20. *Advection-dispersion simulation results after five years for three different layers, from top to bottom: layer 2 (in the Quaternary deposits), layer 6 and layer 9.*

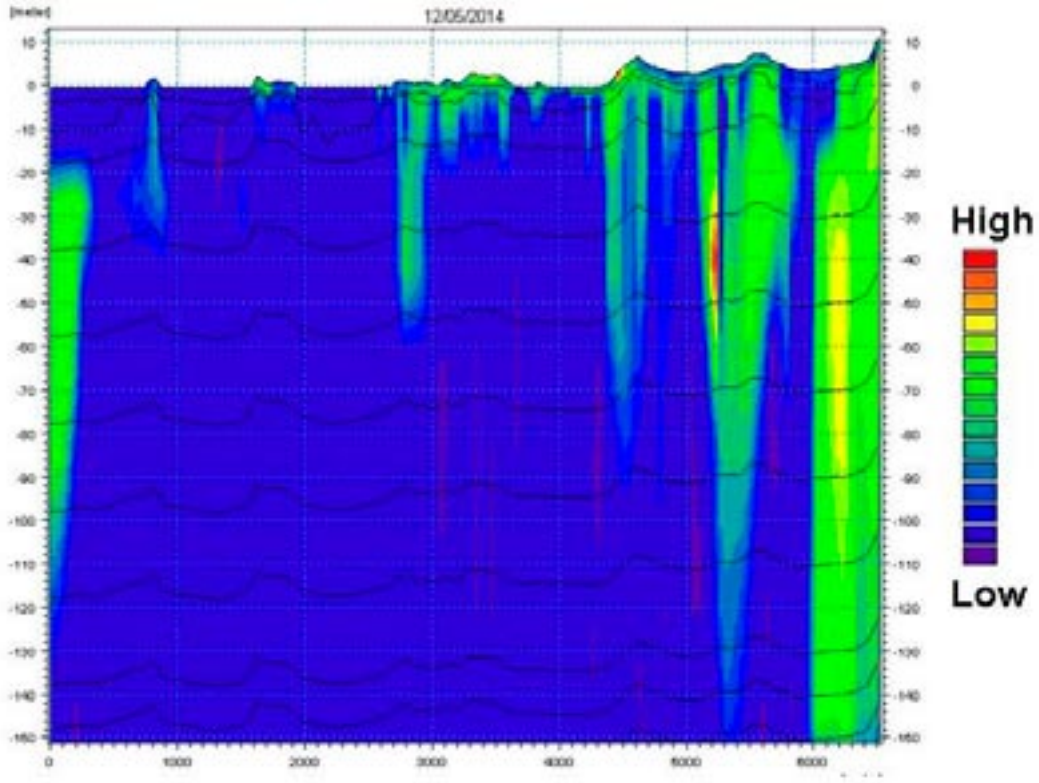

Figure 6-21. *Solute concentrations after 10 years in the profile shown in Figure 6-10 from advection-dispersion modelling of transport from a continuous infiltration source.*

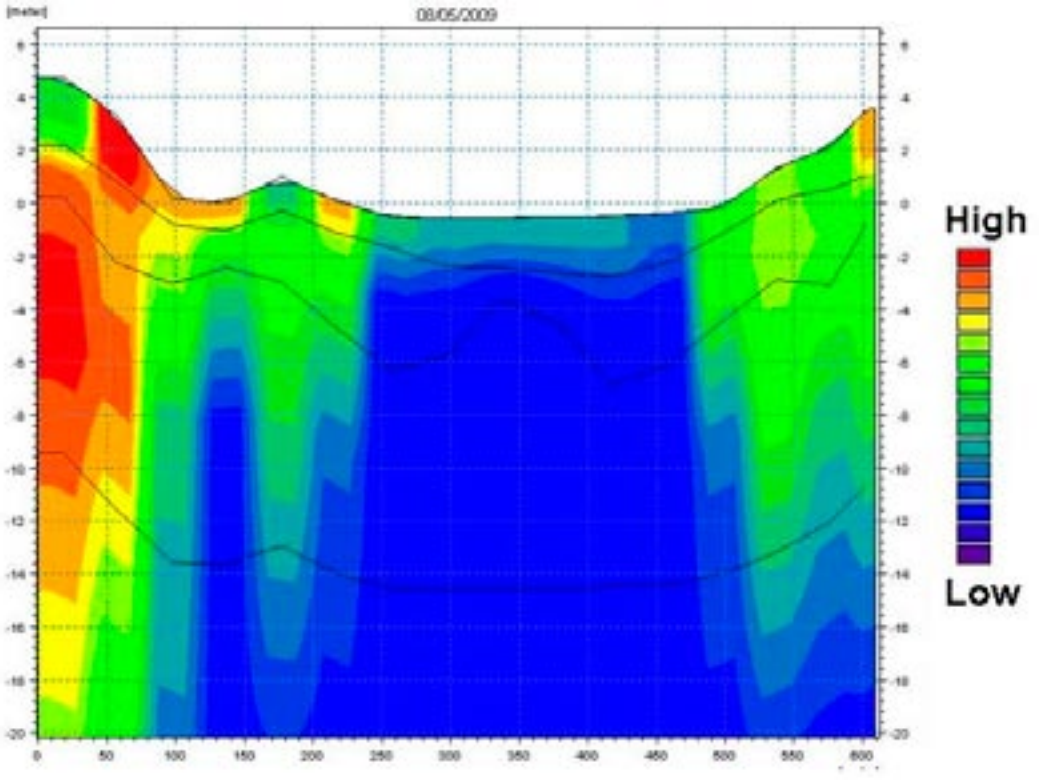

Figure 6-22. *Solute concentrations after 5 years in a profile in the west-east direction through Lake Eckarfjärden, from advection-dispersion modelling of transport from a continuous infiltration source.*

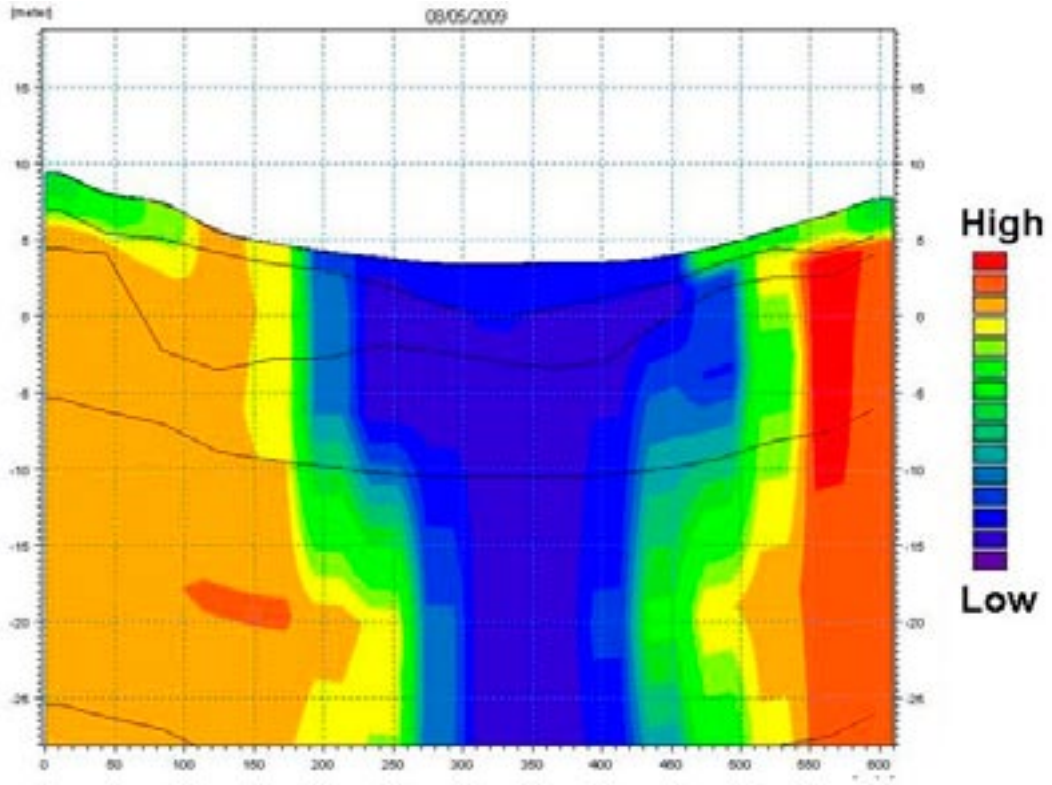

Figure 6-23. *Solute concentrations after 5 years in a profile in the west-east direction through Lake Bolundsfjärden, from advection-dispersion modelling of transport from a continuous infiltration source.*

Table 6-3 shows a summary of sinks where the solute leaves the saturated zone. Each sink parameter is compared to the total saturated zone output at the end of the simulation. The major part of the applied mass goes to the unsaturated zone, which is expected with an infiltration source. Finally, a large part of the applied source mass goes to the sea, which was also noted in the simulation with the bedrock source.

Table 6-3. Summary of model sinks after 200 years advection-dispersion simulation with a continuous infiltration source.

	Accumulated mass in % of total applied source mass after 200 years
Saturated zone to unsaturated zone	56.4
Saturated zone baseflow to streams	1.2
Saturated zone drain to streams	2.4
Saturated zone to the sea	36.4
Saturated zone flow to boundaries	0.4
Saturated zone drain to boundaries	3.2
Total saturated zone output	100.0

7 Conclusions

The main purpose of the transport simulations presented in this report is to present a sensitivity analysis of different transport properties. The simulations described in Chapters 4 and 5 are based on results from the MIKE SHE flow simulations presented as the *"Final calibrated model"* in /Bosson et al. 2008, Chapter 4/. The aim of the different simulation cases is to test the impact of different model parameters, such as the number of calculation layers, and the dispersion and sorption parameters. Based on the conclusions from this sensitivity analysis, transport simulations were performed on the final, re-calibrated Forsmark flow model; results from these are presented in Chapter 6.

The main conclusions from the transport simulations in Chapter 4 and 5 regarding the overall transport behaviour and the impact of different transport parameters can be summarised as follows:

- The solute source mass applied at a level of c. 140 m.b.s.l. is transported both upwards and downwards. The main direction is however upwards. The solute that is transported towards the surface is mainly transported through deformation zones under the lakes and the watercourses. In some of these zones, the transport is rather fast and the solute is transported to the surface in only a few years.
- Besides the vertical transport in the deformation zones, solute is also transported horizontally towards the sea. The transport towards the sea is, however, much slower than that in the deformation zones. In large parts of the area, the transport towards the sea is very slow, although in some high-conductive parts the process is faster. In these zones with higher horizontal hydraulic conductivity in the bedrock, the solute is mainly transported in the horizontal direction towards the sea, cutting off the vertical transport upwards.
- The applied infiltration source produces solute mass in recharge areas only, although a horizontal solute transport from higher recharge areas to lower discharge areas (e.g. lakes) would be expected. On the time scale considered in the present simulations, it seems like the littoral zones act as hydraulic barriers around some of the lakes. This means that in these areas the spreading through horizontal transport in the upper layers is less important than the effects from vertical flow directions, which reduces mass transport in below the lakes considerably.
- The dispersion processes transports solutes from the advective zones into more stagnant zones. The process is important when evaluating the risk for solute spreading into zones in which the transport pattern is more diffuse. Therefore, it is important to estimate the dispersion coefficients and to avoid numerical dispersion in the model.
- Since sorption leads to a delay in the peak arrival time, it is an important factor to include in the simulations when the estimation of the solute peak arrival time is crucial.

The additional main conclusions from the transport simulations in Chapter 6 with the final re-calibrated Forsmark model are:

- The particle tracking results indicates a relative slow transport from the bedrock up to the ground surface. After 300 years, the majority of the introduced particles are still left in the model volume. The areas with high horizontal hydraulic conductivity, which are associated with the so-called horizontal fractures/sheet joints, short circuit the transport paths of particles released in the area where these structures are represented.
- The particles reaching ground surface when introducing particles all over the model area are concentrated to lake areas, the depressions around the streams, and the sea. When activating the drainage in the SFR repository, no particles discharge to the sea. Instead, the particles are removed by the well representing the SFR drainage. Otherwise, the pattern of the exit points at the ground surface is the same.

- When introducing particles inside the planned repository area only, all exit points are found in the sea (in the case without the SFR drainage). No particles discharge in the land part of the model area. The overall pattern of exit points after 300 years does not change when running the model for 5,000 years; however, additional exit points are obtained further out in the sea.
- The advection-dispersion results from the case where the solute is introduced at 140 m.b.s.l. show that the transport is directed both upwards and downwards. The upward transport in the bedrock is mainly directed towards the sea and the lake areas. When the solute reaches a layer where the sheet joints are represented, the horizontal component of the transport is dominating. As a result, only a minor fraction of the solute appears above the areas with high horizontal hydraulic conductivity.
- Vertical profiles confirm the importance of the sheet joints for the overall pattern of the transport. Each time the solute reaches a layer with sheet joints, which are represented at three different levels, a spreading towards the sea can be noticed.
- The modelled discharge from the bedrock to the Quaternary deposits is limited. Only areas above the Eckarfjärden regional fracture zone receive solute from the bedrock in the transport simulations.

8 References

Bosson E, Berglund S, 2006. Near-surface hydrogeological model of Forsmark. Open repository and solute transport applications – Forsmark 1.2. SKB R-06-52, Svensk Kärnbränslehantering AB.

Bosson E, Gustafsson L-G, Sassner M, 2008. Numerical modelling of surface hydrology and near-surface hydrogeology at Forsmark. Site descriptive modelling, SDM-Site Forsmark. SKB R-08-09, Svensk Kärnbränslehantering AB.

DHI Software, 2007. MIKE SHE – User Manual. DHI Water & Environment, Hørsholm, Denmark.

Follin S, Johansson P-O, Hartley L, Jackson P, Roberts D, Marsic N, 2007. Hydrogeological conceptual model development and numerical modelling using CONNECTFLOW, Forsmark model stage 2.2. SKB R-07-49, Svensk Kärnbränslehantering AB.

Hedenström A, Sohlenius G, Strömgren M, Brydsten L, Nyman H, 2008. Depth and stratigraphy of regolith at Forsmark. Site descriptive modelling, SDM-Site Forsmark. SKB R-08-07, Svensk Kärnbränslehantering AB.

Hedenström A, Sohlenius G, 2008. Description of the regolith at Forsmark. Site descriptive modelling, SDM-Site Forsmark. SKB R-08-04, Svensk Kärnbränslehantering AB.

Johansson P-O, 2008. Description of surface hydrology and near-surface hydrogeology at Forsmark. Site descriptive modelling, SDM-Site Forsmark. SKB R-08-08**,** Svensk Kärnbränslehantering AB.

Johansson P-O, Öhman J, 2008. Presentation of meteorological, hydrological and hydrogeological monitoring data from Forsmark. Site descriptive modelling, SDM-Site Forsmark. SKB R-08-10**,** Svensk Kärnbränslehantering AB.

Lindborg (ed), 2008. Surface system Forsmark. Site descriptive modelling, SDM-Site Forsmark. SKB R-08-11, Svensk Kärnbränslehantering AB.

SKB, 2008. Site description of Forsmark at completion of the site investigation phase. SKB TR-08-05, Svensk Kärnbränslehantering AB.

Werner K, Bosson E, Berglund S, 2005. Description of climate, surface hydrology, and near-surface hydrogeology. Simpevarp 1.2. SKB R-05-04, Svensk Kärnbränslehantering AB.